

2016

A Climatological Exploration of Land Change and Land Use on Lightning Patterns over Louisiana

Nicholas James Sokol

Louisiana State University and Agricultural and Mechanical College, Nsokol2@lsu.edu

Follow this and additional works at: https://digitalcommons.lsu.edu/gradschool_theses



Part of the [Social and Behavioral Sciences Commons](#)

Recommended Citation

Sokol, Nicholas James, "A Climatological Exploration of Land Change and Land Use on Lightning Patterns over Louisiana" (2016).
LSU Master's Theses. 4406.
https://digitalcommons.lsu.edu/gradschool_theses/4406

This Thesis is brought to you for free and open access by the Graduate School at LSU Digital Commons. It has been accepted for inclusion in LSU Master's Theses by an authorized graduate school editor of LSU Digital Commons. For more information, please contact gradetd@lsu.edu.

A Climatological Exploration of
Land Change and Land Use on Lightning Patterns over Louisiana

A Thesis

Submitted to the Graduate Faculty of the
Louisiana State University and
Agricultural and Mechanical College
in partial fulfillment of the
requirements for the degree of
Master of Science

in

The Department of Geography and Anthropology

by
Nicholas J. Sokol
B.S., Towson University, 2015
December 2016

Acknowledgments

The completion of this thesis would not have been possible without several people who were there for me. I must extend most heartfelt thanks to my family, who have supported my academic endeavors through innumerable hardships. After them, many of my sincerest thanks go out to the faculty members at Louisiana State University that have impacted my life in many ways. I also must thank my advisor Dr. Robert Rohli, who has provided unyielding support and feedback on my work since my time at LSU began. Without his hard work, dedication, and assistance, I doubt I would have completed this thesis. I also thank Dr. Carol Friedland for granting me an opportunity to work alongside individuals in the College of Engineering at LSU. In addition, I would like to thank my committee members: Dr. Nan Walker (Oceanography), Dr. Michael Leitner (Geography and Anthropology), and Dr. Todd Moore (Geography and Environmental Planning at Towson University). Each of these faculty members provided amazing feedback and counsel on how to make my thesis the best it could be! My gratitude goes to everyone else in the Geography and Anthropology (G&A) department. My interactions with everyone in G&A have made me aware of so many things in life and ultimately changed me as a person.

I would be remiss if I did not mention my gratitude to all my friends and advisors back in Maryland, and other parts of the world. You all have supported me since before I gave graduate school a thought and provided nothing but love and positive energy. Every time I returned home you listened to me whine about being broke and how much I despised the heat and humidity in Louisiana. In return you responded with ways I could make the best of it, took me on crazy adventures to get my mind off work, and spent countless hours enjoying my dark sense of humor – and that kept me going. Thank you all!

Table of Contents

ACKNOWLEDGMENTS.....	ii
LIST OF TABLES.....	iv
LIST OF FIGURES.....	v
ABSTRACT.....	viii
I. INTRODUCTION.....	1
II. LITERATURE REVIEW.....	6
2.1 Diurnal Lightning Studies.....	6
2.2 Seasonal Lightning Studies.....	7
2.3 Lightning Frequency.....	8
2.4 Landsat Based Land Change Studies.....	12
2.5 Land Change Influences on Lightning.....	14
III. DATA/METHODS.....	16
3.1 Landsat Land Classification Data.....	16
3.2 NOAA/Vaisala NLDN Lightning Data.....	28
3.3 Lightning Climatology.....	31
3.4 Linear Regression with a Categorical Variable.....	31
3.5 ANOVA and Scheffé's 95% Confidence Interval Test.....	31
3.6 Geographically Weighted Regression.....	33
IV. RESULTS AND DISCUSSION.....	35
4.1 Lightning Climatology.....	35
4.2 Linear Regression with a Categorical Variable.....	57
4.3 ANOVA and Scheffé's Test.....	61
4.4 Geographically Weighted Regression.....	67
V. CONCLUSION.....	73
REFERENCES.....	76
VITA.....	85

List of Tables

Table 3.1 Colors representing each LULC type within the classification image maps	22
Table 4.1 Results of trend line analysis.....	54
Table 4.2 Results of categorical linear regression for 1996 and 2001.....	60
Table 4.3 Results of categorical linear regression for 2006 and 2010.....	61
Table 4.4 Results of ANOVA.....	62
Table 4.5 Results of Scheffé's test for 1996	63
Table 4.6 Results of Scheffé's test for 2001	64
Table 4.7 Results of Scheffé's test for 2006	65
Table 4.8 Results of Scheffé's test for 2010	67

List of Figures

Figure 1.1 Graupel, hail, sleet, and snow.....	1
Figure 1.2 Process of a stepped leader	2
Figure 1.3 Lightning fatalities in the United States from 1940 to 2015.....	3
Figure 2.1 Lightning climatology derived from LIS/OTD	8
Figure 2.2 Lightning climatology derived from the worldwide lightning location network.....	9
Figure 3.1 Louisiana land classification map for 1996.....	18
Figure 3.2 As in Figure 3.2, for 2001.....	19
Figure 3.3 As in Figure 3.2, for 2006.....	20
Figure 3.4 As in Figure 3.2, for 2010.....	21
Figure 3.5 Majority resampled Louisiana land classification for 1996.....	23
Figure 3.6 As in Figure 3.5, for 2001.....	24
Figure 3.7 As in Figure 3.5, for 2006.....	25
Figure 3.8 As in Figure 3.5, for 2010.....	26
Figure 3.9 LULC totals for the years 1996, 2001, 2006, and 2010.....	27
Figure 3.10 NOAA derived NLDN CG lightning product.....	28
Figure 3.11 Aligned CG lightning raster with resampled Louisiana Land Classes.....	30

Figure 4.1 Histogram of CG lightning along with frequency map for 1995.....	36
Figure 4.2 As in Figure 4.1, for 1996.....	37
Figure 4.3 As in Figure 4.1, for 1997.....	38
Figure 4.4 As in Figure 4.1, for 1998.....	39
Figure 4.5 As in Figure 4.1, for 1999.....	40
Figure 4.6 As in Figure 4.1, for 2000.....	41
Figure 4.7 As in Figure 4.1, for 2001.....	42
Figure 4.8 As in Figure 4.1, for 2002.....	43
Figure 4.9 As in Figure 4.1, for 2003.....	44
Figure 4.10 As in Figure 4.1, for 2004.....	45
Figure 4.11 As in Figure 4.1, for 2005.....	46
Figure 4.12 As in Figure 4.1, for 2006.....	47
Figure 4.13 As in Figure 4.1, for 2007.....	48
Figure 4.14 As in Figure 4.1, for 2008.....	49
Figure 4.15 As in Figure 4.1, for 2009.....	50
Figure 4.16 As in Figure 4.1, for 2010.....	51
Figure 4.17 As in Figure 4.1, for 2011.....	52

Figure 4.18 Bar graph showing the total regional frequency of CG lightning flashes with a trend line fitted (top), and a map showing the spatial distribution of the 4 km x 4 km pixels across the region for all years 1995–2011.....	53
Figure 4.19 Boxplots of each LULC type and their mean, interquartile range, and extremes of CG lightning, by 4 km x 4 km pixel, for 1996 (top) and 2001 (bottom).....	55
Figure 4.20 As in Figure 4.19, for 2006 and 2010.....	56
Figure 4.21 Residuals from a linear regression test between 1996 (top) and 2001 (bottom) LULC and lightning	57
Figure 4.22 As in Figure 4.21, for 2006 and 2010.....	58
Figure 4.23 Resulting conditional number, local R^2 , standard residuals, and predicted values from GWR output between total lightning frequency between 1996 land classes and total lightning.	70
Figure 4.24 As in Figure 4.23, for 2001.....	71
Figure 4.25 As in Figure 4.23, for 2006.....	72
Figure 4.26 As in Figure 4.24, for 2010.....	73

Abstract

Lightning is one of the most impactful weather phenomena but yet little precise and accurate information is known about how its frequency is impacted climatologically by changes in land use/land cover (LULC). This is unfortunate because LULC changes occur ubiquitously as the human influence on the environment proceeds. This research uses NOAA's gridded annual lightning data from the National Lightning Detection Network (NLDN), and LULC classification data from the NOAA coastal change analysis program (C-CAP) to analyze frequency changes in lightning across a swath of Louisiana, coastal Mississippi, and coastal east Texas over the years 1995–2011. Results suggest that urban areas have the highest frequency of CG lightning, but there is little variation in lightning over the course of the temporal period examined. The implications of this work will provide planners and regional analysts more insight as to how some LULC categories attract more lightning than others, as well as how CG lightning is sporadic and complicated to model. Some limitations of this research are that the lightning data utilized in this study are not point data, complicating the measurement of spatial shifts in lightning occurrence since raster cells are fixed to a specific latitude and longitude. Therefore, continued work is needed to further understand the relationship between human influence on the landscape and the lightning risk. Results presented here and in future work will be useful to environmental planners as they work to understand and mitigate the lightning hazard.

Chapter 1. Introduction

Why Study Lightning?

Lightning is a phenomenon that has perplexed, terrified, amazed, and devastated humans and other organisms. It is one of the world's most dangerous, but often underestimated, severe weather phenomena and it continues to claim dozens of lives every year in the United States (Curran et al., 2000; NWS, 2016; Holle, 2016).

Fulminologists—scientists who study atmospheric electricity—have generated substantial information regarding the development of lightning. Lightning is formed when small particles of ice – known as graupel (Figure 1.1) – form inside a cloud. The graupel is ionized through collisions with other particles in the cloud that are driven by powerful updrafts; this process is known as an electron avalanche (Cooray, 2015).



Figure 1.1 Graupel, hail, sleet, and snow, respectively (NWS, 2016).

Once enough electrically charged particles surpass the threshold of atmospheric insulation, a stepped leader (Figure 1.2)—a concentrated current of energy that is negatively or positively charged propagating toward the surface—will connect with a vertically-propagating stepped leader from the surface or object on Earth, and the resulting phenomena is the lightning flash (Cooray, 2015). Thunder is the acoustic aftermath of a lightning flash, caused by rapid

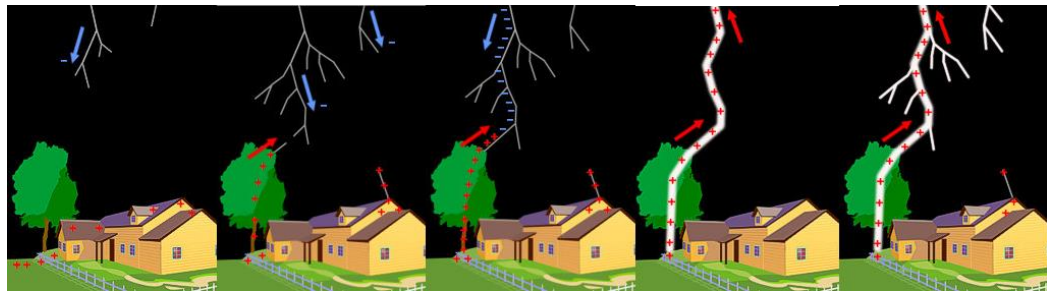


Figure 1.2 The process of a stepped leader and how it creates a Cloud to ground lightning flash. Negative (positive) channels connect with positive (negative) channels propagating from the surface (NWS, 2016).

heating and expansion of the surrounding air, which has been recorded to reach temperatures of up to 6000 K (Rakov and Uman, 2003).

Most people who are aware of the hazard of lightning often jest about the statistical probability of being struck, which is 1 in 1,042,000 (NWS, 2013). This fact likely causes many to neglect the safety methods disseminated by the National Oceanic and Atmospheric Association (NOAA) and the National Weather Service (NWS), and fatalities continue to occur. However, a brief analysis of lightning fatalities shows that the total has decreased over time for the country and Louisiana (Figure 1.3; Curran et al., 2000; Roeder et al., 2015; NWS, 2016).

Louisiana is ranked ninth among the states in lightning-induced deaths per year (Holle, 2016), despite having a population that ranks 25th. Louisiana often has the second highest rate of lightning frequency in the United States. Florida, Texas, Mississippi, and Alabama also have high flash frequencies (Holle, 2016). Florida's high flash rate exists because of its proximity to the atmospheric features required to create a thunderstorm, such as convection, moisture, and heat (Zhu et al., 2015). Louisiana is also in a similar position; although it lacks the persistent convective enhancement of peninsular Florida, the state has a constant supply of warm, moist air from the Gulf of Mexico that fuels atmospheric

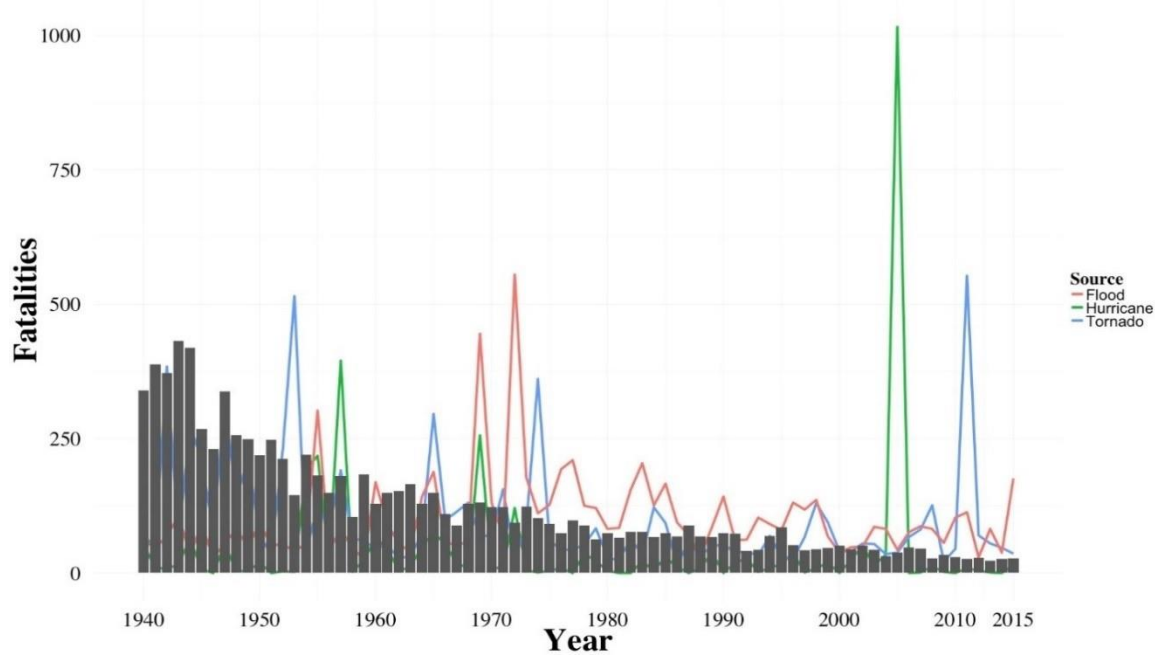


Figure 1.3 Total lightning fatalities in the U.S., 1940 to 2015 (bars), compared with fatalities from other natural hazards (NWS, 2016).

instability for a substantial number of days throughout the year. In addition to moisture (Lericos et al., 2002) and pollution (Smith et al., 2005).

Instrumentation designed to detect lightning has improved in recent decades. This has allowed atmospheric scientists to create climatological averages of lightning over specific areas, and of course to research the spatio-temporal patterns of lightning. Although there have been many tools for examining lightning in past years (e.g. boys cameras, cloud chambers, lightning chimes), modern ground-based electromagnetic sensor and orbiting satellites in space keep a far more accurate and precise count of lightning totals on a near-real-time basis over far wider areas than ever before.

Despite their many advantages, weaknesses of the modern lightning detection systems exist. Specifically, ground-based measurement systems often detect electromagnetic

perturbations only to a limited height of the atmosphere, whereas satellite instrumentation can only sense the perturbations down to a limited depth of the atmosphere and may confuse lightning with other distortions of light in the Earth-atmosphere system (Boccippio et al., 2000; Boccippio et al., 2002; Ushio et al., 2002; Mach et al., 2007; Beirle et al., 2014, Buechler et al., 2014). Studies have consistently shown that ground-based detection systems are more precise, accurate, and reliable than their space-based counterparts (Idone et al., 1998; Biagi et al., 2007; Holle, 2014; Mallick et al., 2014). Rapid technological advancements continue to further lightning observation and study.

Lightning detection systems consistently show that strikes are more frequent on tall, ellipsoid-shaped buildings and surfaces that can generate a large electrical field (Rakov and Uman, 2003). In natural environments, these land covers consist of open fields or bodies of water, tall trees, and high points on a mountain. Built-up environmental features such as parking lots, skyscrapers, communication towers, sports fields, farm plots, and other anthropogenic landscapes are also favored. Data are now available to assess the validity of the notion that land use / land cover (LULC) may modify the spatio-temporal patterns of lightning strikes.

An improved understanding of the spatiotemporal patterns of lightning frequency is important for protecting life and property. Additional understanding of the relationship between natural and anthropogenic landscapes and lightning can improve protection of life and property. The objectives of this thesis are to:

- 1.) Analyze the spatio-temporal distribution of cloud-to-ground (CG) lightning over the northern Gulf Coast region.
- 2.) Investigate the influence of land classes on lightning totals and patterns over the northern Gulf Coast region.

Results from this research will not only serve the people of the Louisiana Gulf Coast region, but will also be useful elsewhere for mitigating lightning damage.

Chapter 2 will provide a more detailed literature review of lightning and LULC change detection research in recent decades. Chapter 3 will explain the data and methods used to address the objectives listed above. In Chapter 4, the results and their implications will be presented. Finally, Chapter 5 will include a summary of the major findings, along with suggestions for future research.

Chapter 2. Literature Review

“An investment in knowledge pays the best interest.”

– Benjamin Franklin

While a majority of recent lightning research is dedicated to understanding the physics of lightning, recent studies have focused on extracting spatio-temporal patterns from lightning data (Roeder et al., 2015; Cecil et al., 2015; Dowdy, 2016). In addition, LULC due to anthropogenic activity has also been explored through geographic research methods (Contiu & Gorza, 2016; Maclaurin and Leyk, 2016). This chapter will review the spatio-temporal and other geographically-focused studies.

2.1 Diurnal Lightning Studies

Diurnal patterns of lightning have been investigated thoroughly. Wallace (1975) found that thunderstorm activity depends upon diurnal kinematic and thermodynamic variables in the U.S., with most locations experiencing a peak in severe thunderstorms in the afternoon. Easterling and Robinson (1985) divided the U.S. into nine regions based on diurnal thunderstorm tendencies and found that the central region’s thunderstorms occur mostly at night, while eastern and western thunderstorms display an afternoon preference, and those in the Northeast and the Pacific coast are rare. López and Holle (1998) showed that Colorado storms are more commonly characterized by a west to east shift in maximum frequency from early morning to late evening, while Florida has lightning patterns that tend to be maximized between Cape Canaveral and Orlando in the afternoon. Carey and Rutledge (2003) analyzed the diurnal characteristics of lightning over the Kansas/Colorado border to Minnesota; their results showed that the amperage of a lightning flash depends upon the strength, size, and location of the storm, but overall the most powerful flashes occur in the afternoon. Smith et al. (2005) found that over the Gulf of

Mexico from 1989 – 2002, warm-season lightning is most prevalent during the day over areas along the coast, and during the night the lightning occurs most frequently over the Gulf.

More recent diurnal studies of lightning have utilized data from recently developed observation techniques such as the World-Wide Lightning Location Network (WWLLN; Jacobsen et al., 2006). Rudlosky & Shea (2013) compared results of the WWLLN to the Lightning Imaging Sensor (LIS) derived lightning counts and found strong similarities between the two data sets. Utilizing data from the LIS satellite to compile a spatial pattern analysis of lightning, Sen Roy and Balling (2013) showed that most lightning flashes occur over land during the day with very few occurring at night. Blakeslee et al. (2014) utilized LIS/Optical Transient Detector (OTD) remotely-sensed data to determine that global lightning maxima tends to occur most frequently in late afternoon, with minima tending to occur in the late morning. Holle (2014) found evidence using data from the National Lightning Detection Network (NLDN) that, over the U.S., lightning tends to occur between 1200 and 1800 local time, but occurrences before noon are more common over areas along the Gulf Coast and portions of the East Coast than elsewhere. Virts et al. (2015) found summer frequencies of lightning strikes to be maximized during the late afternoon and early evening, in general across the contiguous U.S., with lightning tending to occur most frequently from sunrise to late morning in the northern Gulf of Mexico – showing evidence of strong regional influence on diurnal lightning patterns.

2.2 Seasonal Lightning Studies

Seasonal lightning studies have been conducted around the world. Collier et al. (2006) reported that in southern Africa the highest flash rate is in the summer over Madagascar and South Africa. In a global study of seasonal lightning variability Yang et al. (2009) determined that Africa and Asia contains higher rates of CG lightning than any other location on the globe.

Tinmaker et al. (2014) identified a bimodal pattern of frequency over the Indian Seas, with peaks in April and October, corresponding to the timing of the monsoon front. Virts et al. (2015) showed that summer is the most active lightning season over the Gulf of Mexico and surrounding coastal areas and that most lightning activity is concentrated over the land. A lightning climatology for the U.S. Southwest in conjunction with the North American monsoon showed a drastic increase in lightning during the summer, when the monsoon period is at its strongest (Holle and Murphy 2015). Dowdy (2016) concluded that ENSO has the strongest influence on seasonal lightning variability around the globe.

2.3 Lightning Frequency

Climatological studies of lightning across the U.S. have been completed for various regions, with data for global tropical coverage (Figure 2.1) and global coverage (Figure 2.2) also having become recently available. Changnon (1988a, 1988b) showed that the peak frequency of

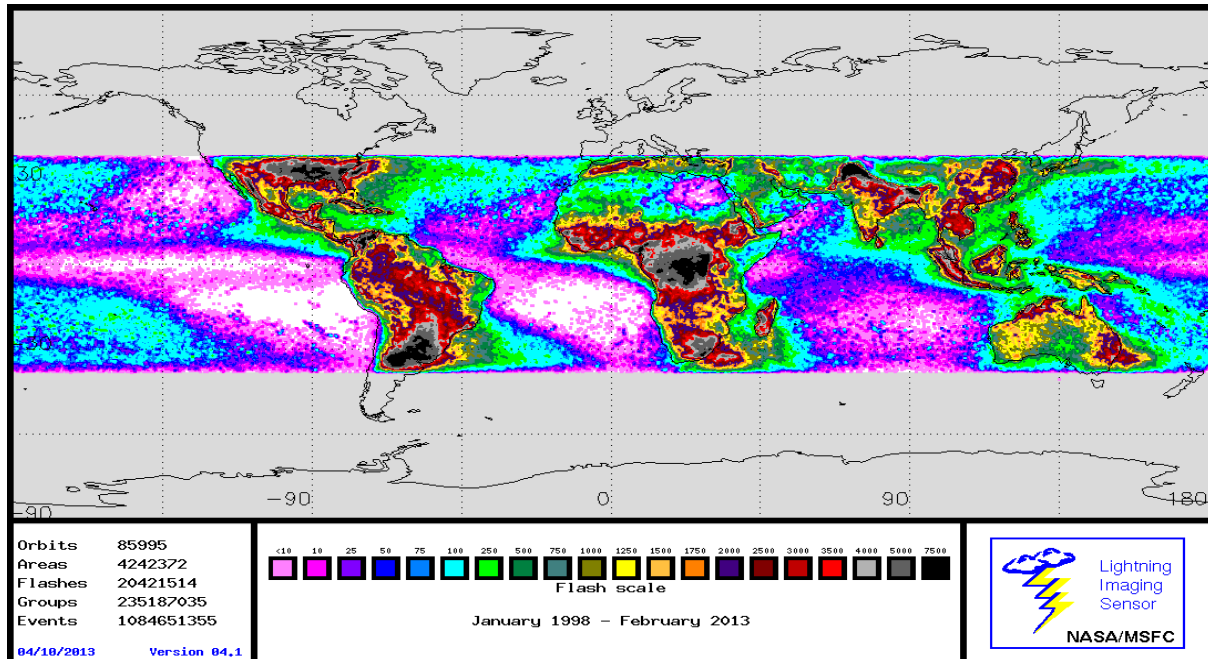


Figure 2.1 A lightning climatology derived from the Lightning Imaging Sensor / Optical Transient Detector sensor, which is aboard the Tropical Rainfall Measuring Mission satellite (NASA, 2016).

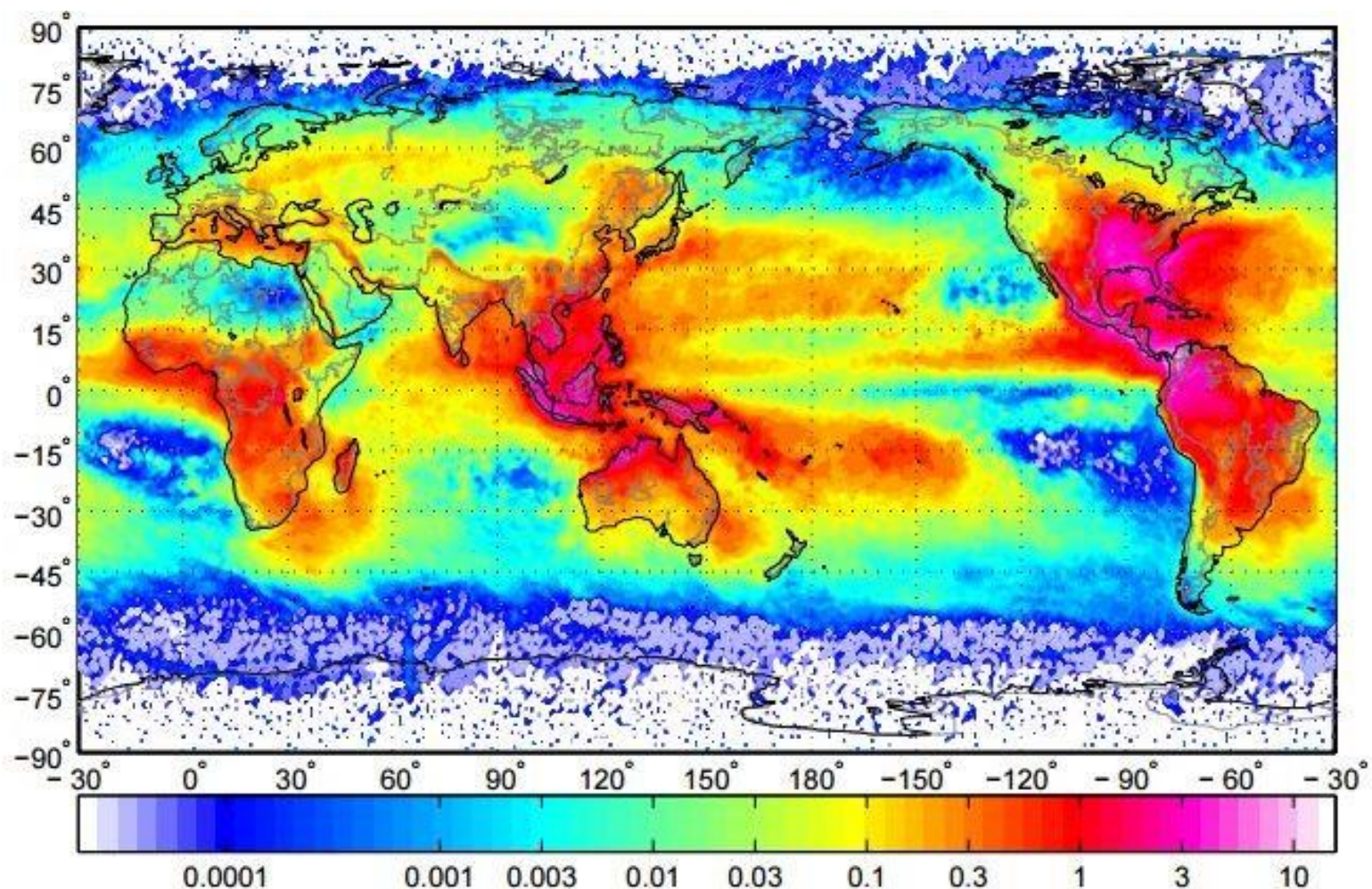


Figure 2.2 A lightning climatology derived from the Worldwide Lightning Location Network showing the mean lightning flashes per hour per year (2008–2011) per km² (Virts et al., 2013).

thunder events in the U.S. tends to occur the most over the Gulf Coast and the least over the West Coast. Watson and Holle (1996) found that in the southeastern U.S., the CG strike frequency is maximized along the shores of Florida and that urban areas often show enhanced frequency. Hodanish et al. (1997) found that for each season, synoptic and mesoscale mechanisms influence the location of lightning occurrence in Florida. Huffines and Orville (1999) found that Florida has the highest lightning strike density in the U.S. due to its unique geographic features that allow convection to promote thunderstorm development rapidly. Orville and Huffines (1999) suggested that Florida and Louisiana have the highest frequency of lightning activity—11 strikes km^{-2} per year—in the U.S., due to abundant moisture, heat, and forcing mechanisms. Zajac and Rutledge (2001) found that U.S. lightning flashes are most frequent over the coastal Southeast, but that high frequencies are also concentrated over the southern Rocky Mountains and the Great Plains. Schuhltz et al. (2011) found that CG lightning comprises of approximately 40% of total lightning in the United States. Villarini and Smith (2013) found that, within the U.S., extreme lightning activity is concentrated in the central U.S. and west of the Appalachian Mountains and increased in frequency from 1999 to 2011.

Sources of lightning frequency variability have also been examined. LaJoie and Laing (2008) showed that, over the Gulf of Mexico, lightning tends to have increased activity during warm El Nino/Southern Oscillation periods. In follow-up research, Laing et al. (2008) identified statistically significant correlations between winter ENSO and lightning activity in the Gulf of Mexico region, but only weak correlation values for the summer.

Synoptic-scale spatial patterns have revealed previously unknown characteristics of thunderstorms. In analyzing summer thunderstorm features over the southeastern U.S., Murphy and Konrad (2005) found, not surprisingly, that larger thunderstorms tend to produce more lightning than more localized thunderstorms. Williams (2005) determined that, while lightning is sensitive to temperature when analyzed under smaller temporal scales, under more extensive temporal analysis the connection diminishes for global lightning occurrences.

Lightning climatologies focused elsewhere in the world have also been completed in recent years, in response to newly-available and detailed lightning data availability. Burrows et al. (2002) reported that Canadian lightning flashes are concentrated most heavily in southern Alberta, southeast of Nova Scotia, and southern Ontario. Burrows and Kochtubajda (2010) concurred, concluding that Canadian lightning maxima tends to occur nearest to the U.S. border in areas where heat, moisture, and instability tend to be abundant. In a review of lightning in the tropical Western Hemisphere, Pinto et al. (2007) found that lightning flash densities vary from 19 to 65 flashes $\text{km}^{-2} \text{ year}^{-1}$. Antonescu and Burecea (2010) showed that the highest density of lightning strikes in Romania are associated with the Romanian plain convergence zone. Makela et al. (2011) found that median values of lightning density per day are similar between the U.S. and Finland, but maximum values per day are much different between the two nations. Virts et al. (2013) showed that the highest lightning frequency globally occurs over tropical Africa. Dowdy and Kuleshov (2014) found maximum lightning frequency in/near Australia over the ocean off the coast during the cooler months. In a global lightning climatology from 1995–2010 using LIS and OTD data, Cecil et al. (2014) showed that the maximum frequency of lightning activity is in central Africa, but the peak monthly average rate is during the summer (July) in Brahmaputra Valley, India. The global spatial patterns of frequencies identified by the above

studies are not static in time; Koshak et al. (2015) found an increase over the 2003–2012 period globally.

2.4 Landsat-Based LULC Change Studies

Because lightning data is to be correlated with land use, a review of recent Landsat-based LULC change is provided here. Singh (1988) defined land change analysis as:

“the process of identifying differences in the state of an object or phenomenon by observing it at different times. Essentially, it involves the ability to quantify temporal effects using multi-temporal data sets.”

Although many LULC change studies have been conducted using satellite imagery and remote sensing techniques, this discussion includes only research analyzing LULC change using Landsat data and the influence of LULC change on meteorological or climatological variables.

Landsat data consist of Earth imagery captured from various wavelength bands on the electromagnetic spectrum. Because these images are capable of capturing such a wide range of spectral signatures, they can be used to analyze a host of environmental issues, including LULC change.

Several LULC change studies have focused on inventorying derived categories of LULC in the United States. For example, an urban and regional LULC for Atlanta, Georgia, identified a slight increase in urban coverage from 1972 to 1974 (Todd, 1977). Vogelmann et al. (1998) used Landsat data to develop a LULC characterization for the Mid-Atlantic region; their results found that pesticide runoff could influence land cover change. A detailed analysis of Minnesota by Yuan et al. (2005) revealed that urban development had increased by up to 32% and natural environments had decreased by 69% from 1986 to 2002. Huang et al. (2009) found that 30 to 40% of national forest lands in the eastern U.S. have been disturbed between 1990 and 2005.

Much Landsat-based research of this type has focused on development in China. For example, Seto et al. (2002) used an image pixel change technique to illustrate the relationship between economic growth and LULC in the Pearl River Delta between 1988 and 1996. Similarly, Zhang et al. (2002) employed two images – one from 1984 and the other from 1997 – to determine LULC in Beijing by calculating spectral differences using three different methods, with results showing that changes in structural buildup are more noticeable using the image differencing technique. Complementary work in China by Liu et al. (2005) revealed the rate of change from cropland to urban development from 1990 to 2000, with the newly-claimed cropland less productive than the former cropland. This work was corroborated by Fan et al. (2007), who found a rapid decrease in cropland in Guangzhou from 1977 to 2007.

LULC change studies abound for other parts of the world too. For example, Lyon et al. (1998) showed using Landsat imagery for Chiapas, Mexico, that vegetation indices are affected by the type of statistical calculation used to ascertain the differences in land use, but the normalized difference vegetation index proved to be the most accurate. Cardille and Foley (2003) used integrated Landsat imagery along with census data to identify the rapid increase in agricultural land use in Brazil from 1980 to 1995. Shalaby and Tateishi (2007) showed that tourist-focused development caused vegetation degradation, water logging, and urban development in northeastern Egypt from 1987 to 2001. Dewan and Yamaguchi (2009) found that between 1975 and 2003 much of the green space and bodies of water in Greater Dhaka, Bangladesh, had been replaced with human-made structures. By using land surface temperature to calculate the total amount of land change in Malaysia from 1999–2007, Tan et al. (2010) found that urban area increased substantially, grassland area increased moderately, and barren and forest area decreased (Tan et al., 2010).

Environmental impacts of development have become a ubiquitous concern in recent decades, with a number of studies using Landsat data to highlight connections between land modification and the environmental change created by it. For example, Kalnay and Cai (2003) found that a drastic reduction in diurnal temperature range accompanied urbanization globally. Tang et al. (2005) found that an increase in urbanization would subsequently lead to an increase in runoff of harmful chemicals into the Muskegon River watershed in Michigan. Scanlon et al. (2005) suggested that urban development reduces the amount of moisture in the soil. Seneviratne et al. (2006) showed that an increase in climatic variability in Europe would place a greater stress on moisture availability in soil – which in turn would be increasingly limited should urban expansion continue. Chen et al. (2006) determined that urban heat island patterns were scattered among the land types in the Pearl River Delta of China, with developed areas (concrete) and bare land being the warmest. Fortunately, even the long-problematic constraint of cloud cover in Landsat based studies was found to be of only minor concern in such LULC change studies, since these typically only require one cloud-free image per year (Ju and Roy, 2008).

2.5 Land Change Influences on Lightning

Despite the abundance of literature on lightning climatology and use of Landsat imagery for environmental change analysis, there remains a gap in the literature on the overlap of these two important topics. This section will focus on explaining how changes to atmospheric particulate flux, often derived from LULC, near developed areas may influence lightning, as well as how urban environments can perturb the typical lightning behaviors.

Urban areas are well-known to increase the frequency and intensity of thunderstorms (Ashley et al., 2012; Harberlie et al., 2015). Urban influences on lightning flash frequency could occur due to increases in atmospheric particulates, enhanced convection, or a greater availability

of attractive objects. In an analysis of lightning patterns around 16 major U.S. cities from 1989–1992, Westcott (1995) found that areas downwind and over cities experienced a 40-80% increase in lightning activity over adjacent environs. Naccaroto et al. (2003) found a 60–100% enhancement in CG lightning over urban areas in Brazil, with this increase attributed to enhanced heat output from urban surfaces. Bentley and Stallins (2005) found that in Atlanta, Georgia, July is the most active lightning month, and that each season has its own predominant synoptic conditions for producing lightning when coupled with urban enhancement. In a follow-up study by Stallins and Bentley (2006), the northeast quadrant of Atlanta was found to support the most lightning, with the enhancement attributed to increased urban-induced instability.

While high-quality work on the relationship between LULC change and environmental factors has been conducted, more work is needed to for a more complete understanding. In the next chapter, data and methods of how this thesis will explore the relationship between LULC change and lightning flash patterns will be completed.

Chapter 3. Data and Methods

“The goal is to turn data into information, and information into insight.”

— Carly Fiorina

Data that will be used for addressing the research objectives described in Chapter 1 consist of NOAA’s gridded lightning data from 1995 to 2011, and National Aeronautics and Space Administration’s (NASA’s) Geostationary Operational Environmental Satellite (GOES) Landsat 4–5 imagery from 1996 to 2010. Methods that are to be implemented on these data sets include a descriptive statistical analysis of lightning frequencies, One-way Analysis of Variance (ANOVA) and Scheffé’s 95% confidence interval (Scheffé, 1959) test to determine differences between lightning frequency for each LULC and annual lightning count dataset, linear regression with a categorical variable (James et al., 2013), and geographically weighted regression (GWR; Fotheringham, 2002). This chapter will describe how these data sets and procedures will be manipulated and how they work. In addition, handling of the data prior to analysis will also be explained.

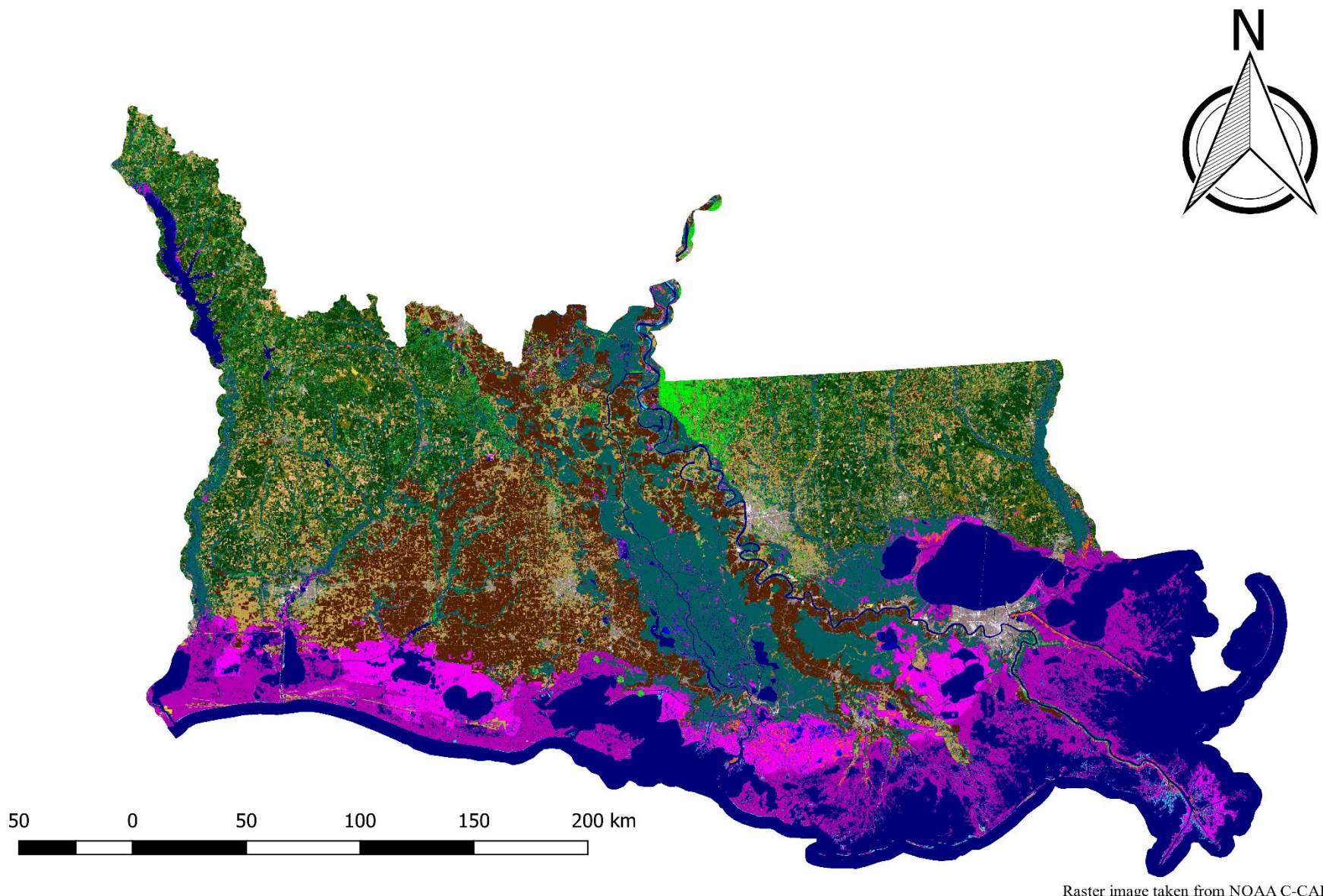
3.1 Landsat Imagery

The United States Geological Survey (USGS) provides Landsat 4–5 (L4 and L5) data from 1982 to 2012 through its EarthExplorer portal. Landsat 4–5 images were captured using the Landsat 4 and 5 satellites, respectively. Aside from a communications update on the L5 satellite, there are no differences between L4 and L5 bands. The sensors aboard the two satellites are a multispectral scanner (MSS) and thematic mapper (TM). MSS Images from L4 and L5 comprise four spectral bands: Band 4 Visible (0.5 to 6 μm), Band 5 Visible (0.6 to 0.7 μm), Band 6 Near-Infrared (0.7 to 0.8 μm), and Band 7 Near-Infrared (0.8 to 1.1 μm), all with pixel sizes of 57 x 79 m. TM images from L4 and L5 include seven spectral bands: Band 1 Visible (0.45 to 0.52 μm),

Band 2 Visible (0.52 to 0.60 μm), Band 3 Visible (0.63 to 0.69 μm), Band 4 Near-Infrared (0.76 to 0.90 μm), Band 5 Near-Infrared (1.55 to 1.75 μm), Band 6 Thermal (10.40 to 12.50 μm) and Band 7 Mid-Infrared (2.08 to 2.35 μm) – TM pixel sizes are 30 m x 30 m for all bands except for the thermal band, which has a 120 m x 120 m pixel size. Total scene size of images is 170 km x 185 km.

L4-5 data are utilized because of the generally high quality and because the access to imagery matches the temporal period of the project. While L7 and L8 both provide accurate data sets, their temporal periods are limited, in comparison with L4–5, because they were launched in 1999 and 2013, respectively. While change analysis on the imagery available from these sensors would be possible, it would not match with the temporal period of the gridded lightning data set used in this study.

NOAA Coastal Change Analysis Program (C-CAP) provides LULC change data for coastal locations using Landsat imagery, including data for 1996 (Figure 3.1), 2001 (Figure 3.2), 2006 (Figure 3.3), and 2010 (Figure 3.4). These years of data were selected for use instead of a manual land classification due to the amount of quality control from a reputable source and the adequate spatial coverage of the data. Because land classification can be a monotonous process prone to error, utilizing data that are considered high quality by NOAA will minimize concern of erroneous pixel classification. Due to the extensive number of LULC types, the color corresponding to each in Figures 3.1–3.4 is shown in Table 3.1.



Raster image taken from NOAA C-CAP

Figure 3.1 Raw image of 1996 NOAA Coastal Change Analysis Program (C-CAP) Louisiana LULC classification.

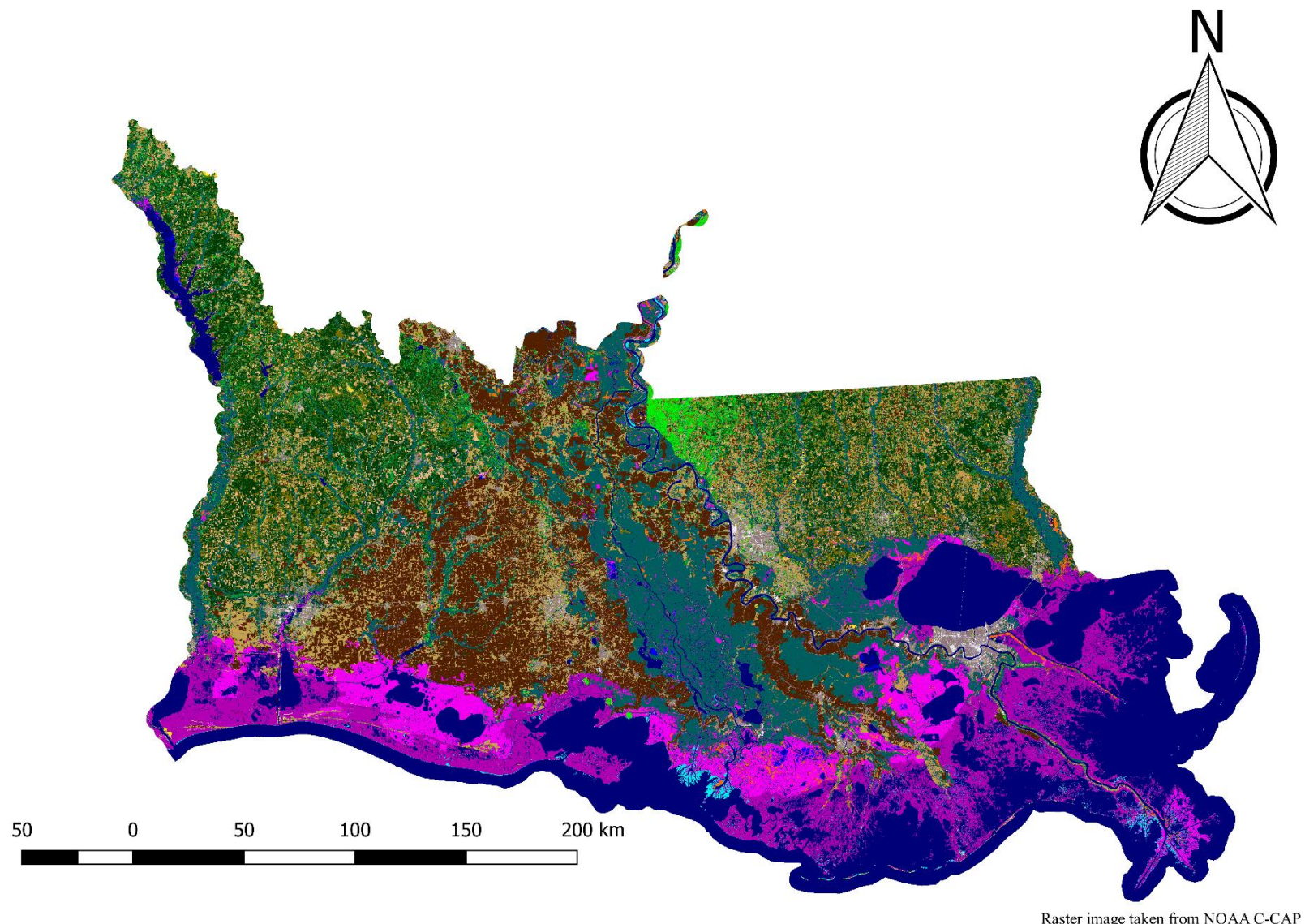


Figure 3.2 As in Figure 3.1, but for 2001.

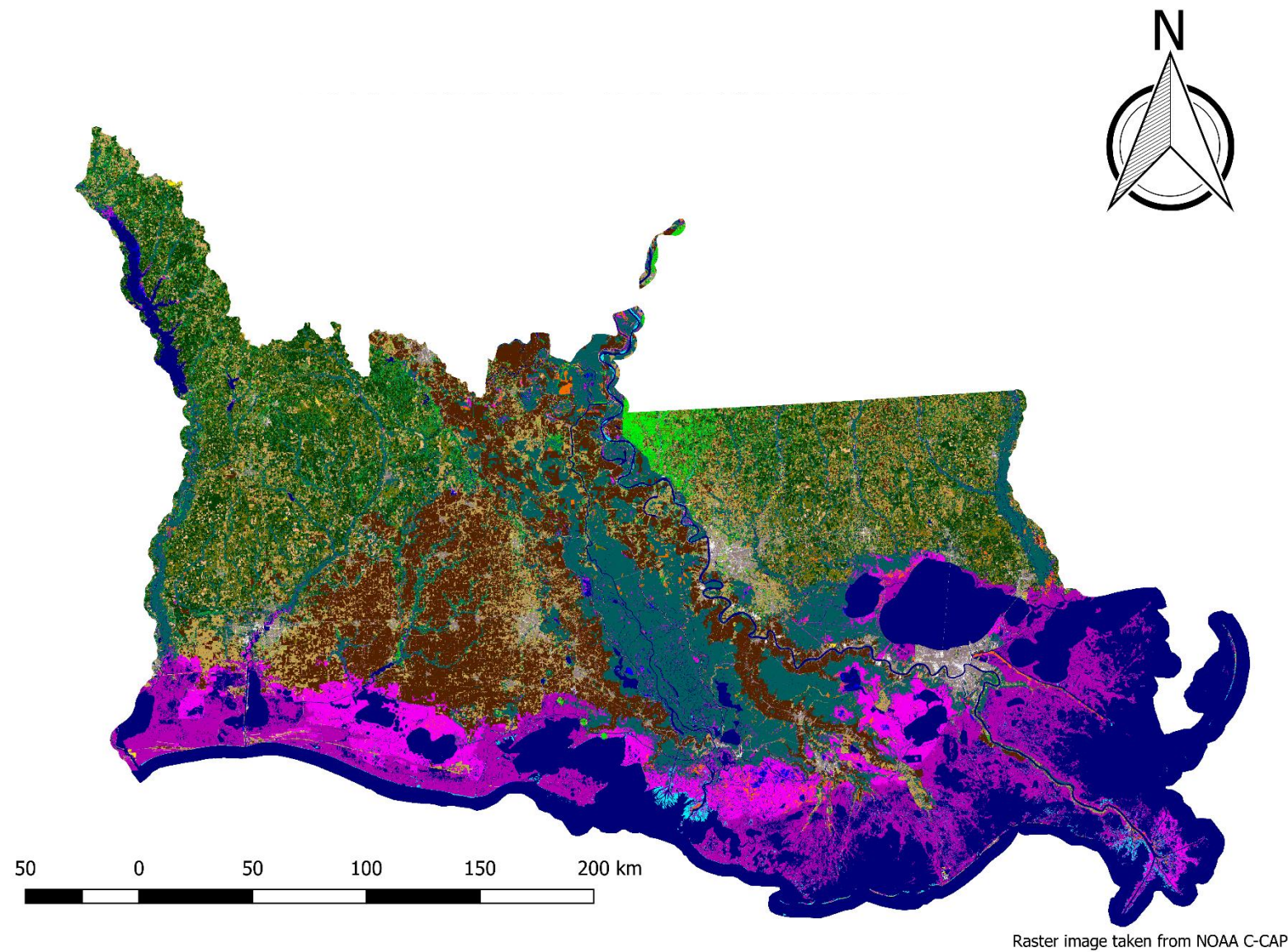


Figure 3.3 As in Figure 3.1, but for 2006.

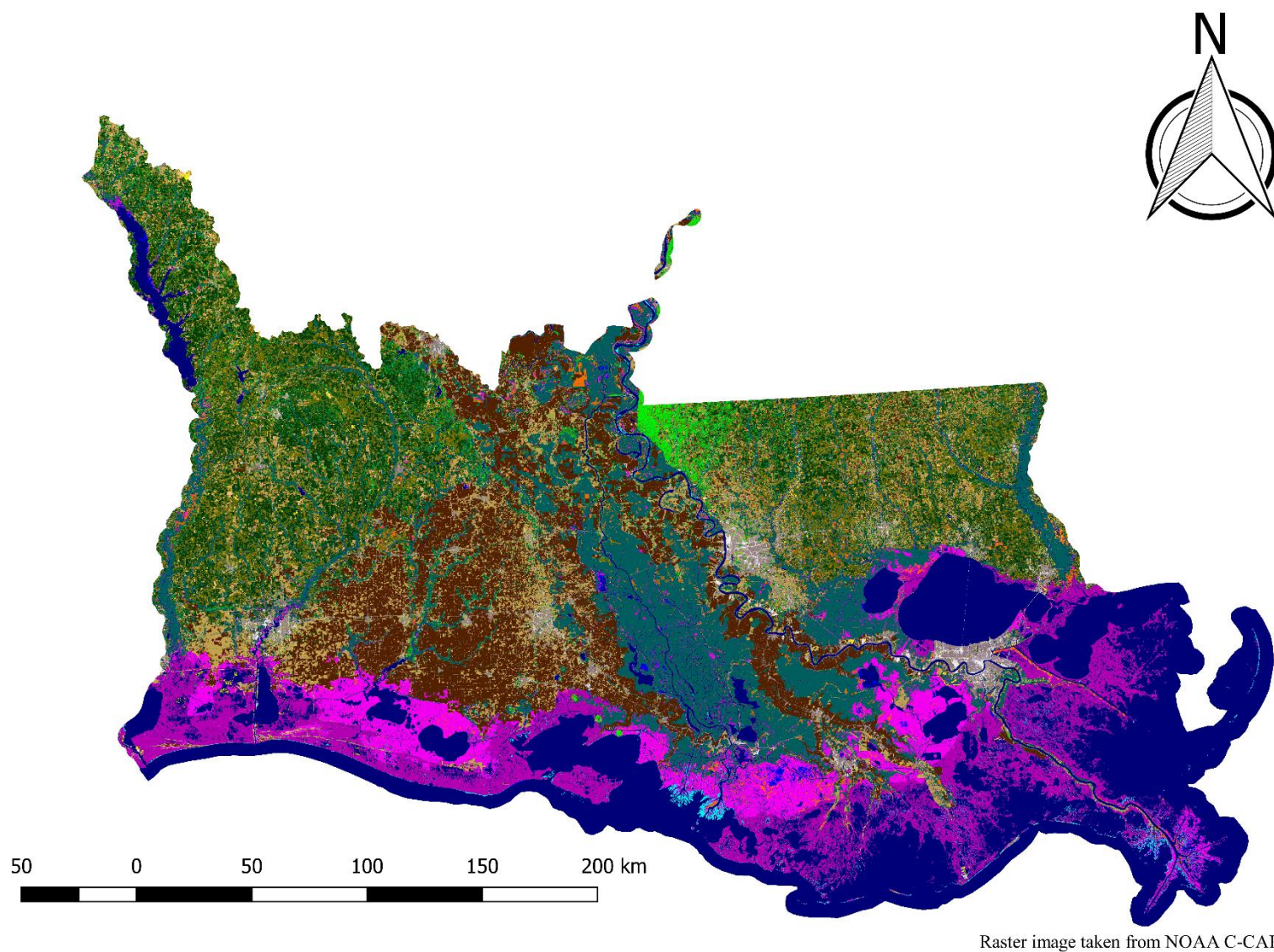


Figure 3.4 As in Figure 3.1, but for 2010.

Table 3.1 Colors representing each LULC type within the classification image maps.

Land Classification Types

	Background
	Unclassified
	Developed, High Intensity
	Developed, Medium Intensity
	Developed, Low Intensity
	Developed, Open Space
	Cultivated Crops
	Pasture/Hay
	Grassland/Herbaceous
	Deciduous Forest
	Evergreen Forest
	Mixed Forest
	Scrub/Shrub
	Palustrine Forested Wetland
	Palustrine Scrub/Shrub Wetland
	Palustrine Emergent Wetland
	Estuarine Forested Wetland
	Estuarine Scrub/Shrub Wetland
	Estuarine Emergent Wetland
	Unconsolidated Shore
	Bare Land
	Open Water
	Palustrine Aquatic Bed
	Estuarine Aquatic Bed

Data handling complications for these images are minimal. Since NOAA's team of remote sensing scientists has already completed classification as well as latitude and longitude adjustment, data correction required only a majority resampling interpolation technique. The purpose was to match the cell sizes and locations to the lightning dataset (Figures 3.5–3.8). Majority resampling works by recalculating the average value of a 2 x 2 cell of the input raster based on the majority value within that cell (Esri, 2016). This type of transformation is preferred for transformations of LULC data because no new values are calculated, but the majority are maintained. Means of land classes per year are provided as well (Figure 3.9).

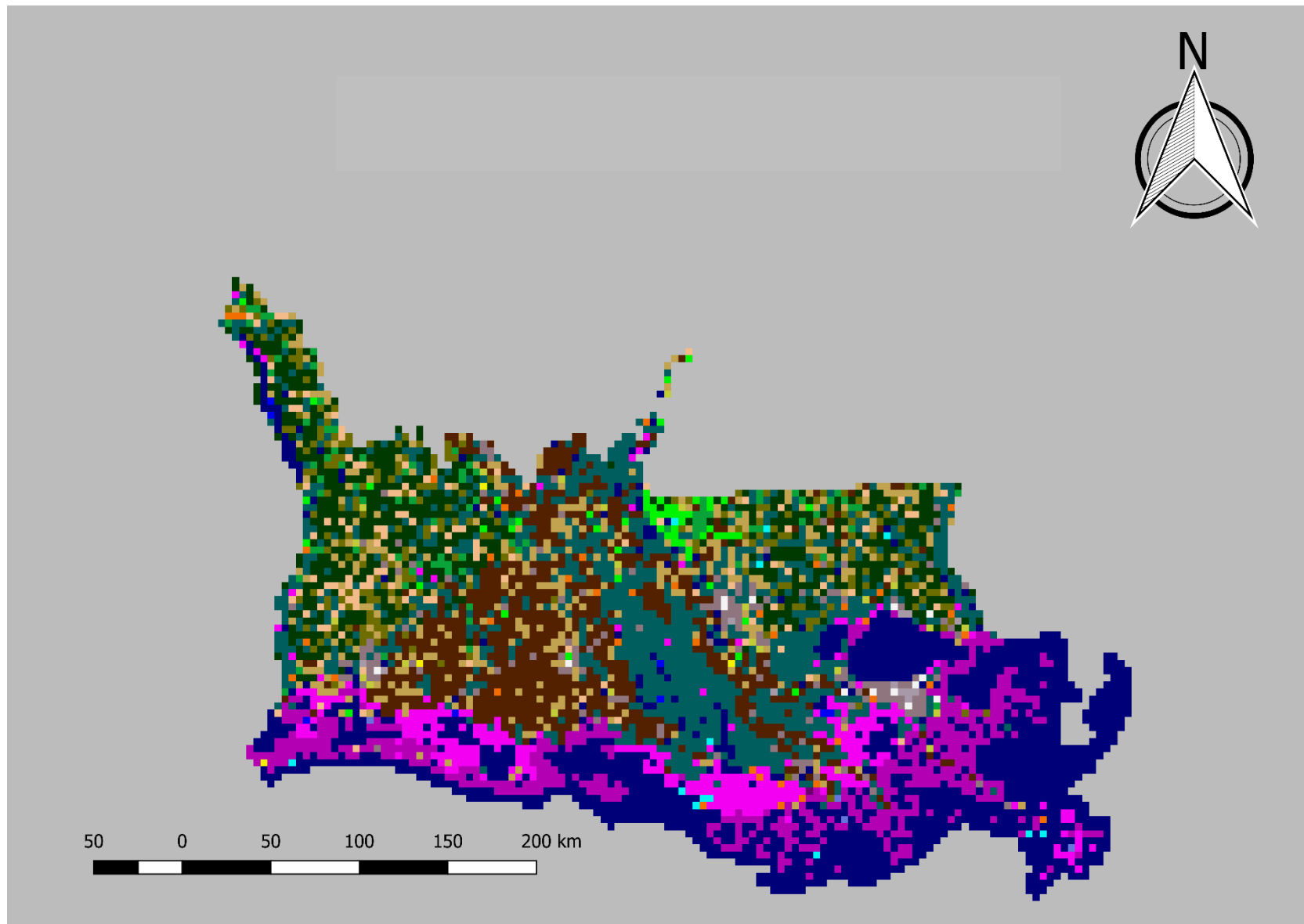


Figure 3.5 Majority resampled 1996 Louisiana LULC map.

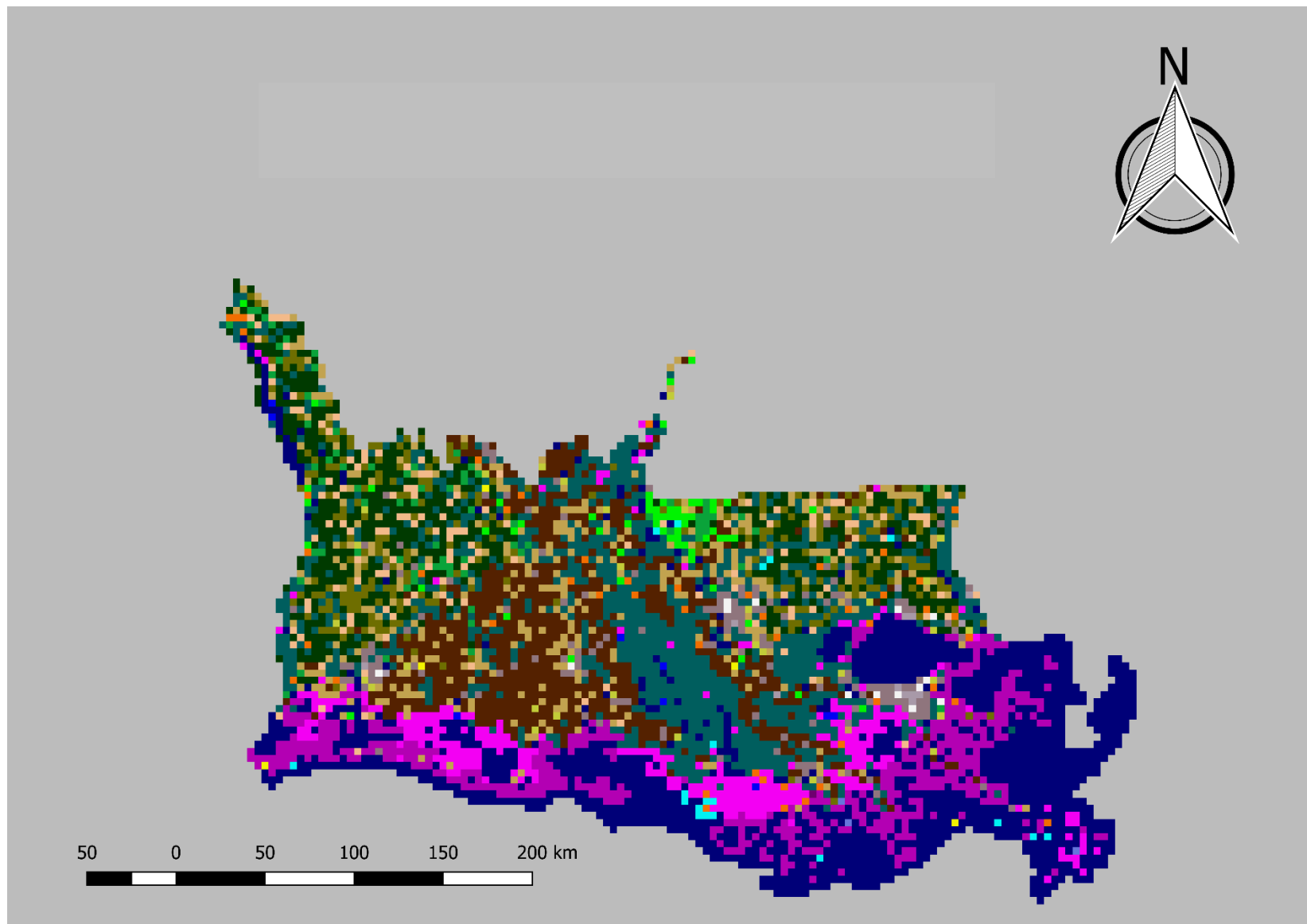


Figure 3.6 As in Figure 3.5, but for 2001.

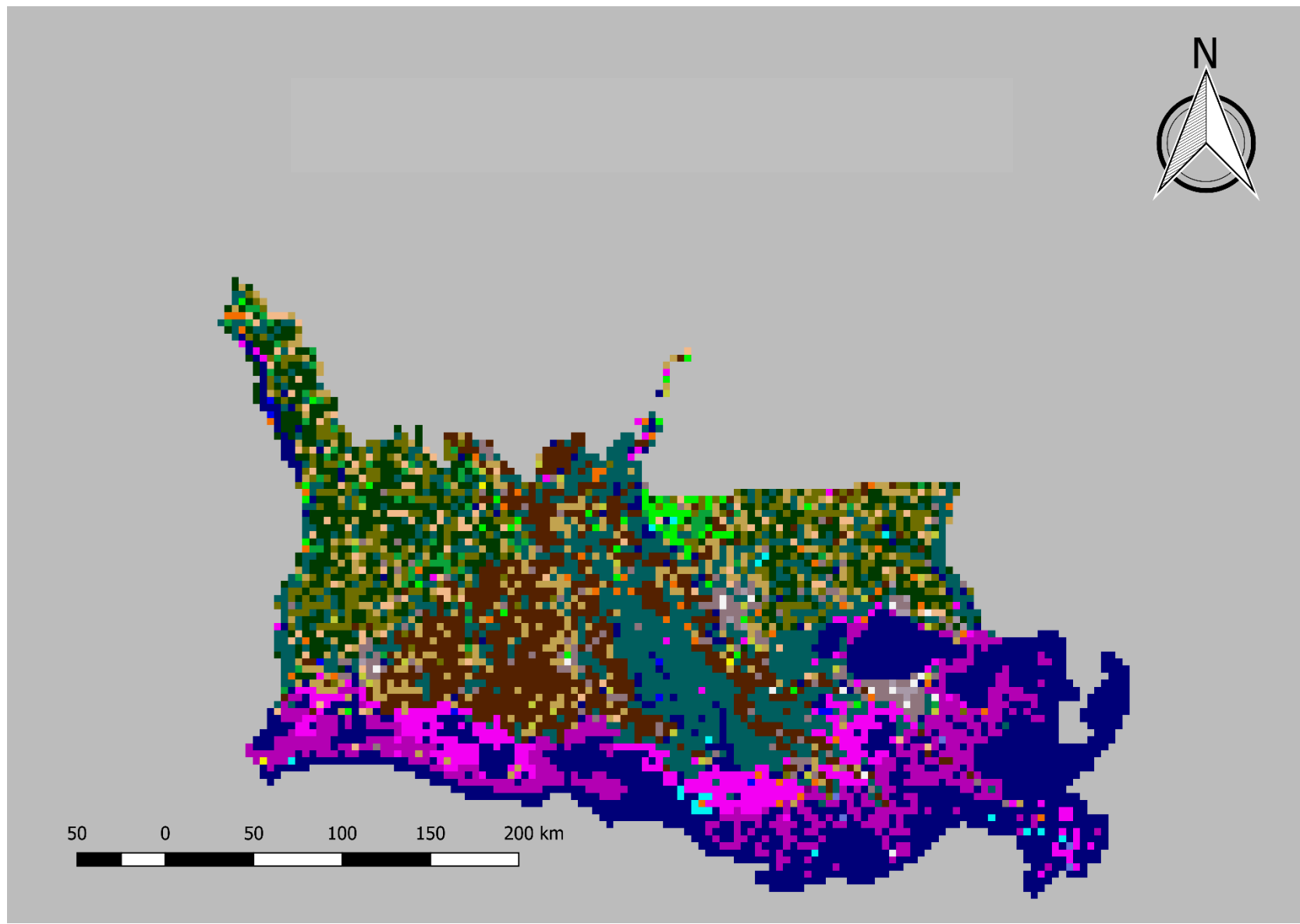


Figure 3.7 As in Figure 3.5, but for 2006.

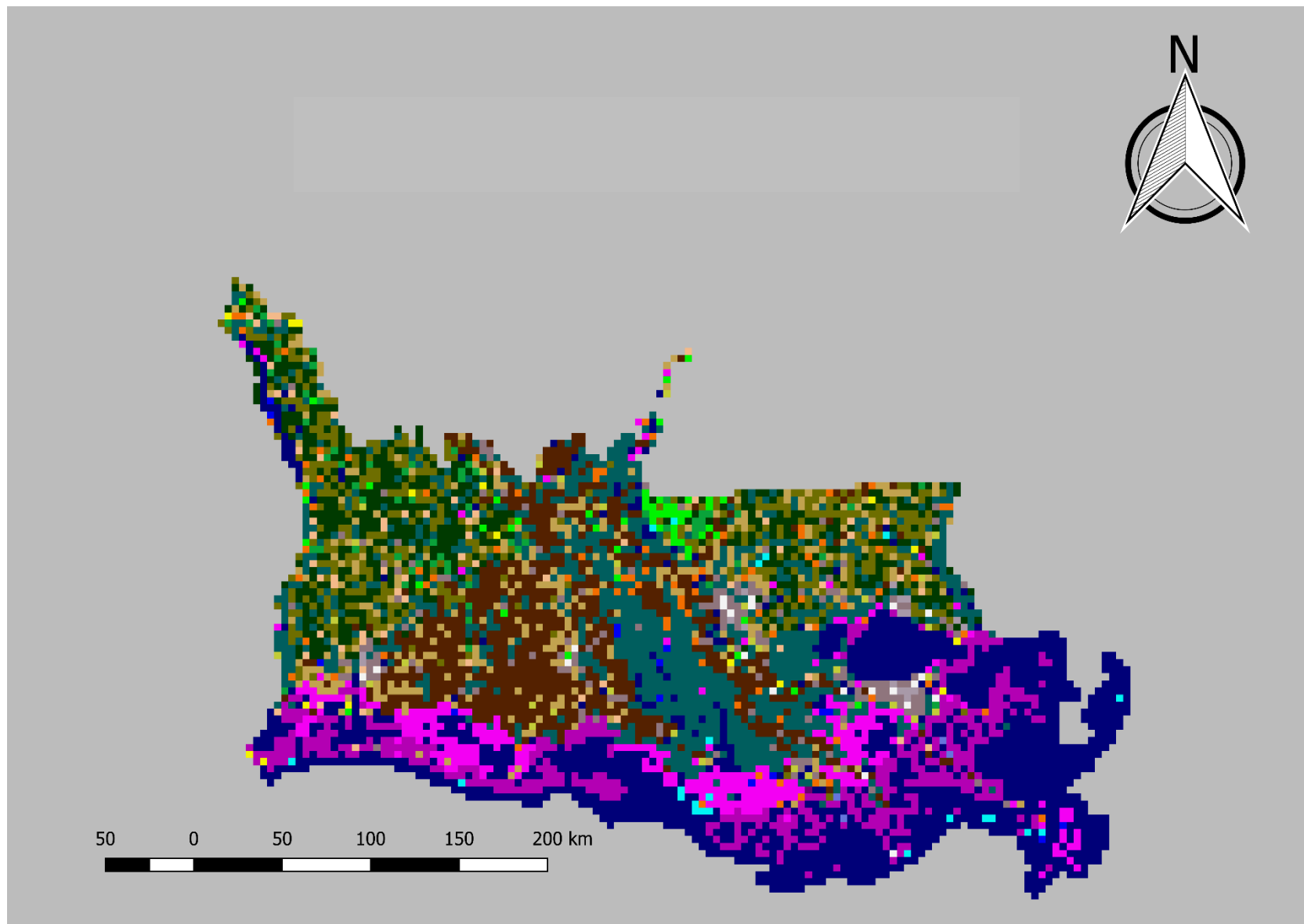


Figure 3.8 As in Figure 3.5, but for 2010.

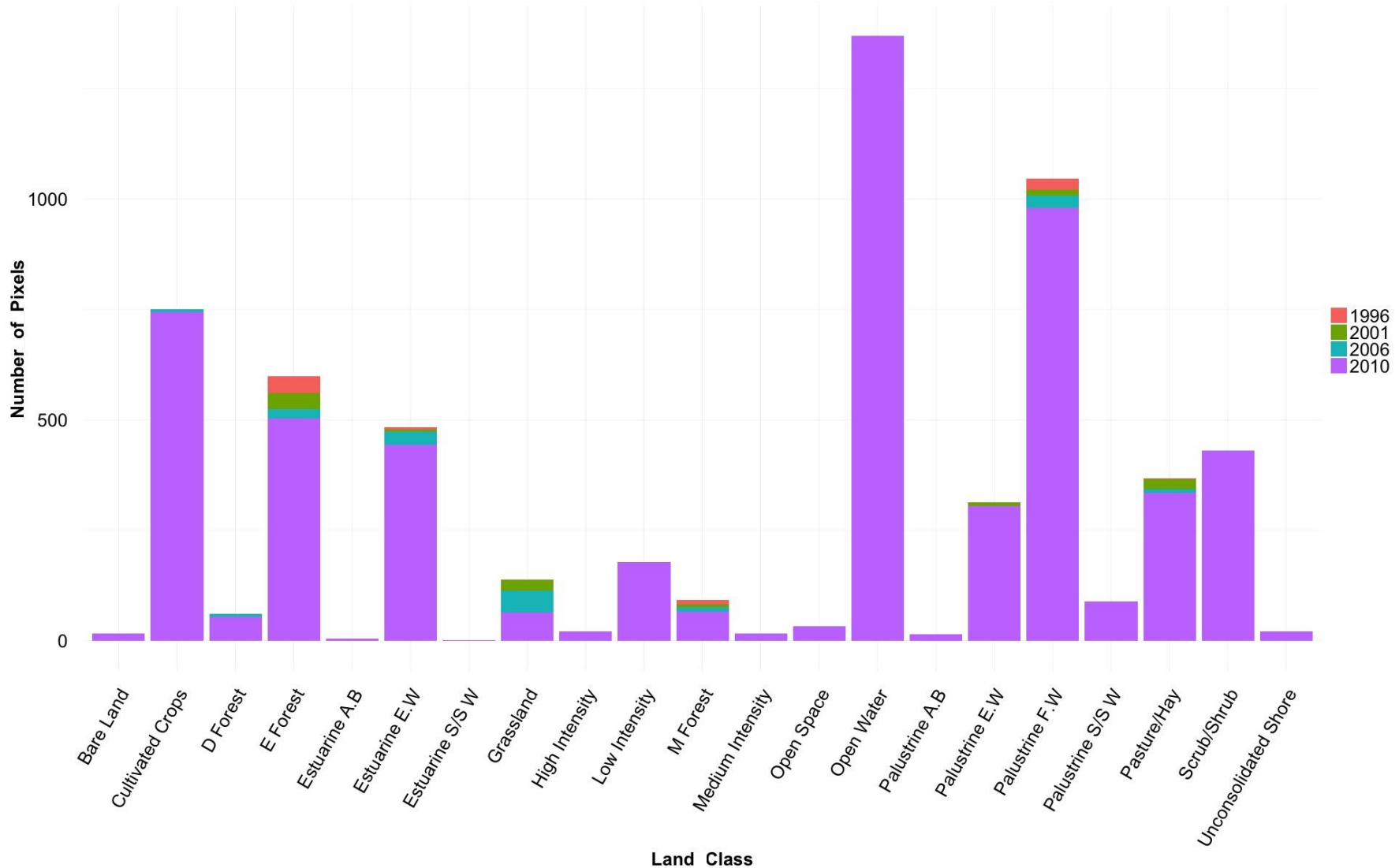


Figure 3.9 LULC totals for the years 1996, 2001, 2006, and 2010. Each line represents a year of the total four periods studied.

After completion of the resampling, and after the data have been imported into the R programming language, the background and unclassified classes are removed to eliminate software error messages from calculation non-applicable values.

3.2 NOAA/Vaisala NLDN Lightning Data

NOAA provides CG lightning data from 1986 to 2013 through its National Centers for Environmental Information (NCEI) web portal. For this project, data from 1995 to 2011 are analyzed, so as to overlap with the temporal period of available data in the NOAA C-CAP data set. The data are provided to NOAA through a contract with Vaisala Inc.'s NLDN (Figure 3.10). These data come with their own coordinate reference system, which displays coordinates in meters instead of latitude/longitude. An adjustment of this projection was made, so that the lightning data projection matches the LULC classification data.

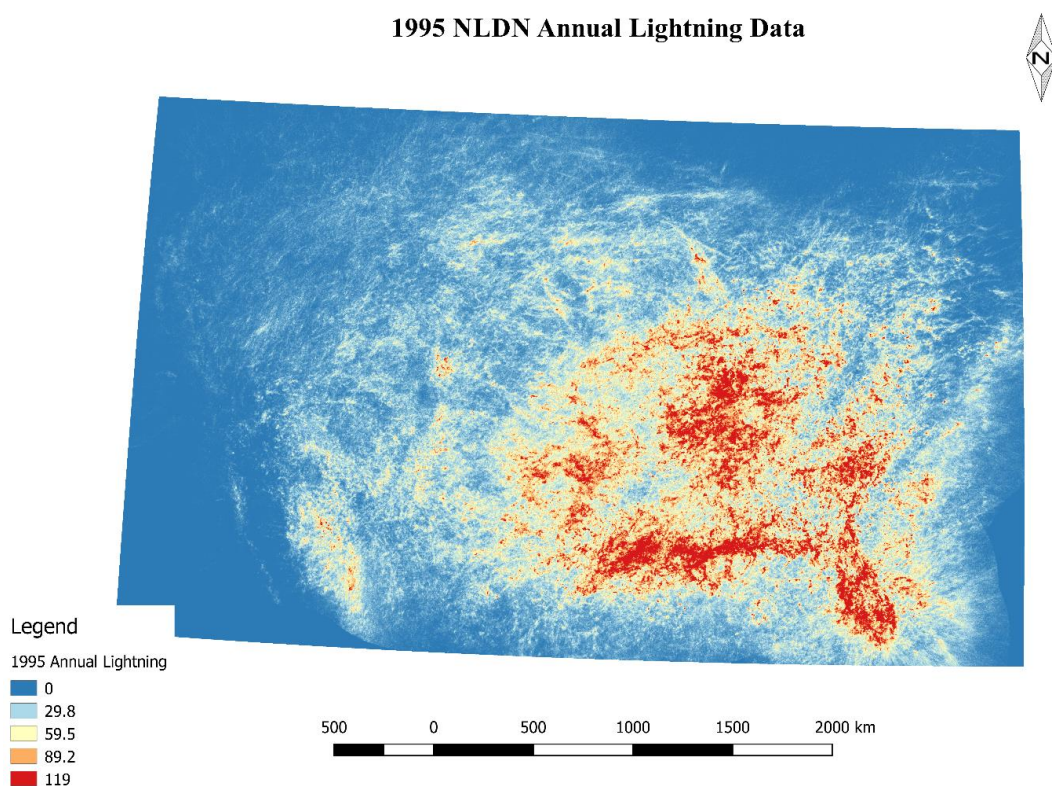


Figure 3.10 A sample of the lightning data over the U.S. observed by the NLDN and distributed by NOAA for the year 1995.

Because raw data are not available for open distribution to the public, NOAA makes derived products that can be disseminated. These products include daily tile summaries, daily, county and state counts for the continental U.S., and 4 km x 4 km Albers Equal Area gridded summaries, which are distributed in frequency by hour per month, by hour per year, by day, by month, and by year. In addition, NOAA's lightning products also consist of a positive polarity only database. Albers Equal Area was the map projection selected because of the importance of preserving area in any display of spatial density of lightning strikes.

Frequency per month and per year data are utilized for addressing Research Objective 1 ("Analyze the spatio-temporal distribution of cloud-to-ground lightning in the northern Gulf Coast region"). Data sets such as the satellite-based LIS/OTD have far too much noise for such an analysis, because it detects intra-cloud, cloud-to-cloud, and cloud-to-air lightning flashes. This would misconstrue the sample and introduce bias to the study, because non-CG flashes are presumably not as directly related to LULC. Therefore, only CG data are used.

The cost of acquiring data from the NLDN directly has largely confined the examination of the accuracy of the NOAA database to Vaisala employees themselves. Vaisala associated scientist Kenneth Cummins confirmed that the NLDN was the most accurate of all lightning location systems in 2009 and would rapidly improve its accuracy in the coming years (Cummins and Murphy, 2009). Soon afterwards, scientists affiliated with Vaisala revealed accuracy ranges of their network between 90–95% in the U.S. and 86–92% for the entire globe, with little variation at night (Demetriades et al., 2010; Cramer and Cummins, 2014).

Data manipulation requirements are minimal. Because this database is a derived product, most errors have already been corrected. The first step was importing the netCDF into QGIS and implementing a projection change from Albers to the projection of the LULC change data used in this project, which is Albers Conformal Conic, which does not affect the frequency of the data at all. The second step was completing a “raster align” in QGIS, which is equivalent to the raster registration tool in ArcMap. This procedure allows the cells of the lightning data to be superimposed on the cells of the LULC classification data. The raster align function in QGIS also clips the portion of data from the entire file so that analysis of data can be restricted to the intended region. A sample of the extracted data is provided for the northern Gulf Coast (Figure 3.11). Lastly, all files were exported as GRID files, which maintains their values in a geocoded format.

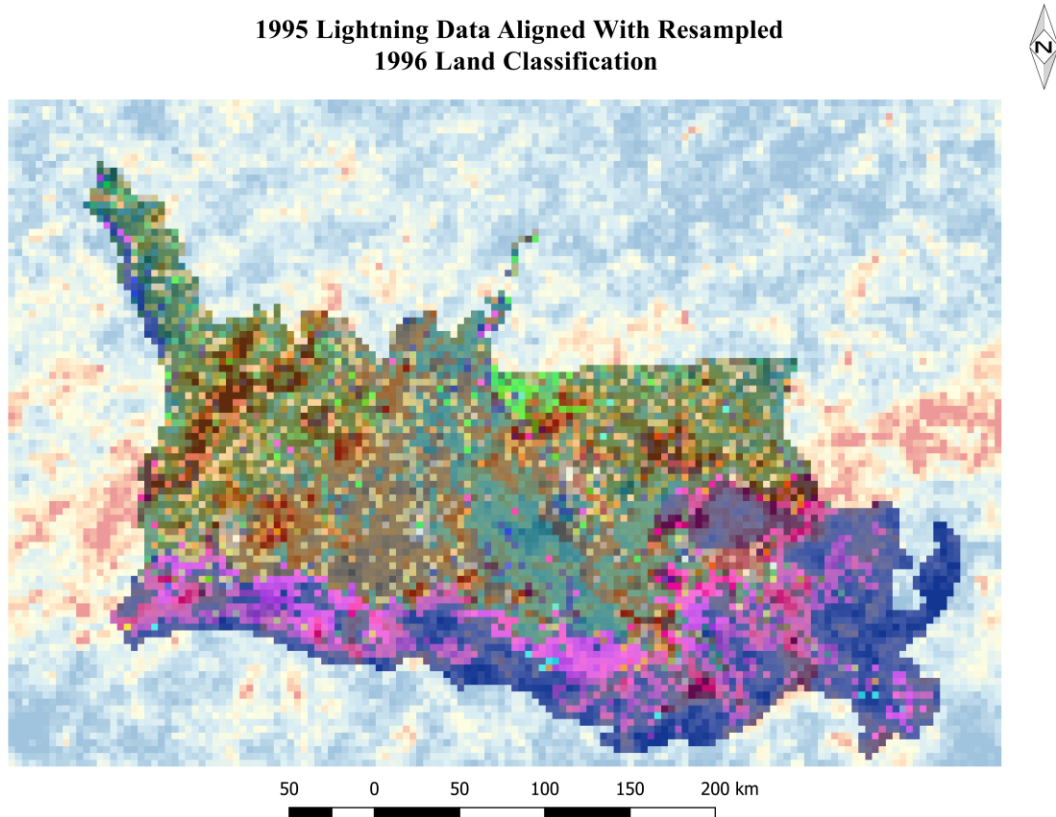


Figure 3.11 Aligned lightning data from the NLDN/NOAA overlaid on the 1995 resampled LULC map.

3.3 Lightning Climatology

Data for histograms are collected by importing the data into R statistical programming software. Once each NetCDF file of gridded lightning data has been imported, annual totals are compiled and reported as a bar graph, with an overlaying trend line. The presence of anomalies will inform further analysis.

3.4 Linear Regression with a Categorical Variable

Linear regression (James et al., 2013) is a statistical test used to assess the relationship between two variables. The assumptions for linear regression are independence of the variables, homoscedasticity (variance around the regression line is the same for all values), no or little multicollinearity (independent variables are not related), and normality (variables are distributed in a bell shape over time). A linear regression with a categorical variable simply takes a dependent variable and tests it among factors – or LULC in this case.

3.5 One-way Analysis of Variance and Scheffé’s 95% Simultaneous Confidence Interval Test

One-way ANOVA is a statistical method that tests for a difference between means among sample sets of two or more variables. Specifically, it determines whether any differences amongst the means exist between two or more samples. Any significant difference of means between two or more variables are indicated by a small enough p-value for the ANOVA (generally > 0.05) that allows one to reject the null hypothesis of no significant differences of mean between any of the sampled variables. The assumptions for ANOVA are identical to that of a linear regression test. As such, ANOVA is an appropriate inferential statistical method for analyzing differences between data sets, and influences of extraneous variables on other various

variables within a data set. It offers the advantage over t-tests of providing comparisons of the mean from multiple variables, taken two at a time, simultaneously. This minimizes the possibility of committing a type I error (Freund et al., 2010) as compared to conducting multiple t-tests. The equation for ANOVA is as follows:

$$F = \frac{MST}{MSE}$$

where F is the ANOVA coefficient, MST is the mean sum of squares due to treatment, and MSE is the mean sum of squares due to error.

ANOVA will be employed with the LULC classification type being the treatment variable; gridded lightning frequencies represent the cases for which the mean is calculated and tested for difference against the mean of the other LULC types. Because the study area is relatively small, differences in synoptic patterns conducive to lightning are assumed to be negligible. This analysis will show whether differences exist between groups, and, with further information on how LULC changes have occurred over time, could give an improved explanation for changes in lightning totals over the total period of record. ANOVA is easily executed in R, QGIS, and ArcGIS through add-on modules and packages.

If ANOVA results suggest significant differences in lightning frequency by LULC type (i.e., a rejection of the null hypothesis), Scheffé's 95% Simultaneous Confidence Interval Test (Scheffé, 1959) will be conducted to determine which LULC types differ statistically significantly from which others.

3.6 Geographically Weighted Regression

A GWR (Fotheringham, 2002) and one-way ANOVA test will be completed to address Research Objective 2 (“Investigate the influence of LULC types and land change on lightning frequency and patterns over the northern Gulf Coast region”) by determining the extent to which LULC is associated with lightning patterns over Louisiana. GWR is a geospatial method of determining the change in relationship across time and space between two spatially similar values. In contrast to linear regression, GWR considers spatial bounds as a means of weighting the relationship. GWR is represented by the following equation:

$$Y_i = \mathbf{X}_i^t \beta(u_i, v_i) + \varepsilon_i = \beta_0(u_i, v_i) + \sum_{k=1}^p X_{ik} \beta_k(u_i, v_i) + \varepsilon_i$$

where $\beta(u_i, v_i)$ indicates the vector of the location-specific parameter estimates, (u_i, v_i) represents the geographic coordinates of location i in space, and ε_i is the error term with mean zero and common variance σ^2 (GEOPOPSCI, 2016). The assumptions for GWR are the same as linear regression or ordinary least squares regression (Fotheringham, 2002). Specifically, the data must be normally distributed, have no multicollinearity, be homoscedastic, and have random variance for all independent and dependent variables (Fotheringham, 2002).

GWR will provide evidence regarding whether local LULC changes are associated with lightning frequency. Potential pitfalls of GWR are location bias and the inability to detect anomalous LULC-related climatic patterns that could lead to a sudden shift in lightning patterns. GWR is easily executable in R, QGIS, and ArcGIS through add-on modules and packages. First, however, an amalgamated lightning raster and the classification rasters must be converted to point shapefiles in ArcMap. This is because GWR only accepts point data for analysis and must be given specified coordinate boundaries. Once this step is completed using the raster-to-point

tool in ArcMap, each LULC file and lightning file are conjoined to be analyzed by the GWR tool in ArcMap.

Chapter 4 will describe and interpret the results of these methods.

Chapter 4. Results

“Insanity: doing the same thing over and over again and expecting different results.”

– Albert Einstein

4.1 Lightning Climatology

Figures 4.1–4.17 depict histograms showing the number of pixels experiencing various ranges of a lightning flash annually, in the region bounded by 32.76281°N, -88.0726°W, 28.55081°N, and -94.8024°W, from 1995 to 2011. Figures 4.1 – 4.17 suggest that in most years most pixels report between 80 and 100 CG flashes, which means that most areas in the Gulf Coastal region experience a high frequency of CG lightning per year $5\text{-}6 \text{ km}^{-2}\text{yr}^{-1}$. Relatively lower amounts of flashes occur in 2000, 2007, 2010, and 2011, when lightning was placed in lower count brackets within the histograms. The 2002 through 2005 period experienced the highest lightning frequencies of pixels with 31 flashes per $\text{km}^{-2}\text{yr}^{-1}$. In addition, these years also had pixels with more than 500 CG flashes for the year. Based on the maps provided with the histograms, it is apparent that the highest lightning frequencies tend to occur along the southeastern southcentral portion of the study area near the Louisiana and Mississippi coast.

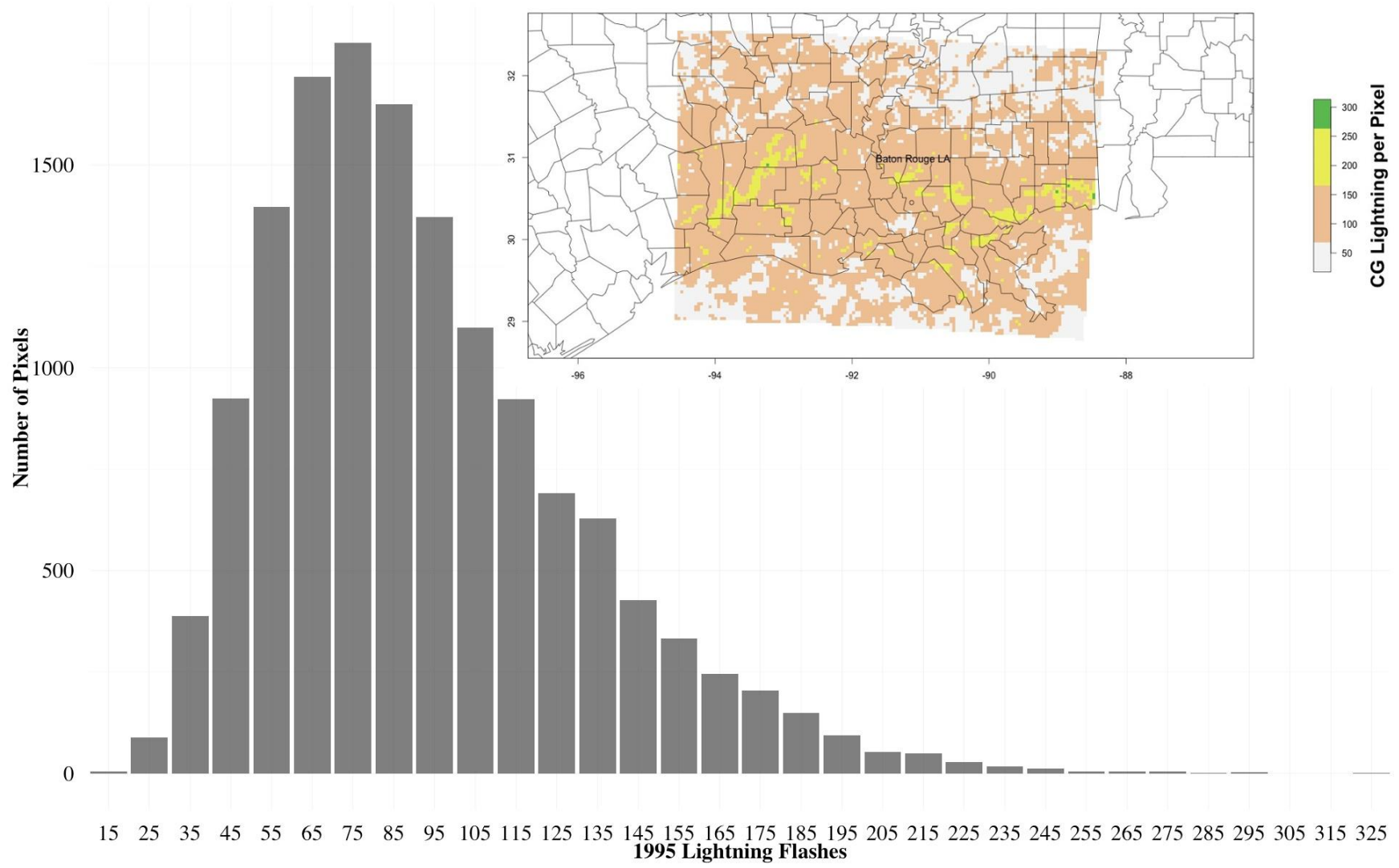


Figure 4.1 Histogram showing number of pixels with 1995 CG lightning frequency ranges at the midpoint shown (i.e., 0–20, 21–30, 31–40, etc.), across the northern Gulf Coast, with mapped frequencies shown in the inset.

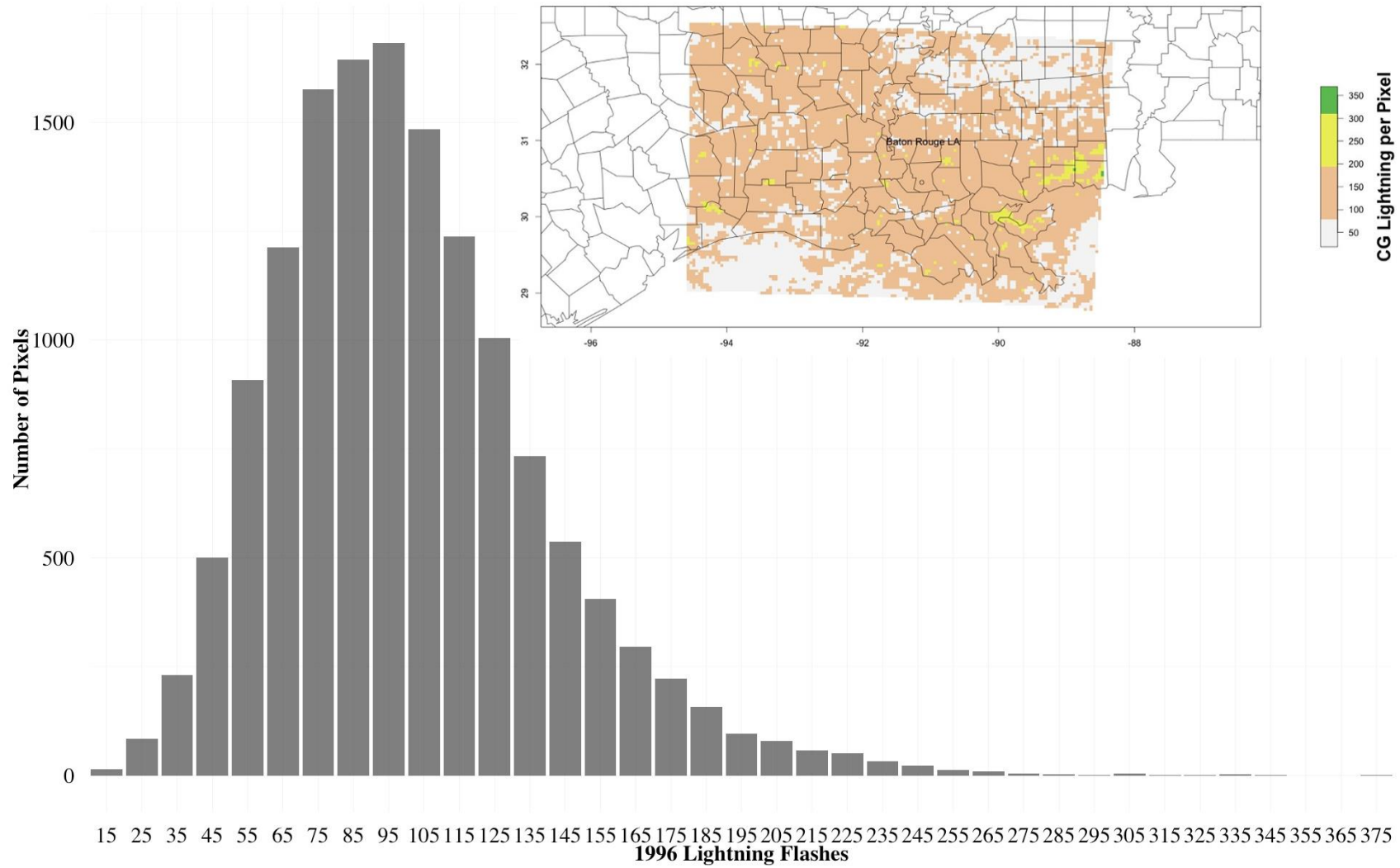


Figure 4.2 As in Figure 4.1, but for 1996.

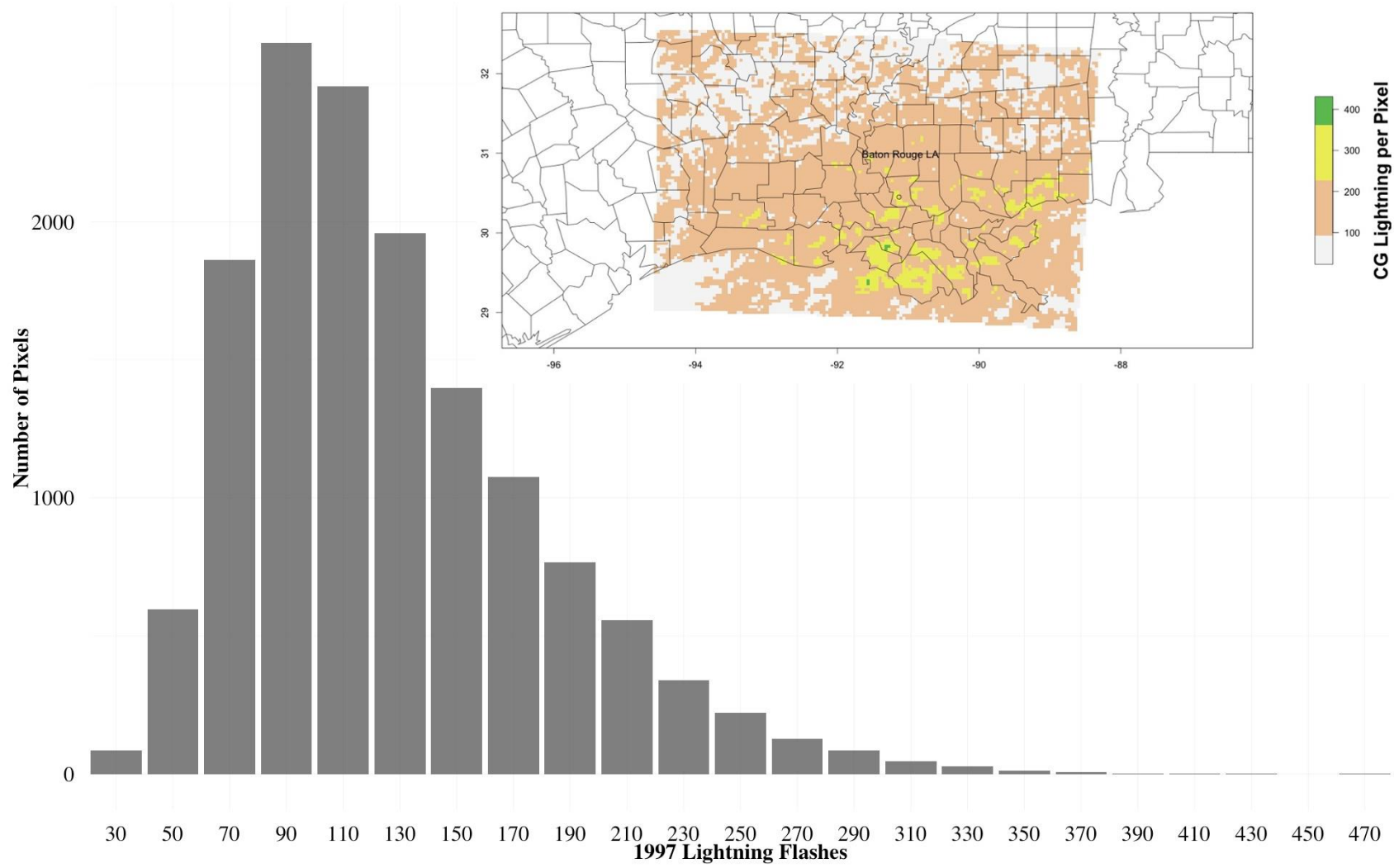


Figure 4.3 As in Figure 4.1, but for 1997.

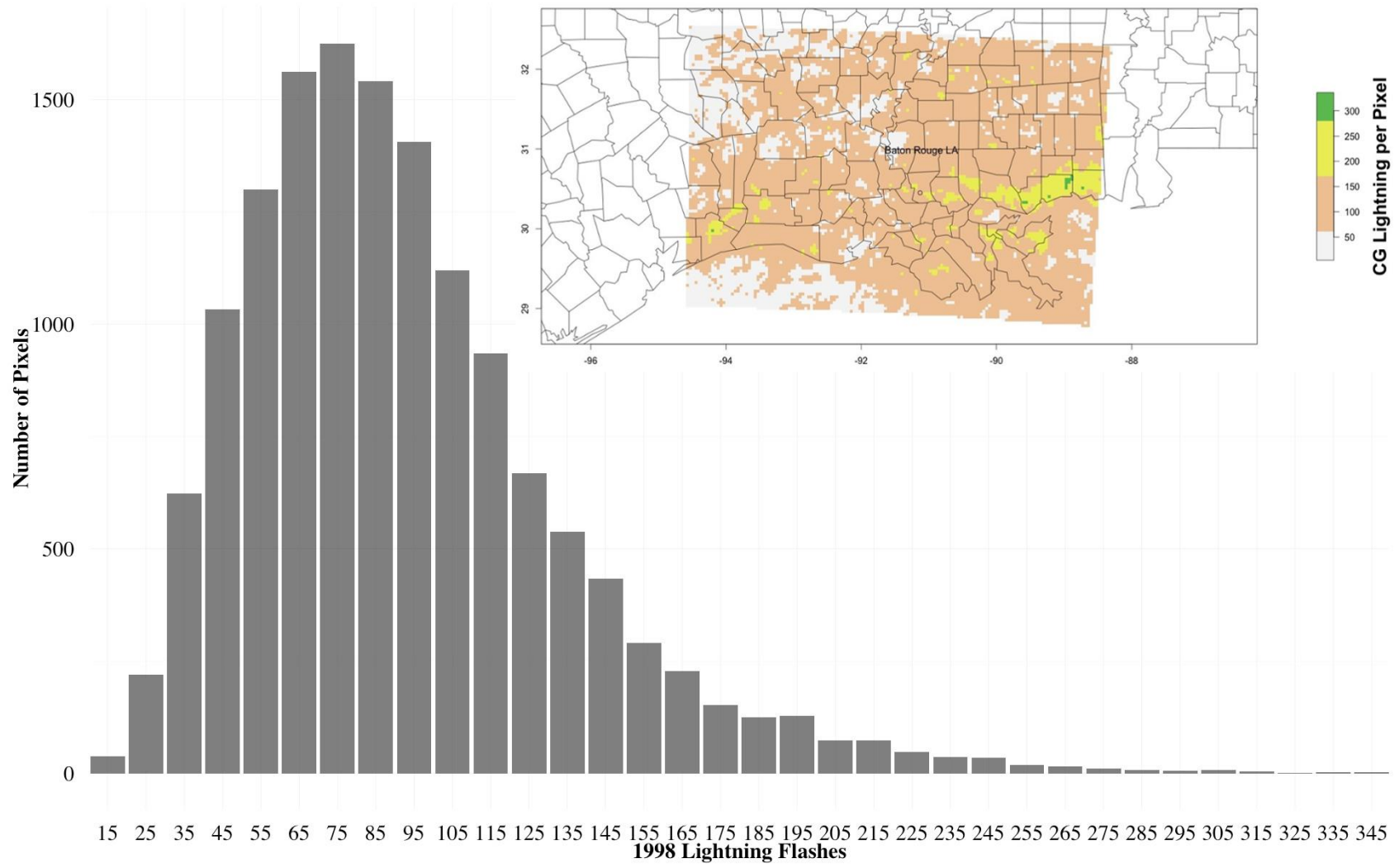


Figure 4.4 As in Figure 4.1, but for 1998.

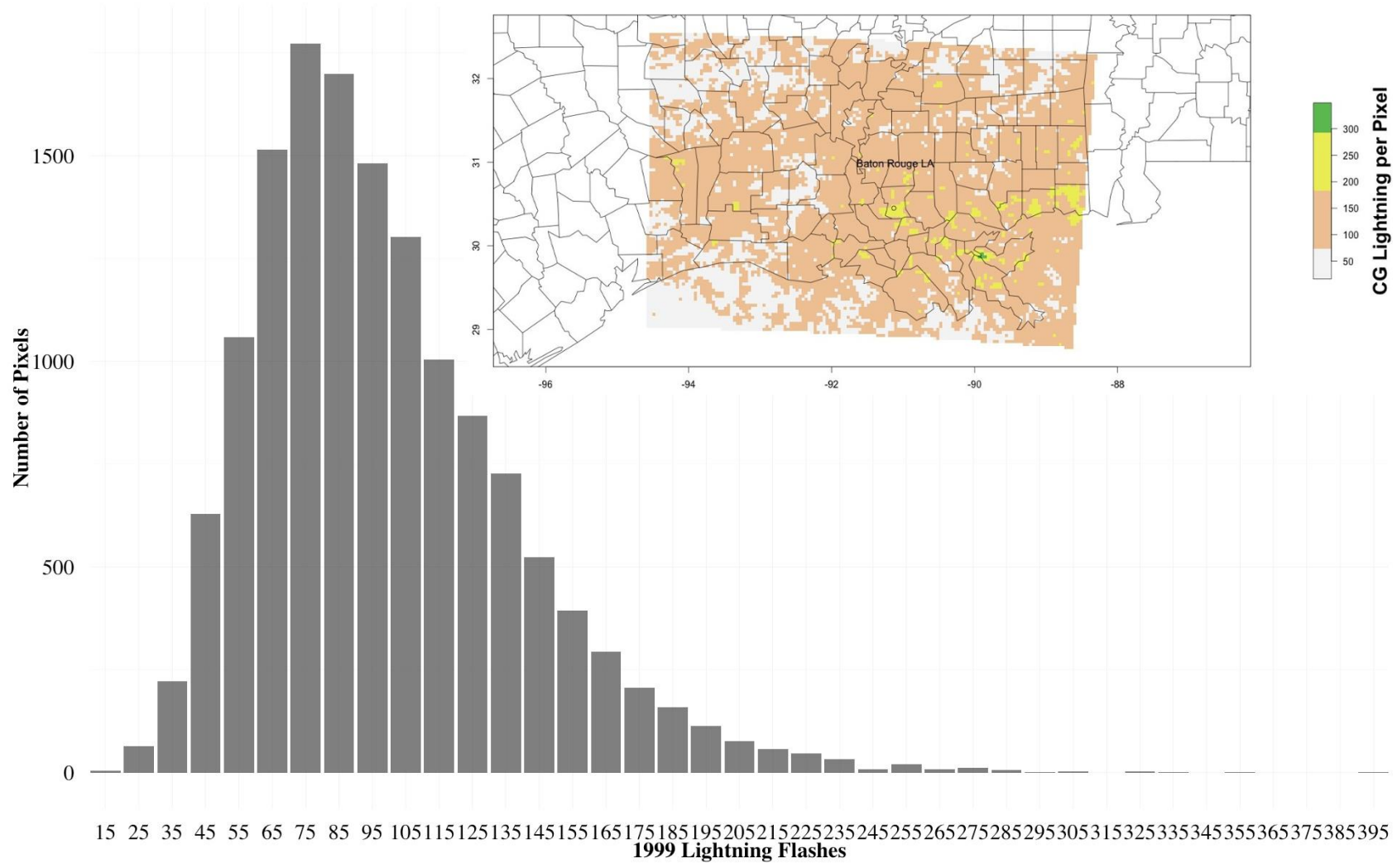


Figure 4.5 As in Figure 4.1, but for 1999.

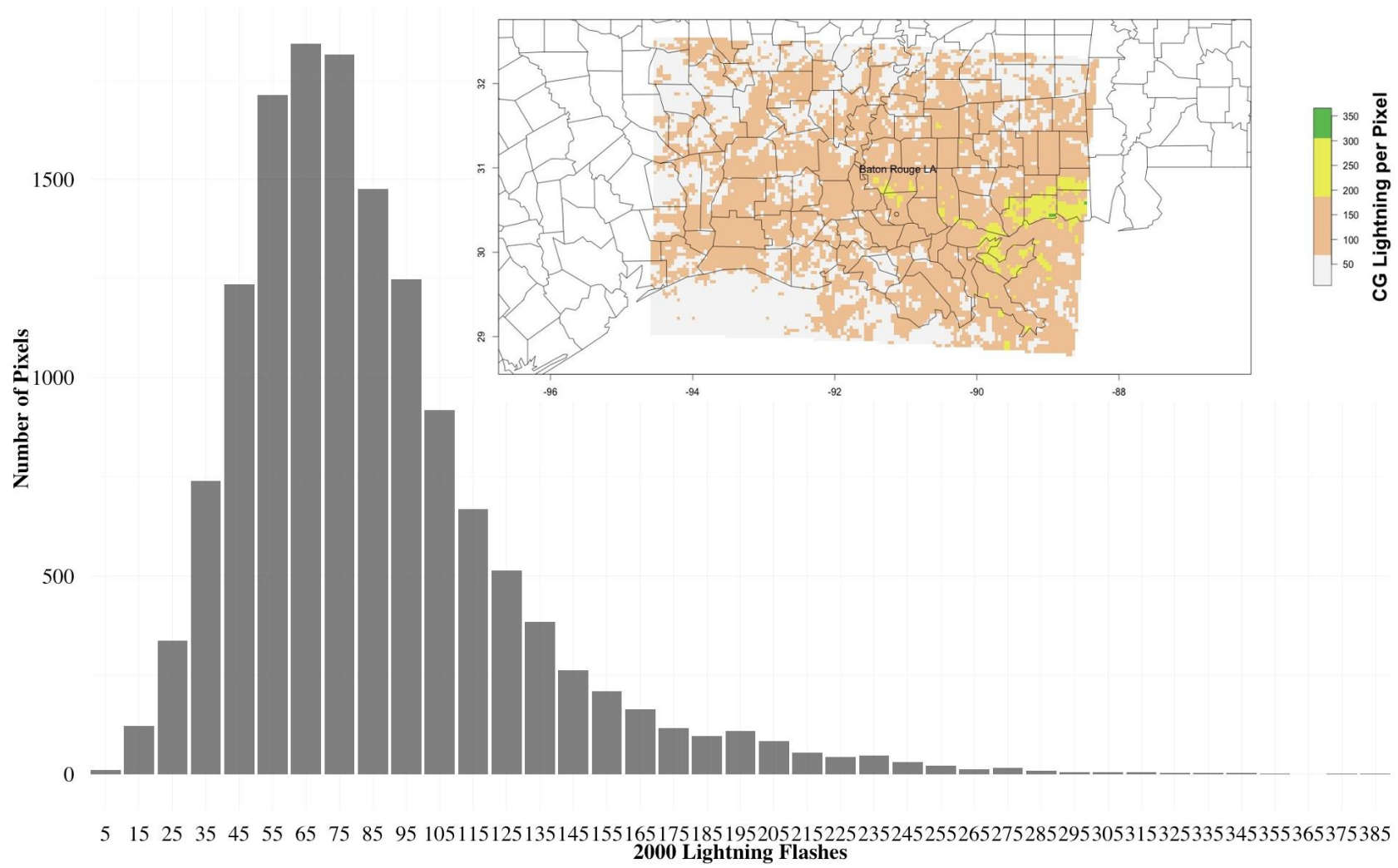


Figure 4.6 As in Figure 4.1, but for 2000.

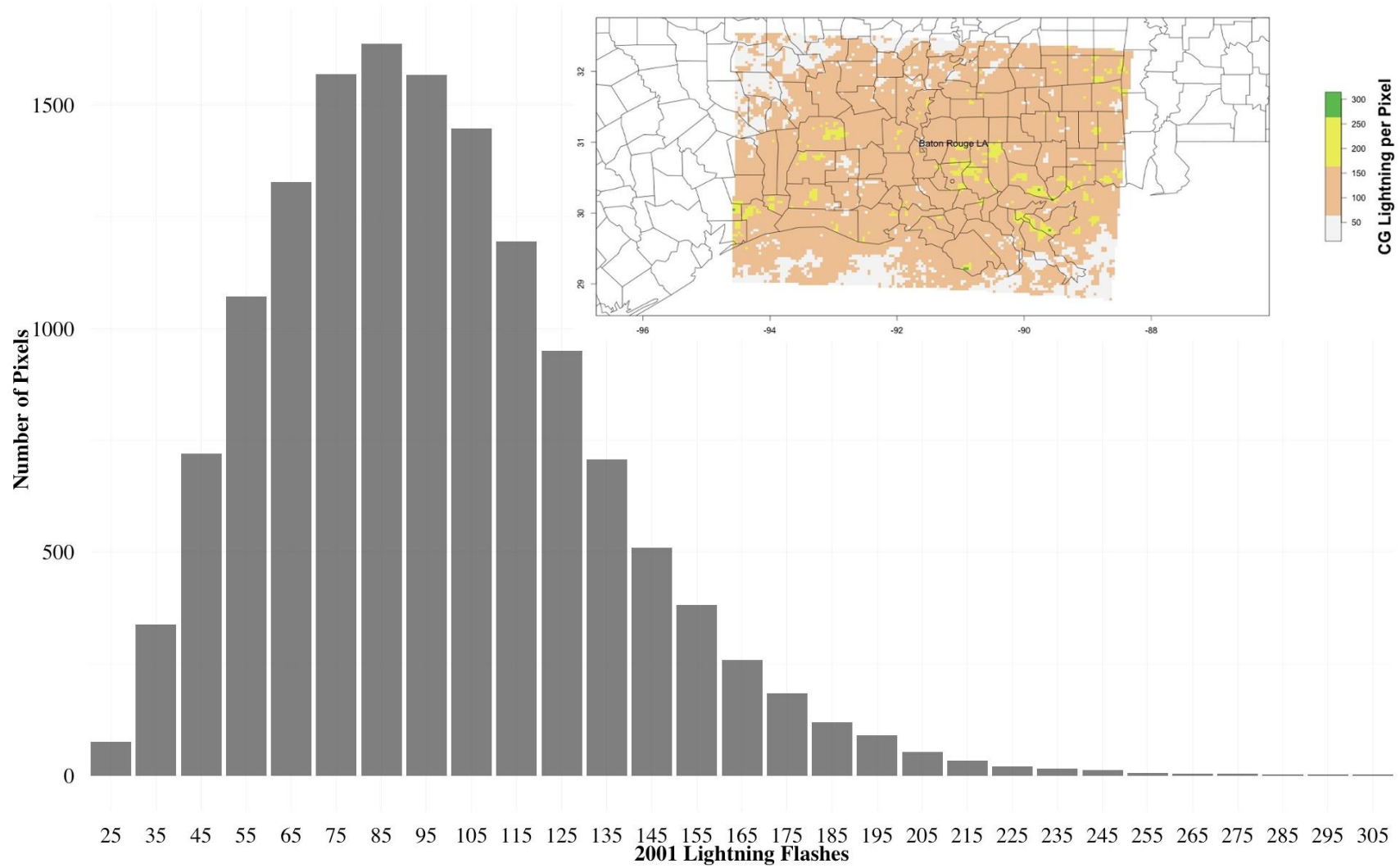


Figure 4.7 As in Figure 4.1, but for 2001.

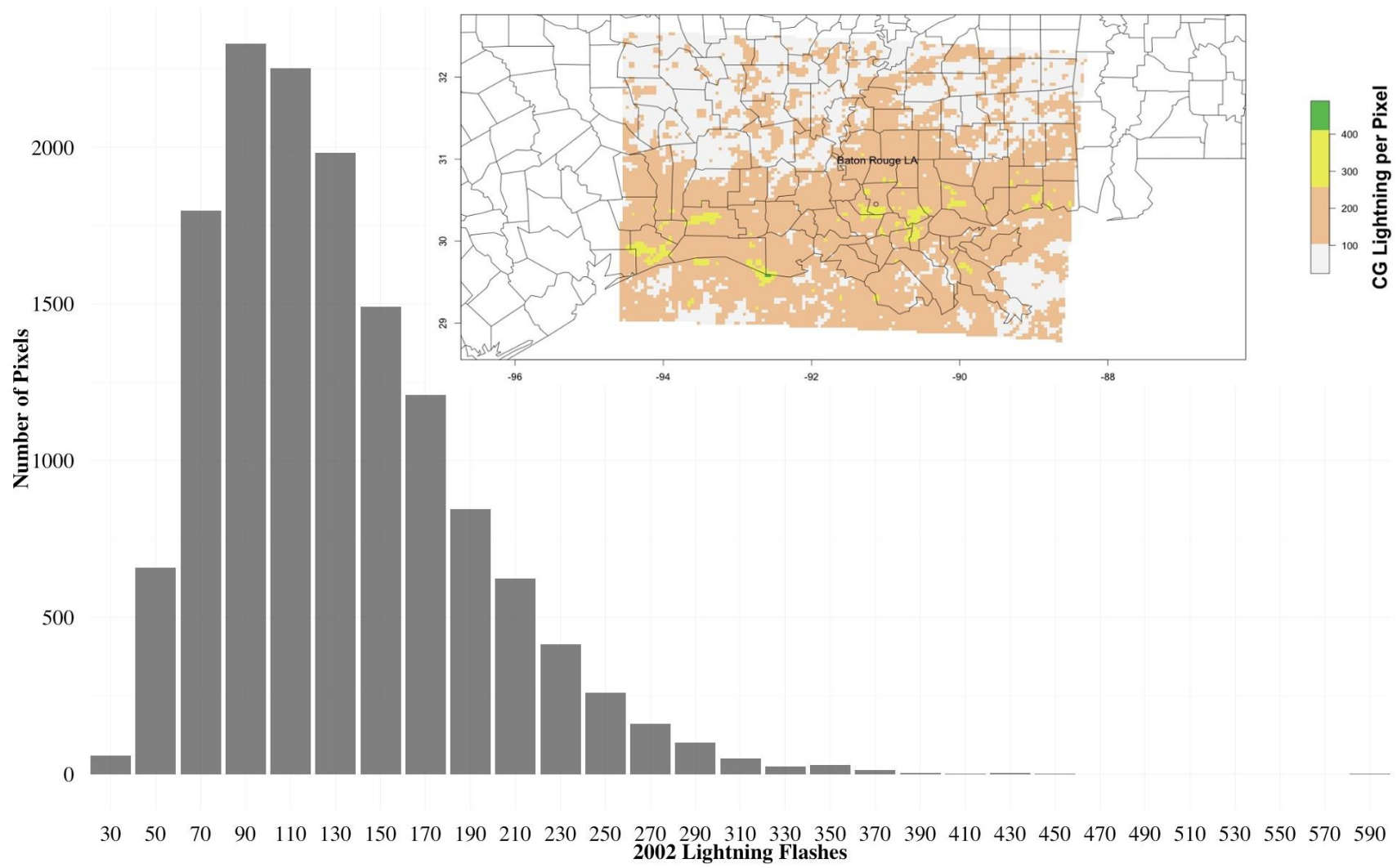


Figure 4.8 As in Figure 4.1, but for 2002.

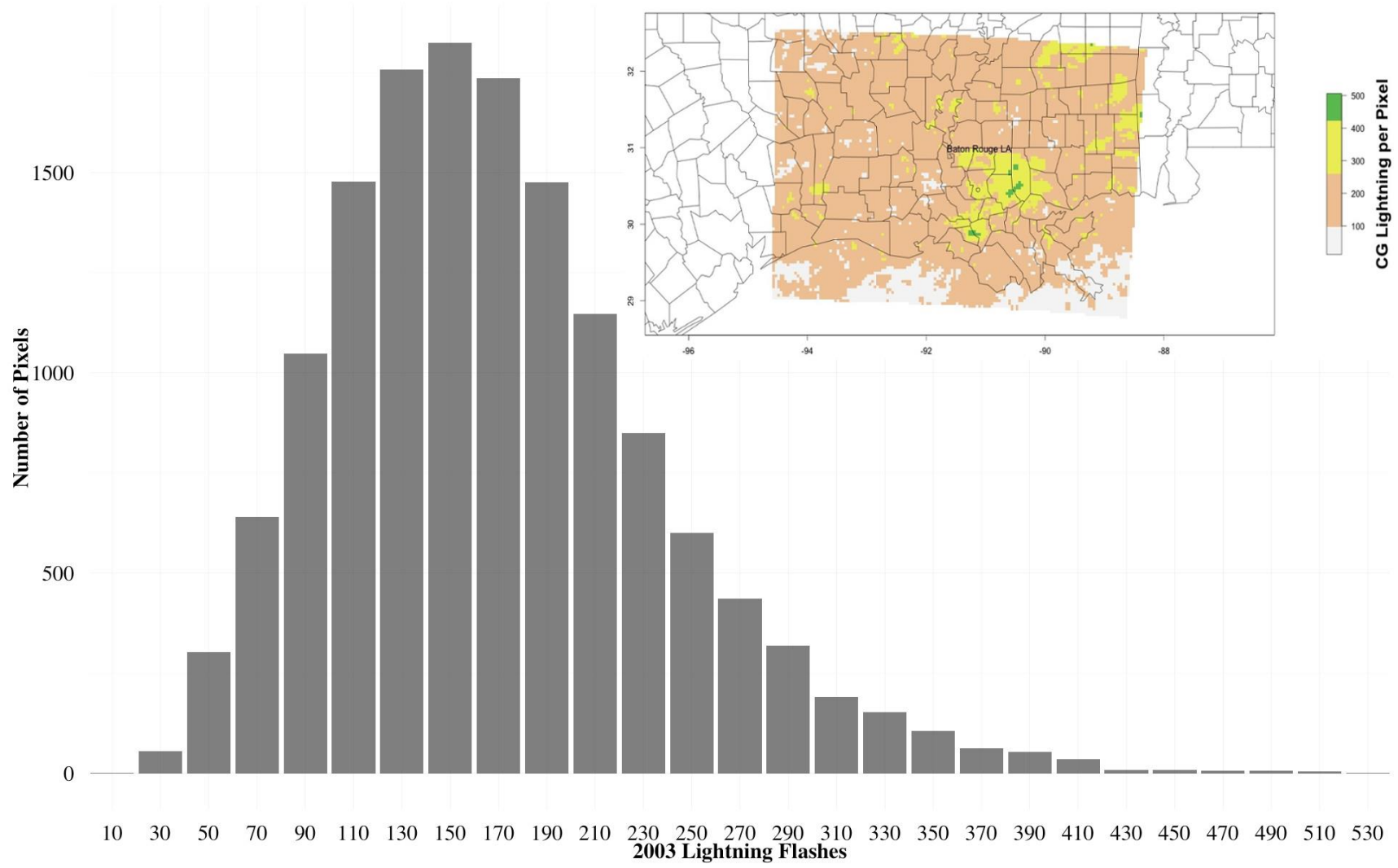


Figure 4.9 As in Figure 4.1, but for 2003.

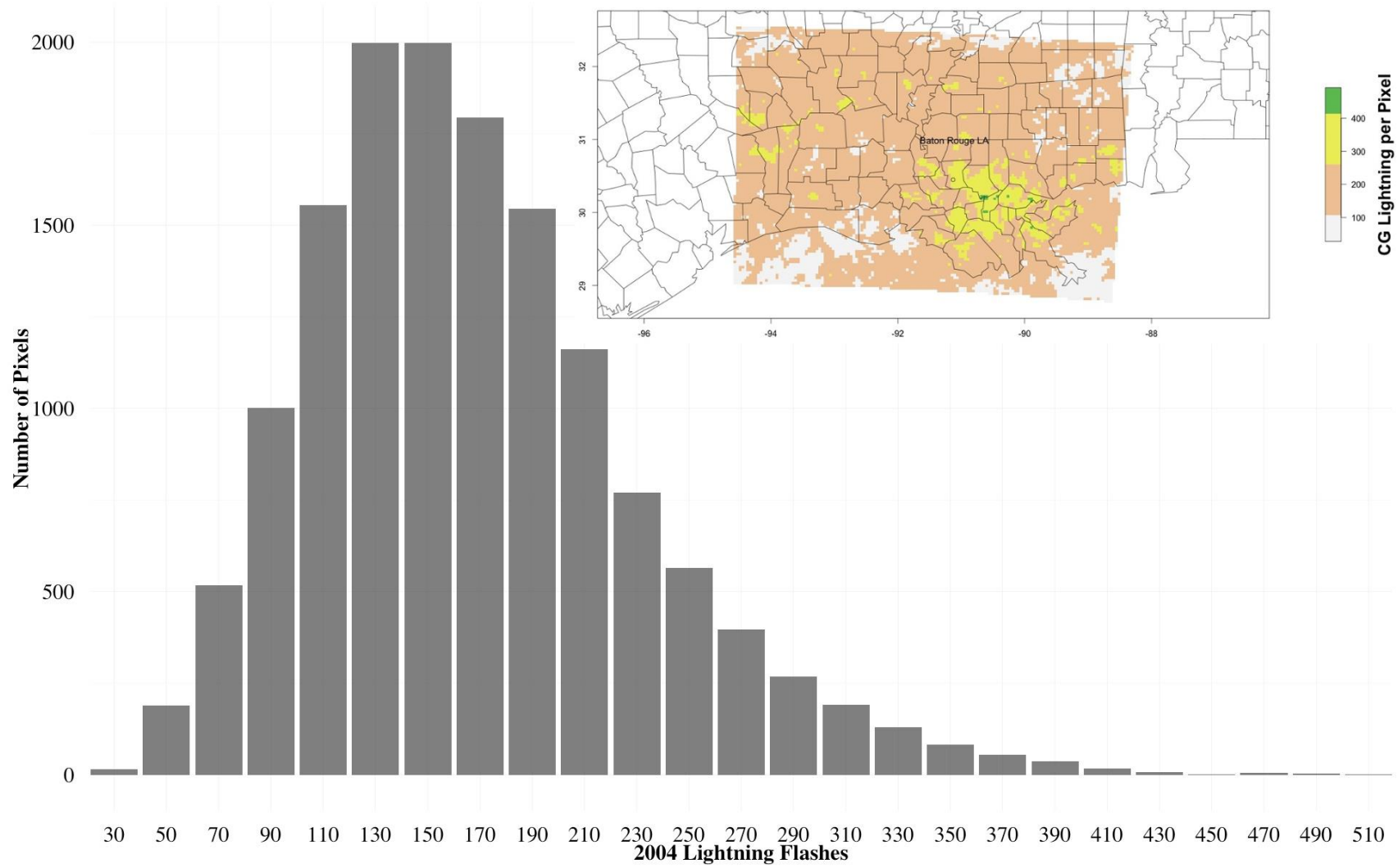


Figure 4.10 As in Figure 4.1, but for 2004.

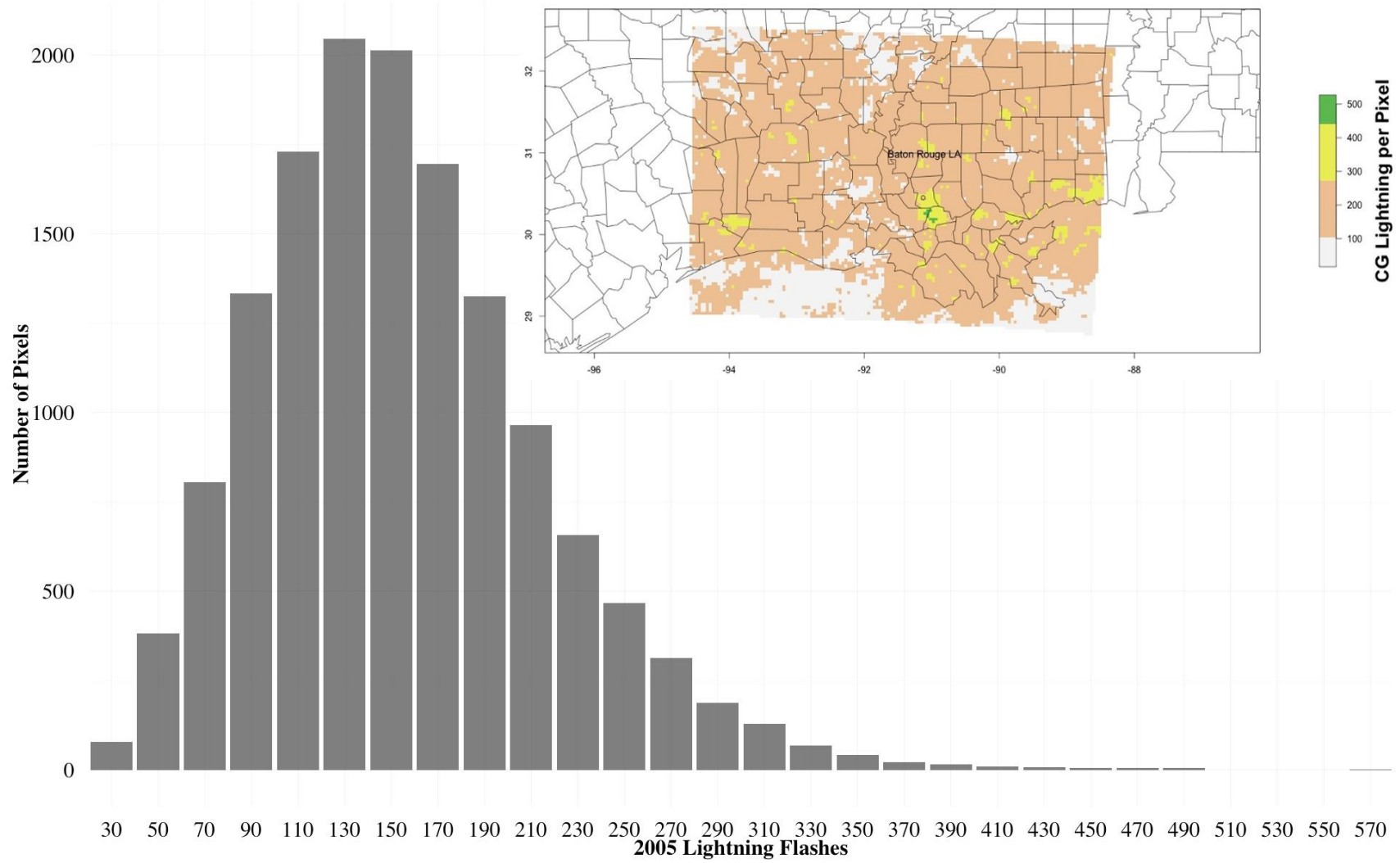


Figure 4.11 As in Figure 4.1, but for 2005.

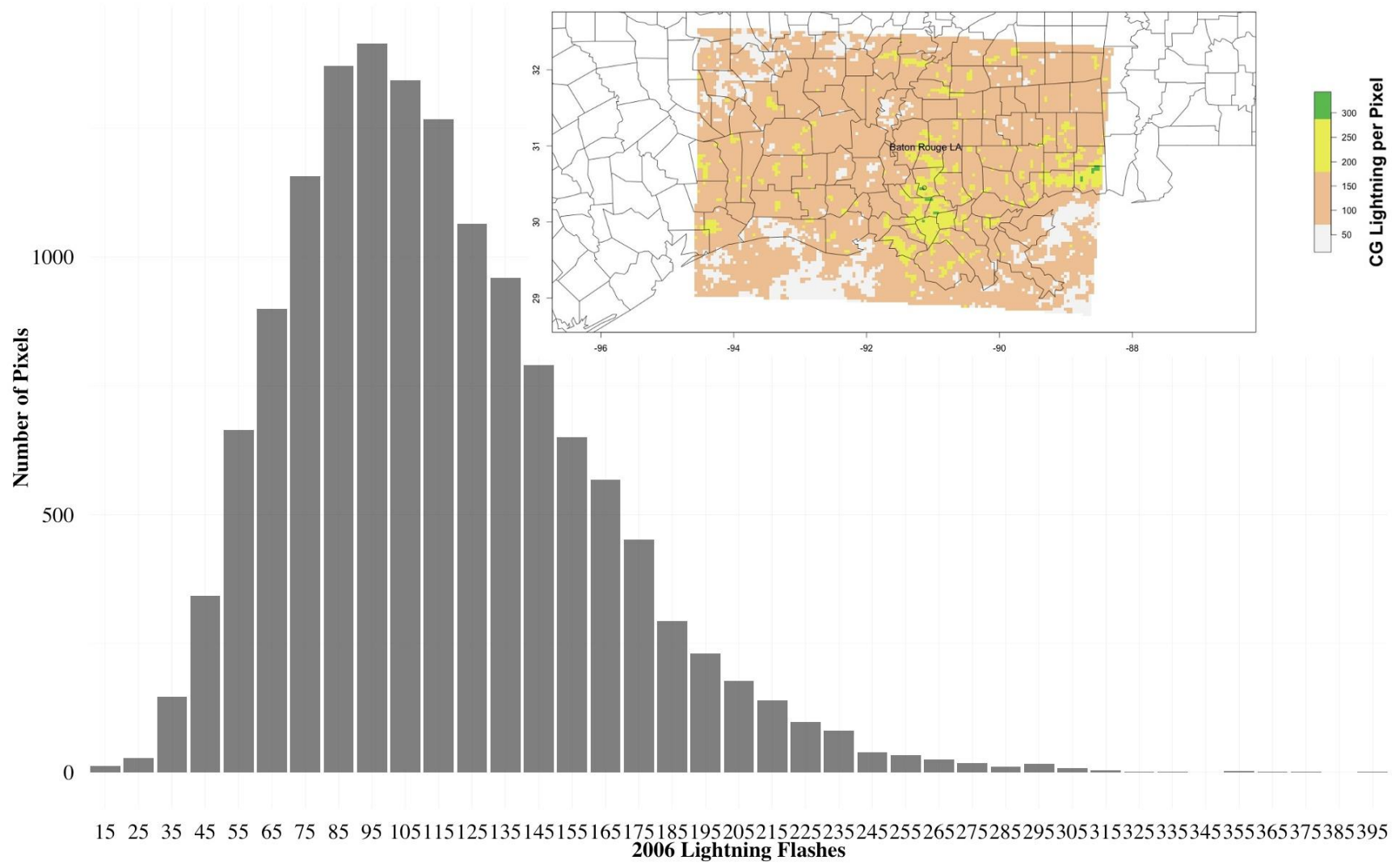


Figure 4.12 As in Figure 4.1, but for 2006.

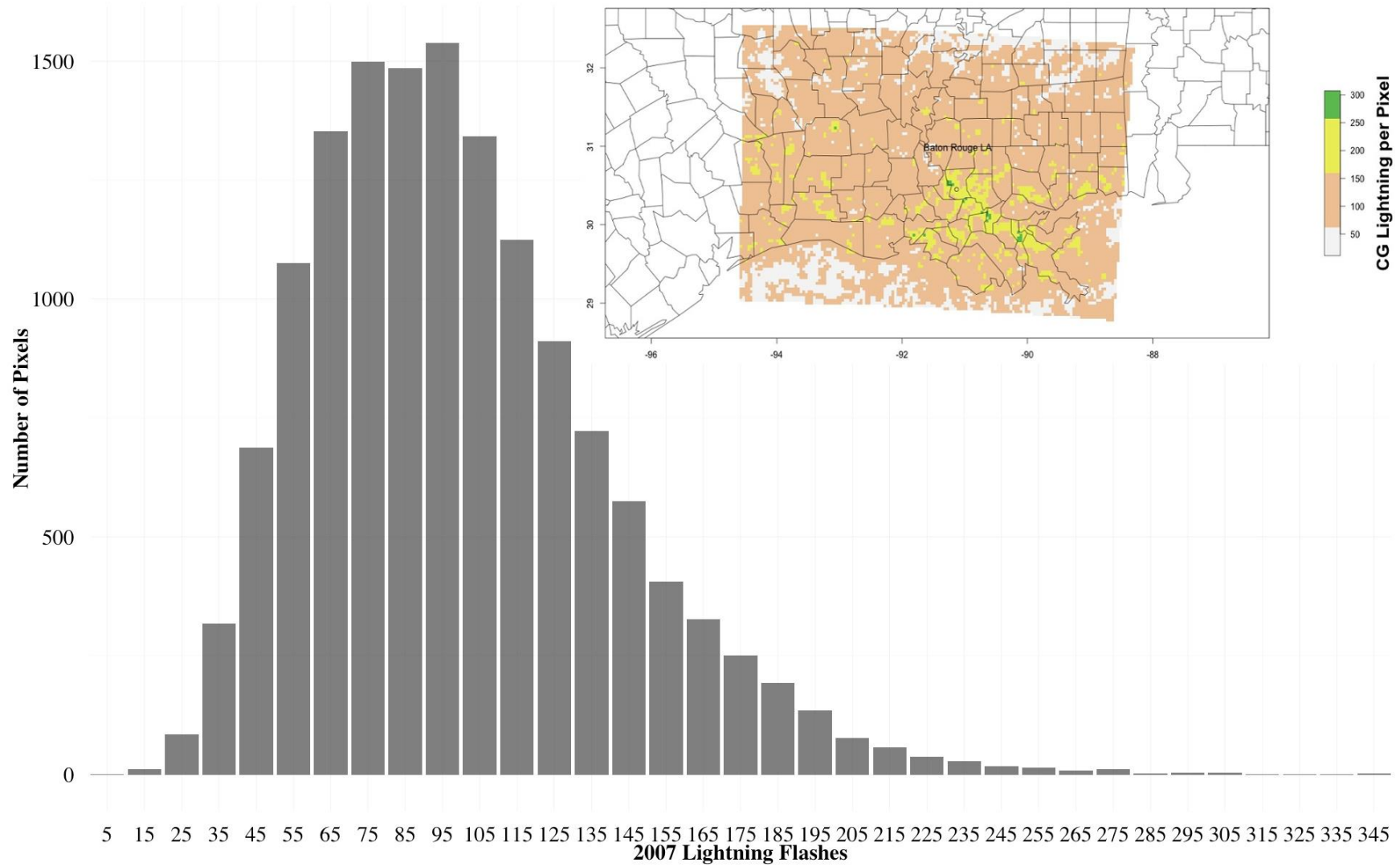


Figure 4.13 As in Figure 4.1, but for 2007.

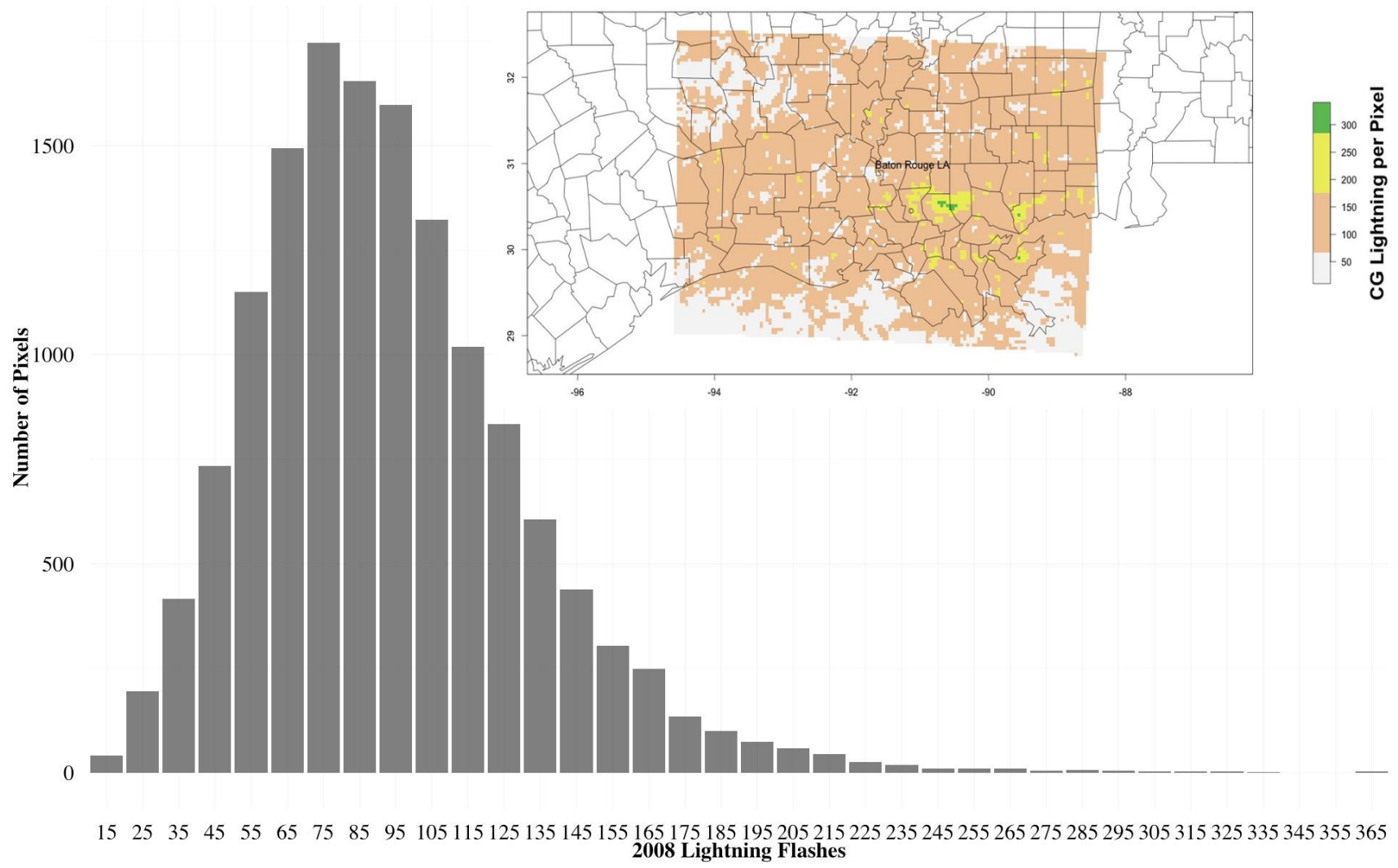


Figure 4.14 As in Figure 4.1, but for 2008.

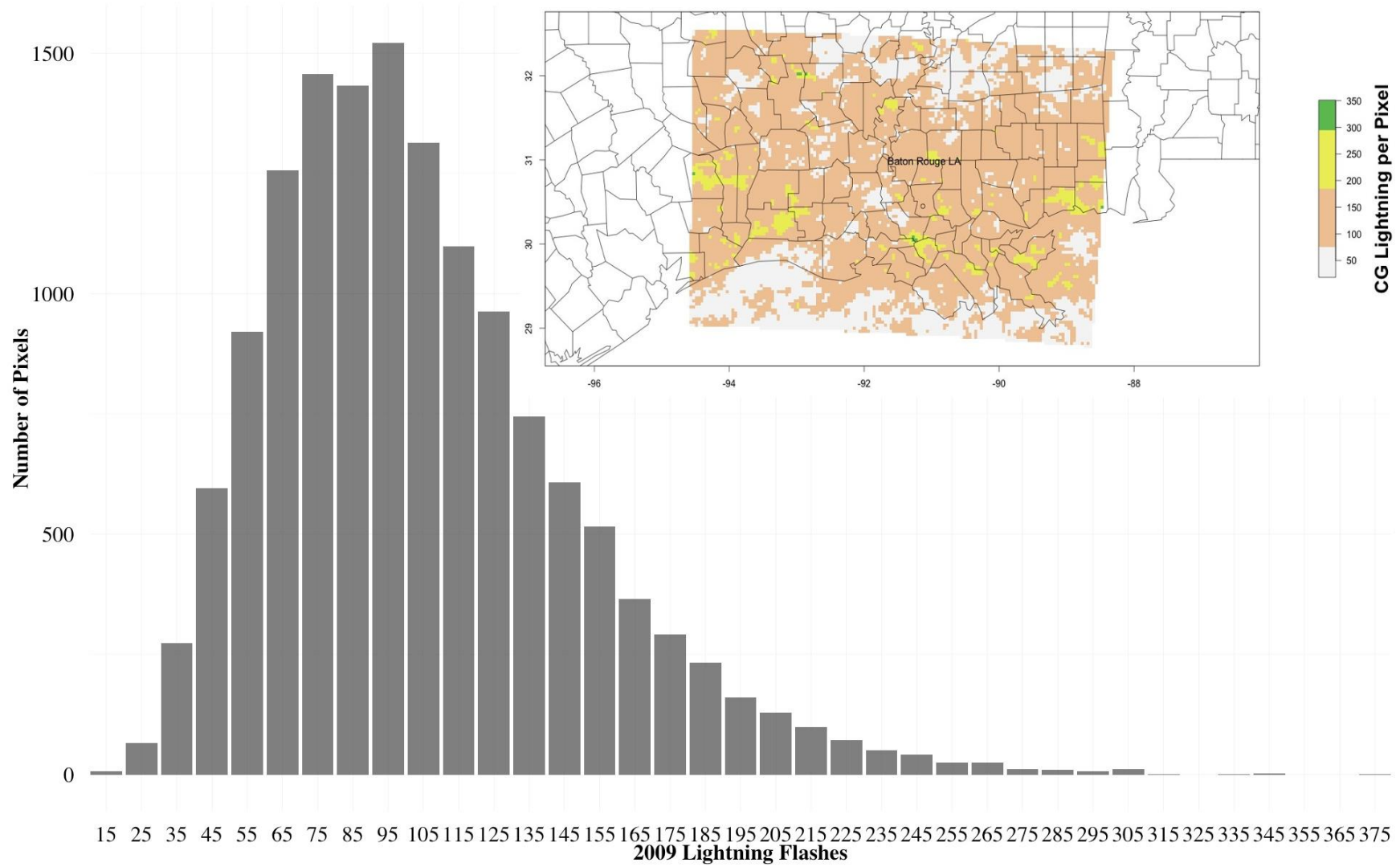


Figure 4.15 As in Figure 4.1, but for 2009.

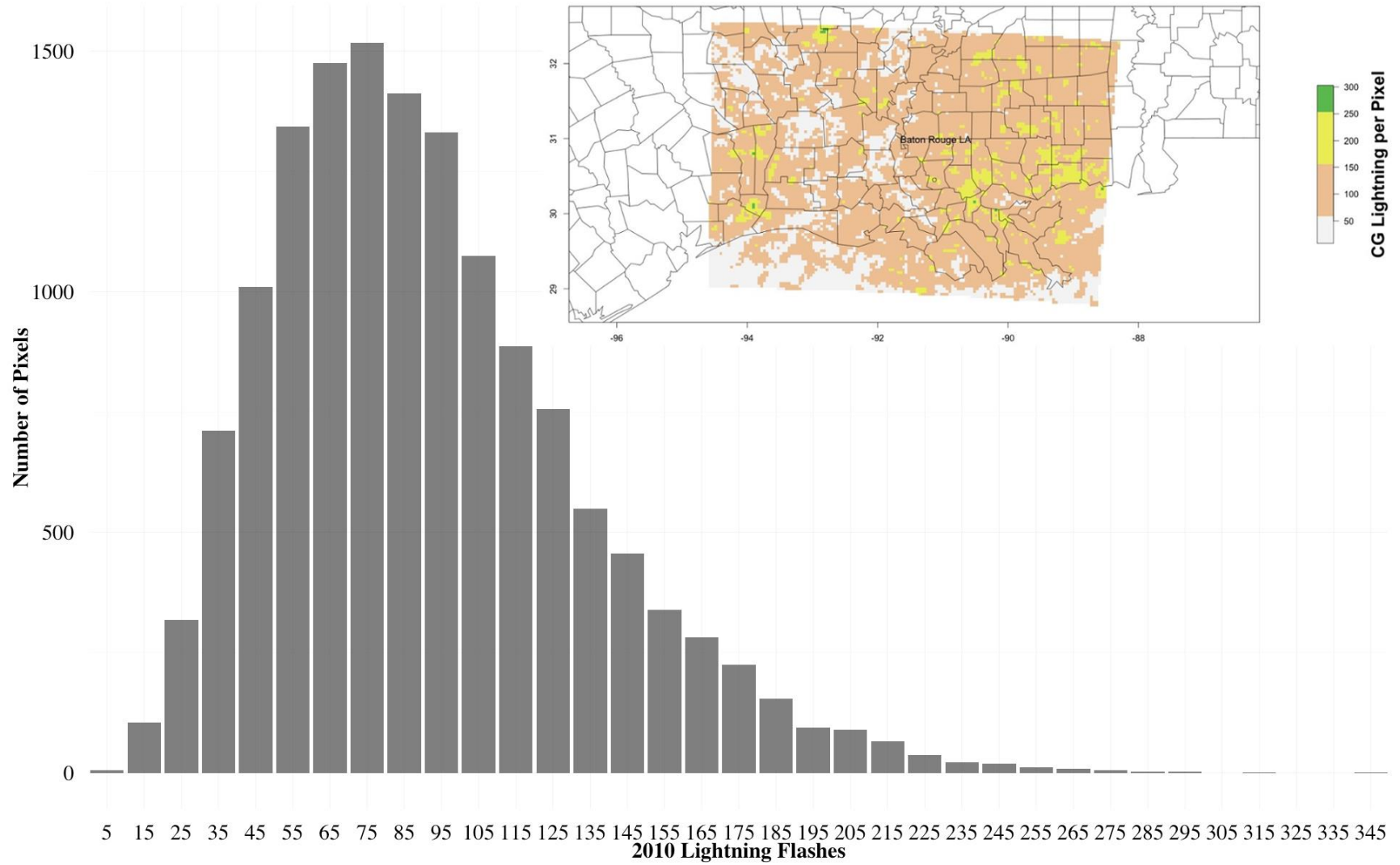


Figure 4.16 As in Figure 4.1, but for 2010.

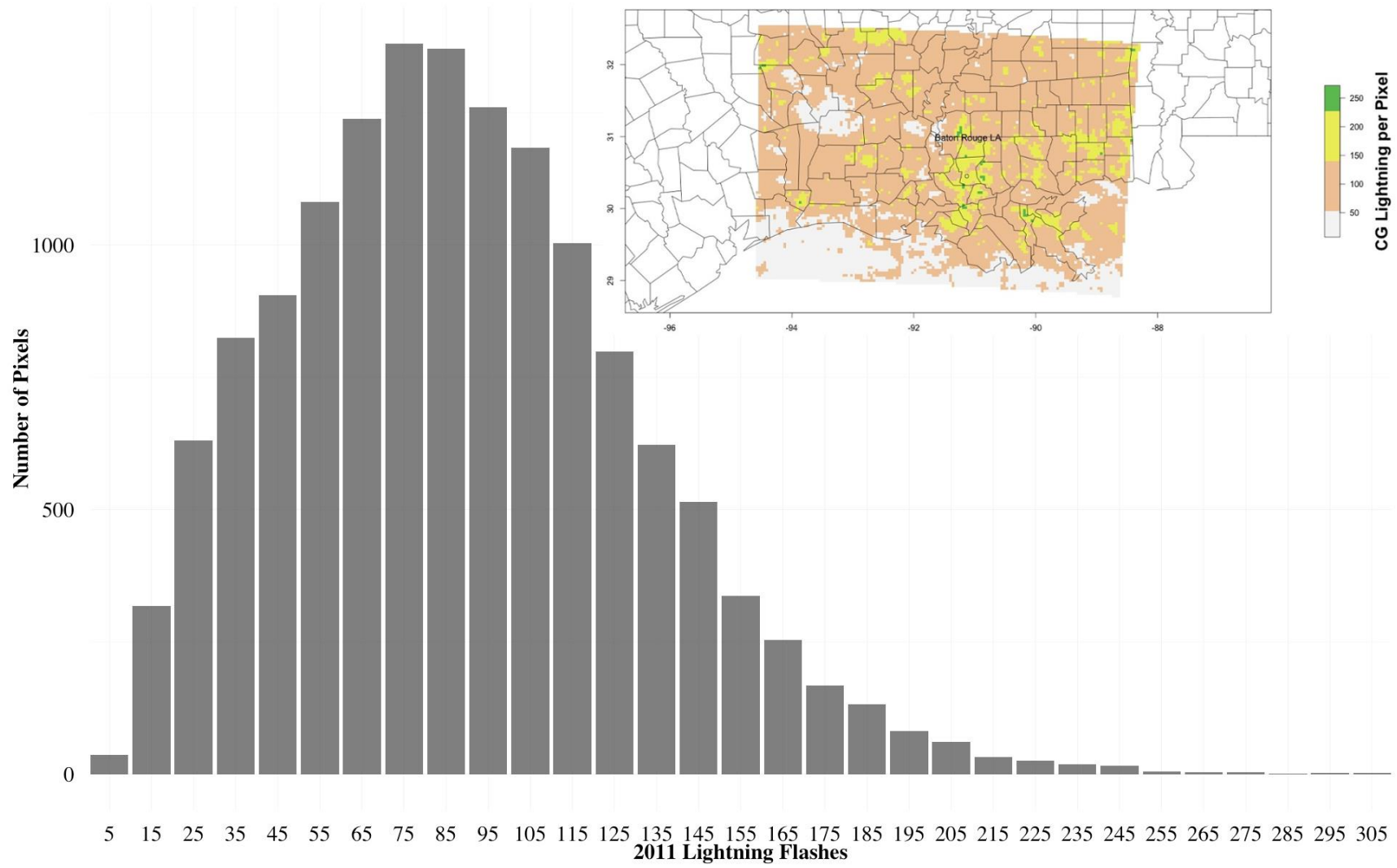


Figure 4.17 As in Figure 4.1, but for 2011.

Figure 4.18 shows the total number of CG lightning strikes in the entire study area by year, with a temporal trend line. A maximum occurred in 2003, with 2,420,859 CG flashes. The low value was observed in 2000, when only 1,216,910 CG flashes were recorded. A linear test for trend identifies no significant temporal trend in areal lightning frequency over the period (Table 4.1).

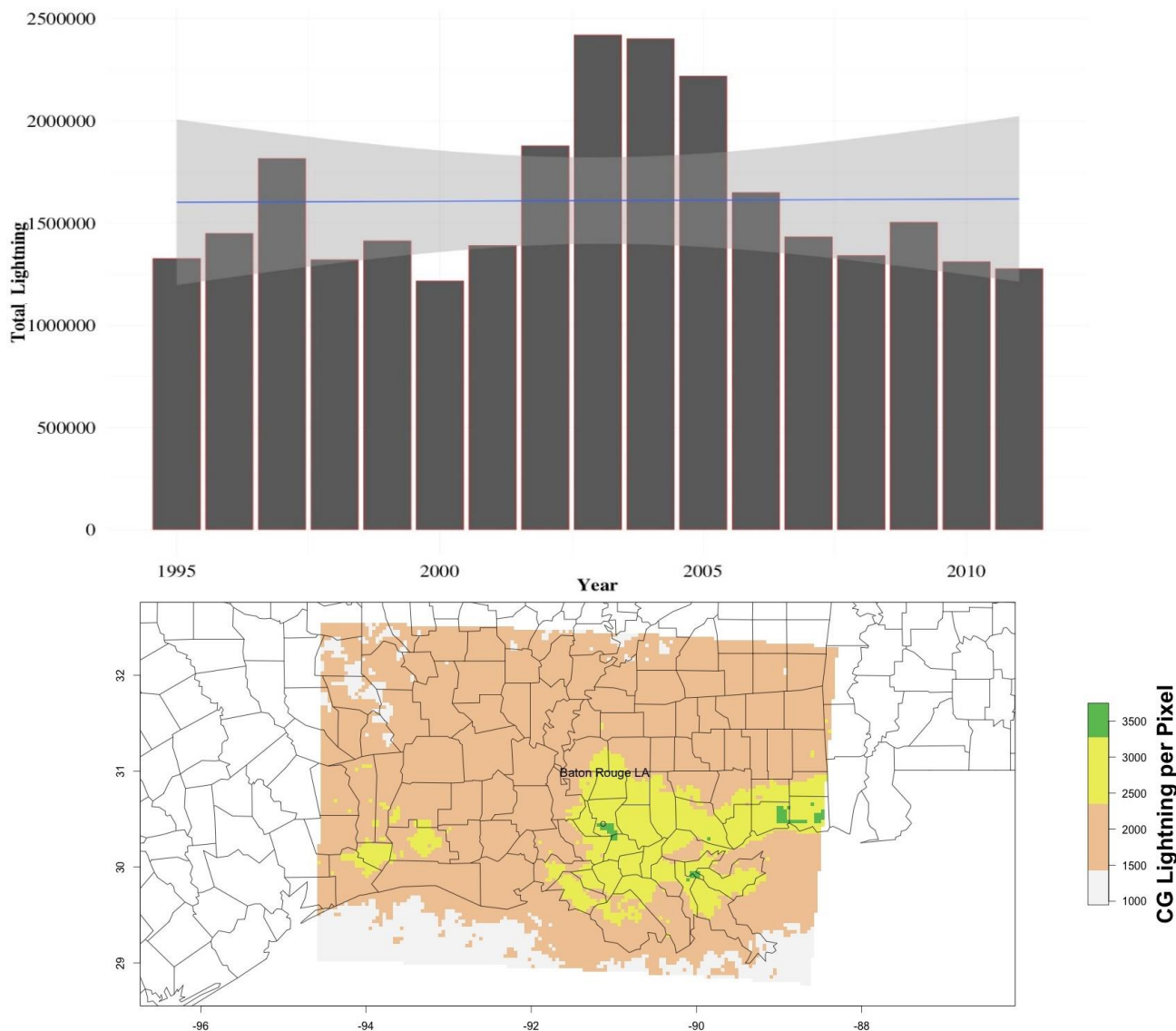


Figure 4.18 Bar graph showing the total regional frequency of CG lightning flashes with a trend line fitted (top), and a map showing the spatial distribution of the 4 km x 4 km pixels across the region for all years 1995–2011.

Table 4.1 Shows resulting statistics for trend line fitted to 17-year lightning climatology.

Intercept	Slope	P-value	Adjusted R-Sq
2.00E+03	1.62E-07	0.992	0.02158
Slope		0.9612	

The low R-squared value could either be related to erratic annual frequencies in lightning occurrence or a small number of years in the data set. A sudden peak in CG lightning activity existed from 2003–2005, and a decrease in lightning activity after that year.

The 17-year climatology map shows that most of the area over land sees an abundance of CG lightning flashes per year. Interestingly, there are areas in southern Louisiana (eg. Lake Charles) on land that see less-frequent lightning than nearby surrounding areas. In addition, areas near Baton Rouge and the I-10/I-12 corridor heading to New Orleans and Biloxi, respectively, both show local maxima in lightning frequencies. This could be evidence of the sea breeze effect, but most likely it is due to the abundance of taller objects that attract lightning by weakening the electric field between the cloud and the ground. CG lightning over the Gulf of Mexico appears to be significantly less than CG lightning over land. Aside from the absence of built-up areas over water, ocean mixing due to winds in a storm make it difficult for an electric field with the appropriate charge to develop to attract a stepped leader.

Figures 4.19 and 4.20 show the distributions of lightning frequency by LULC. From the boxplots, it can be noted that developed land types tend to have higher means than the other land

classes. The largest minimum and maximum flashes are also observed in the developed tiles, this is strong evidence towards an urban-lightning relationship over the temporal period studied.

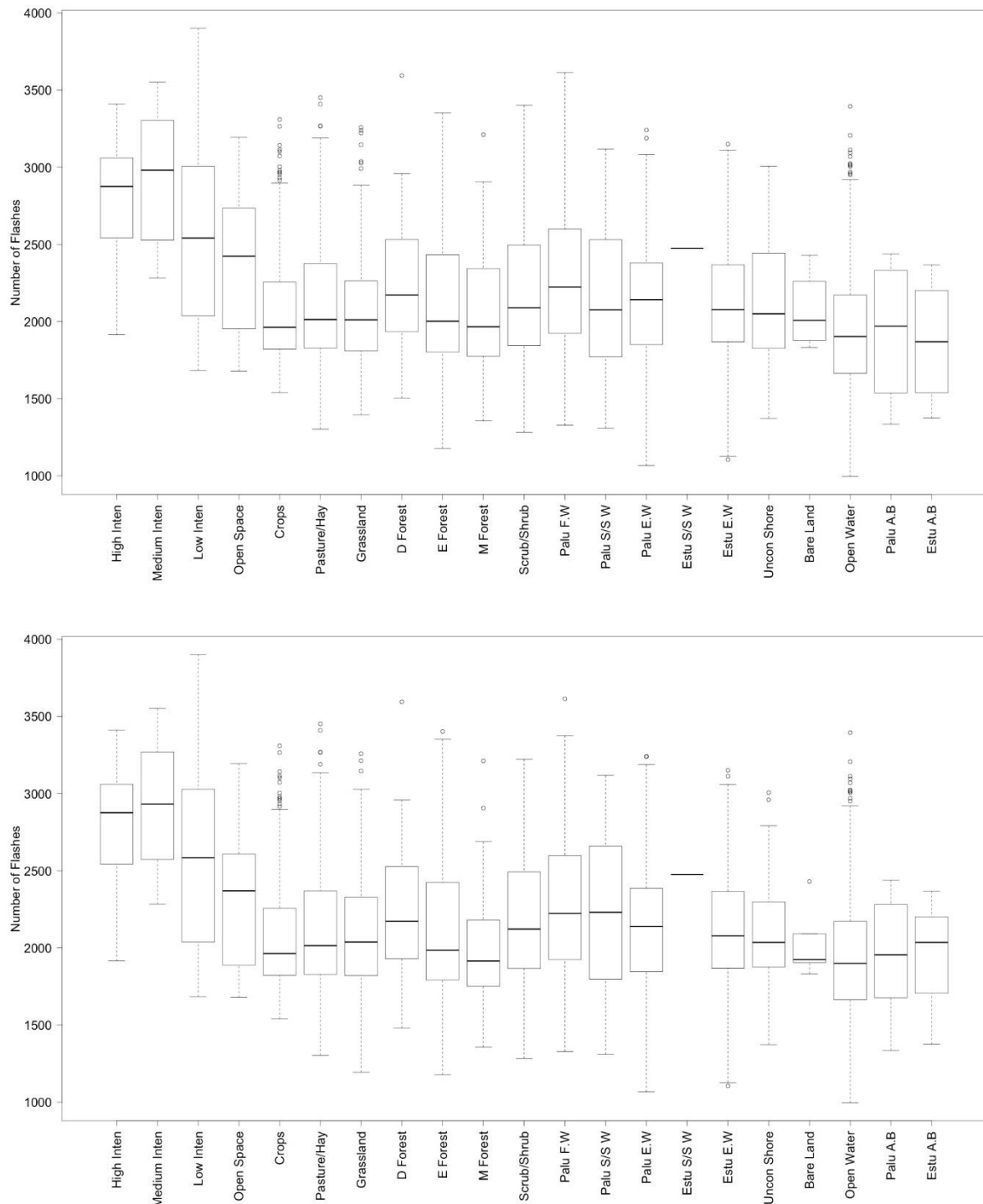


Figure 4.19 Boxplots of each LULC type and their mean, interquartile range, and extremes of CG lightning, by 4 km x 4 km pixel, for 1996 (top) and 2001 (bottom).

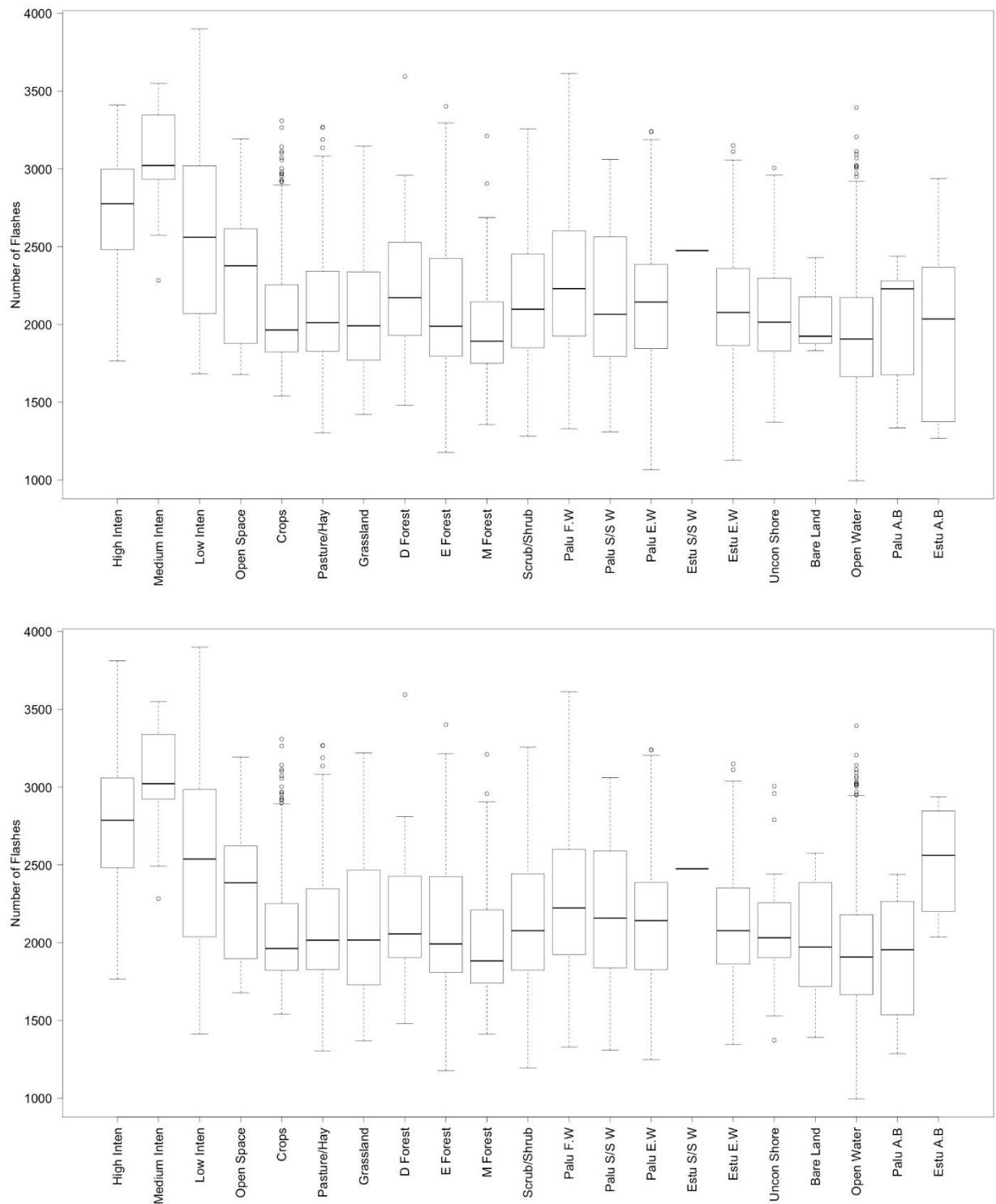


Figure 4.20 As in Figure 4.19, but for 2006 (top) and 2010 (bottom).

4.2 Linear Regression

A Kolmogorov-Smirnoff test for normality was completed before proceeding with the linear regression test, and a p-value below 0.0001 was recorded (Massey, 1951). Figures 4.21 – 4.22 show plots of the residuals between LULC types and the respective years (1996, 2001, 2006, 2010) for the Louisiana portion of this study. Residuals are based on the observed and

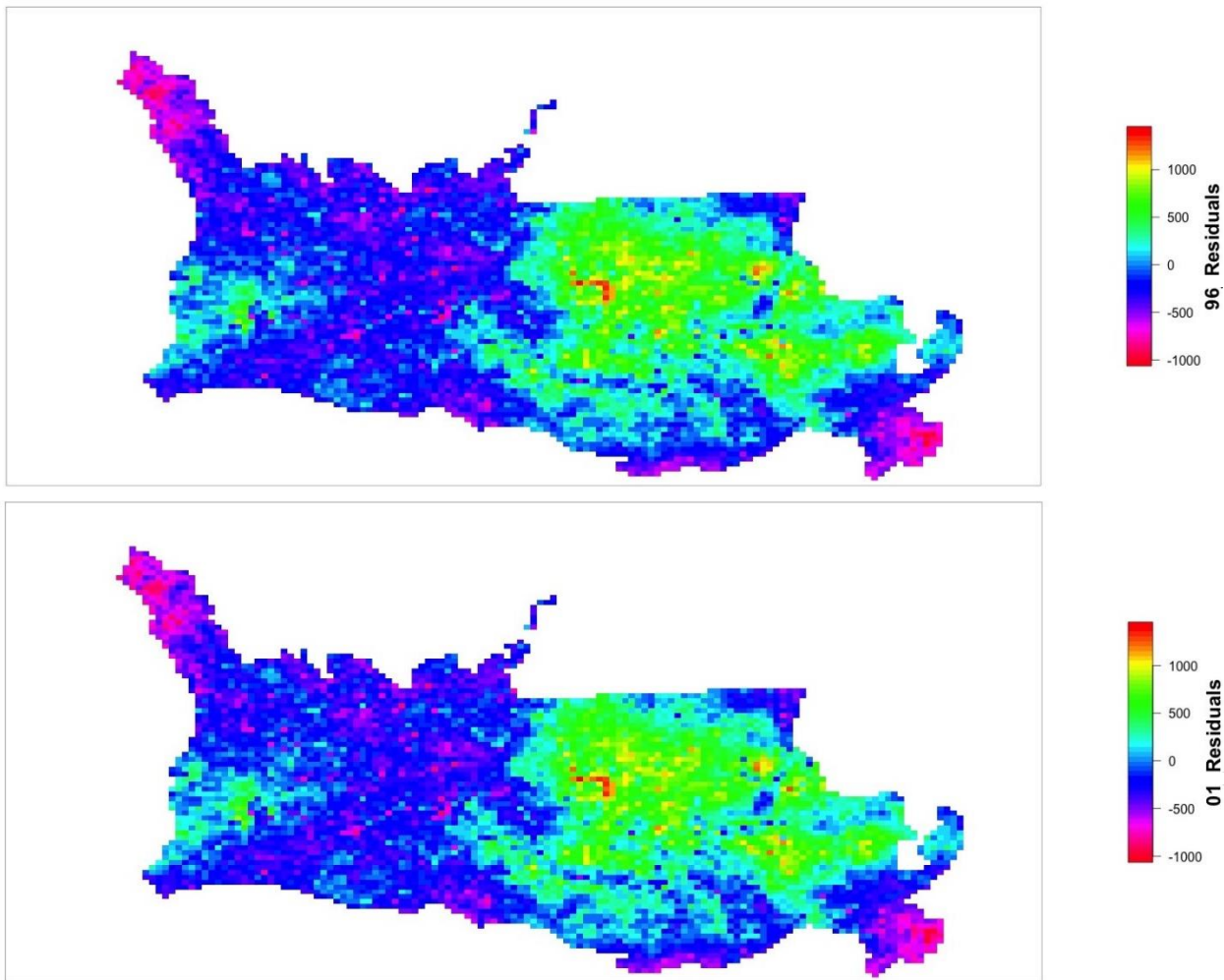


Figure 4.21 Residuals from a linear regression test between 1996 (top) and 2001 (bottom) LULC and lightning.

predicted values, and since the amount of lightning is so large, high residual values are found. The negative residuals represent areas of under estimation and the positive residuals represent over estimation. We observe the highest residuals in urban environments but also in south central

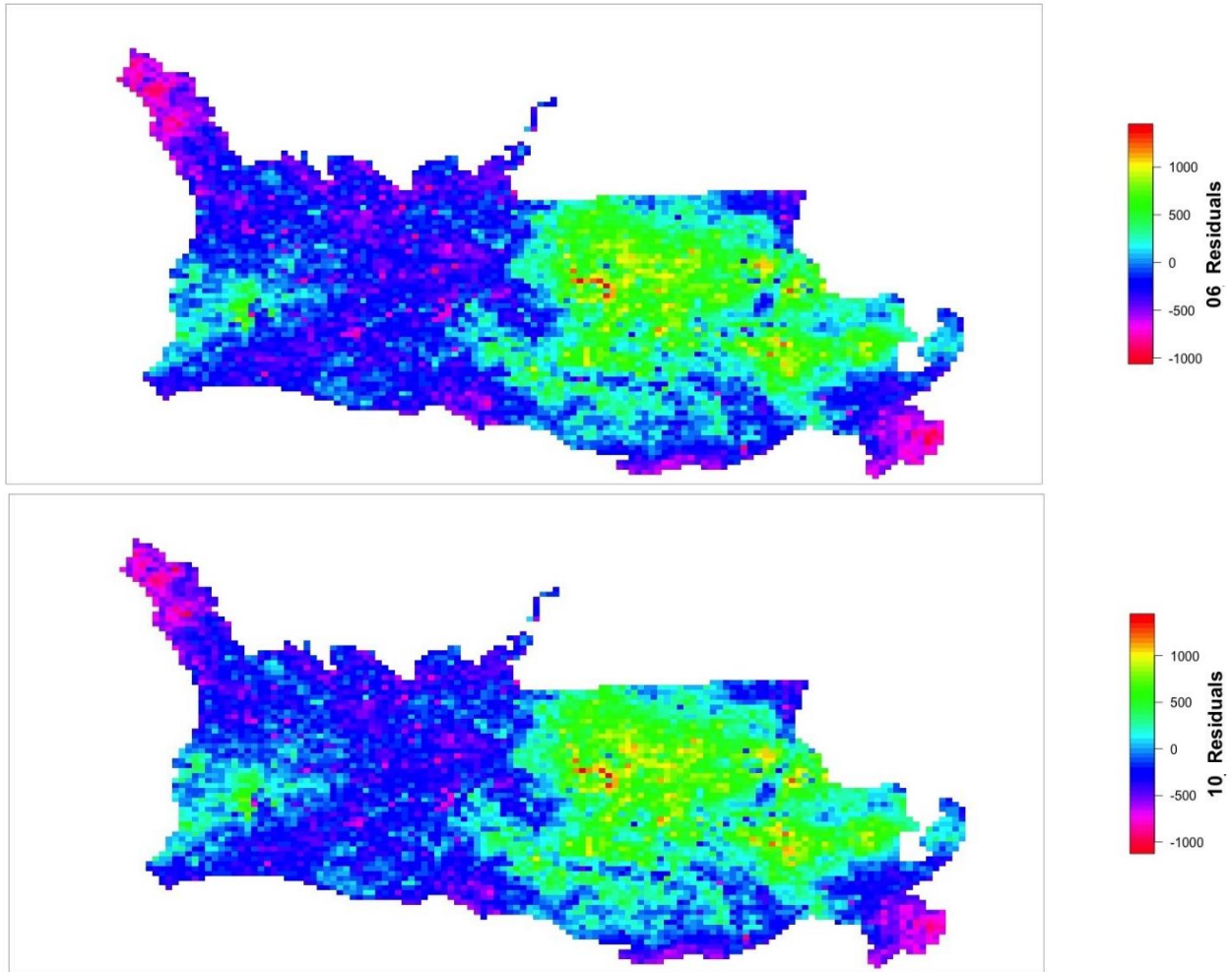


Figure 4.22 As in Figure 4.21, except 2006 (top) and 2010 (bottom).

Louisiana. The lowest residuals occur in southwestern Louisiana, with some clustering of high residuals near the Texas border.

Tables 4.2 – 4.3 show the output of a categorical linear regression between LULC class and the total CG lightning frequency by year. While few differences exist between years, the regression analysis identifies a statistically significant relationship between LULC type and lightning frequency. The level of significance is from 90% to 99%, and most classifications are significant at the 99% confidence interval. There are no background or unclassified classes

present because these were discarded during data handling to prevent error due to the presence of unavailable data and unnecessary zero values.

Table 4.2 1996 (left) and 2001 (right) linear regression results between LULC classification and lightning.

LULC	Coefficients	Std. Error	t-value	P-value
(Intercept)	2815.2857	107.7868	26.12	<0.001
Medium Intensity	132.0476	158.6579	0.83	0.4053
Low Intensity	-257.6494	112.2665	-2.29	0.0218
Open Space	-432.6607	135.6288	-3.19	0.0014
Cultivated Crops	-744.3474	108.7936	-6.84	<0.001
Pasture/Hay	-678.639	109.818	-6.18	<0.001
Grassland	-718.3264	113.7558	-6.31	<0.001
Deciduous Forest	-586.3705	119.895	-4.89	<0.001
Evergreen Forest	-692.461	109.0392	-6.35	<0.001
Mixed Forest	-779.1244	115.6155	-6.74	<0.001
Scrub/Shrub	-635.9409	110.9914	-5.73	<0.001
Palustrine Forested Wetland	-540.7012	108.5051	-4.98	<0.001
Palustrine Scrub/Shrub Wetland	-663.2857	124.8404	-5.31	<0.001
Palustrine Emergent Wetland	-684.4011	110.1786	-6.21	<0.001
Estuarine Scrub/Shrub Wetland	-340.2857	417.4567	-0.82	0.415
Estuarine Emergent Wetland	-683.356	109.3346	-6.25	<0.001
Unconsolidated Shore	-673.9011	155.3374	-4.34	<0.001
Bare Land	-746.0357	228.6504	-3.26	0.0011
Open Water	-875.4381	108.3464	-8.08	<0.001
Palustrine Aquatic Bed	-884.1607	178.7443	-4.95	<0.001
Estuarine Aquatic Bed	-945.2857	228.6504	-4.13	<0.001

LULC	Coefficients	Std. Error	t-value	P-value
(Intercept)	2815.2857	107.5224	26.18	<0.001
Medium Intensity	107.2857	152.0597	0.71	0.4805
Low Intensity	-250.9269	111.8622	-2.24	0.0249
Open Space	-506.0599	129.5461	-3.91	0.0001
Cultivated Crops	-742.999	108.5307	-6.85	<0.001
Pasture/Hay	-676.2394	109.5541	-6.17	<0.001
Grassland	-703.5466	112.8447	-6.23	<0.001
Deciduous Forest	-598.5152	119.2243	-5.02	<0.001
Evergreen Forest	-712.4158	108.8558	-6.54	<0.001
Mixed Forest	-828.7556	116.2374	-7.13	<0.001
Scrub/Shrub	-609.3413	110.2748	-5.53	<0.001
Palustrine Forested Wetland	-541.0222	108.2571	-5	<0.001
Palustrine Scrub/Shrub Wetland	-604.9388	121.919	-4.96	<0.001
Palustrine Emergent Wetland	-683.8335	109.8933	-6.22	<0.001
Estuarine Scrub/Shrub Wetland	-340.2857	416.4326	-0.82	0.4139
Estuarine Emergent Wetland	-681.173	109.0824	-6.24	<0.001
Unconsolidated Shore	-694.0752	141.7031	-4.9	<0.001
Bare Land	-779.0857	209.5998	-3.72	0.0002
Open Water	-877.4899	108.0818	-8.12	<0.001
Palustrine Aquatic Bed	-855.0635	171.8865	-4.97	<0.001
Estuarine Aquatic Bed	-889.619	255.9546	-3.48	0.0005

Table 4.3 As in Table 4.6, but for 2006 (left) and 2010 (right).

LULC	Coefficients	Std. Error	t-value	P-value	LULC	Coefficients	Std. Error	t-value	P-value
(Intercept)	2687.4118	97.3957	27.59	<0.001	(Intercept)	2734.2727	85.7421	31.89	<0.001
Medium Intensity	379.2549	142.2555	2.67	0.0077	Medium Intensity	303.6096	129.8679	2.34	0.0194
Low Intensity	-118.4345	101.9911	-1.16	0.2456	Low Intensity	-196.7278	90.8864	-2.16	0.0305
Open Space	-384.7451	121.9069	-3.16	0.0016	Open Space	-391.697	110.6925	-3.54	0.0004
Cultivated Crops	-612.9124	98.4919	-6.22	<0.001	Cultivated Crops	-663.3561	87.0005	-7.62	<0.001
Pasture/Hay	-565.3884	99.7801	-5.67	<0.001	Pasture/Hay	-607.8638	88.5127	-6.87	<0.001
Grassland	-595.9732	104.4054	-5.71	<0.001	Grassland	-609.679	99.3924	-6.13	<0.001
Deciduous Forest	-470.6413	110.1342	-4.27	<0.001	Deciduous Forest	-561.7455	101.4514	-5.54	<0.001
Evergreen Forest	-579.2632	98.96	-5.85	<0.001	Evergreen Forest	-626.8104	87.5934	-7.16	<0.001
Mixed Forest	-717.8384	107.8706	-6.65	<0.001	Mixed Forest	-752.9848	99.0064	-7.61	<0.001
Scrub/Shrub	-504.1378	99.7069	-5.06	<0.001	Scrub/Shrub	-573.289	87.9031	-6.52	<0.001
Palustrine Forested Wetland	-410.1806	98.2136	-4.18	<0.001	Palustrine Forested Wetland	-459.4595	86.6991	-5.3	<0.001
Palustrine Scrub/Shrub Wetland	-538.7936	111.4358	-4.84	<0.001	Palustrine Scrub/Shrub Wetland	-520.6547	95.7548	-5.44	<0.001
Palustrine Emergent Wetland	-556.3359	100.0906	-5.56	<0.001	Palustrine Emergent Wetland	-600.6845	88.7708	-6.77	<0.001
Estuarine Scrub/Shrub Wetland	-212.4118	413.215	-0.51	0.6072	Estuarine Scrub/Shrub Wetland	-259.2727	411.2045	-0.63	0.5284
Estuarine Emergent Wetland	-554.5172	99.1269	-5.59	<0.001	Estuarine Emergent Wetland	-607.0944	87.8453	-6.91	<0.001
Unconsolidated Shore	-601.6618	132.4725	-4.54	<0.001	Unconsolidated Shore	-623.8182	121.2576	-5.14	<0.001
Bare Land	-625.4118	251.4746	-2.49	0.0129	Bare Land	-727.0227	132.1374	-5.5	<0.001
Open Water	-746.6081	98.0048	-7.62	<0.001	Open Water	-788.9776	86.4283	-9.13	<0.001
Palustrine Aquatic Bed	-690.5229	165.5409	-4.17	<0.001	Palustrine Aquatic Bed	-818.1394	134.6633	-6.08	<0.001
Estuarine Aquatic Bed	-690.8118	204.299	-3.38	0.0007	Estuarine Aquatic Bed	-210.5227	218.6002	-0.96	0.3356

In 1996, there is a relationship between every LULC class and lightning except for developed medium intensity and estuarine forested wetland (Table 4.2). P-values for both categories were just above the threshold required for significance (0.4053 and 0.4150). The results for 2001 (Table 4.6) are similar to those for 1996, which most likely suggests that there were no LULC changes significant enough to change the relationship, or that the climatology of lightning is too chaotic to detect a pattern. For 2006 (Table 4.3), high intensity urban is significantly related to lightning frequency, which could mean that enhanced development of this type of LULC allowed for an increase in relationship. In 2010 (Table 4.3), high intensity urban class is still significantly related to lightning frequency, but estuarine aquatic bed is no longer significantly related. The sudden change could be due to coastal erosion, as much of this type of classification diminished greatly from 1996 to 2010.

4.3 ANOVA & Scheffé's Analysis

ANOVA results for 1996, 2001, 2006, and 2010 show a statistically significant difference of means in lightning by LULC type, for all four years studied (Table 4.4). To ascertain which LULC types differed significantly from which others, a Scheffé's 95% Simultaneous Confidence Interval test (Scheffé, 1959) was implemented to test significant differences between groups.

Table 4.4

Results of ANOVA test to test for difference of mean lightning strikes by LULC type, 1996, 2001, 2006, and 2010.

Year	Df	Sum Sq	Mean Sq	F value	P-Value
1996	20	121865538	6093276.9	37.46	<0.001
	5673	922725155.7	162652.06		
2001	20	126387289.9	6319364.49	39.04	<0.001
	5673	918203403.9	161855		
2006	20	129758712.4	6487935.62	40.23	<0.001
	5673	914831981.4	161260.71		
2010	20	127054334.2	6352716.71	39.28	<0.001
	5673	917536359.6	161737.42		

The results from Scheffé's analysis show that certain LULC types consistently hold higher mean frequencies of CG lightning than certain other land types (Table 4.5 – 4.8). LULC categories denoted by "a" in tables 4.5 - 4.8 are in the group of LULCs with the highest means (while not differing significantly from each other), those denoted by "b" in the tables are in the group of LULCs with the second-highest means (while not differing significantly from each other), those denoted by "c" are in the group with the lowest means and are not significantly different from

Table 4.5 Output of Scheffé's comparison test for 1996 and all years of lightning.

Degrees of Freedom	Number of Treatments	F	Scheffe	alpha
5673	21	1.572378	5.607813	0.05
Rankings	Land Class	Means	Groupings	
1	Developed, Medium Intensity	2947.333	a	
2	Developed, High Intensity	2815.286	ab	
3	Developed, Low Intensity	2557.636	ab	
4	Estuarine Scrub/Shrub Wetland	2475	abc	
5	Developed, Open Space	2382.625	abc	
6	Palustrine Forested Wetland	2274.585	bc	
7	Deciduous Forest	2228.915	bc	
8	Scrub/Shrub	2179.345	c	
9	Palustrine Scrub/Shrub Wetland	2152	c	
10	Unconsolidated Shore	2141.385	c	
11	Pasture/Hay	2136.647	c	
12	Estuarine Emergent Wetland	2131.93	c	
13	Palustrine Emergent Wetland	2130.885	c	
14	Evergreen Forest	2122.825	c	
15	Grassland/Herbaceous	2096.959	c	
16	Cultivated Crops	2070.938	c	
17	Bare Land	2069.25	c	
18	Mixed Forest	2036.161	c	
19	Open Water	1939.848	c	
20	Palustrine Aquatic Bed	1931.125	c	
21	Estuarine Aquatic Bed	1870	c	

Table 4.6 As in Table 4.5, but for 2001.

Degrees of Freedom	Number of Treatments	F	Scheffé	alpha
5673	21	1.572378	5.607813	0.05
Rankings	Land Class	Means	Groupings	
1	Developed, Medium Intensity	2922.571	a	
2	Developed, High Intensity	2815.286	ab	
3	Developed, Low Intensity	2564.359	ab	
4	Estuarine Scrub/Shrub Wetland	2475	abc	
5	Developed, Open Space	2309.226	abc	
6	Palustrine Forested Wetland	2274.263	bc	
7	Deciduous Forest	2216.77	bc	
8	Palustrine Scrub/Shrub Wetland	2210.347	bc	
9	Scrub/Shrub	2205.944	bc	
10	Pasture/Hay	2139.046	c	
11	Estuarine Emergent Wetland	2134.113	c	
12	Grassland/Herbaceous	2131.452	c	
13	Unconsolidated Shore	2121.211	c	
14	Grassland/Herbaceous	2111.739	c	
15	Evergreen Forest	2102.87	c	
16	Cultivated Crops	2072.287	c	
17	Bare Land	2036.2	c	
18	Mixed Forest	1986.53	c	
19	Palustrine Aquatic Bed	1960.222	c	
20	Open Water	1937.796	c	
21	Estuarine Aquatic Bed	1925.667	c	

Table 4.7 As in Table 4.5, but for 2006.

Degrees of Freedom	Number of Treatments	F	Scheffé	alpha
5673	21	1.572378	5.607813	0.05
Rankings	Land Class	Means	Groupings	
1	Developed, Medium Intensity	3066.667	a	
2	Developed, High Intensity	2687.412	ab	
3	Developed, Low Intensity	2568.977	ab	
4	Estuarine Scrub/Shrub Wetland	2475	abc	
5	Developed, Open Space	2302.667	bc	
6	Palustrine Forested Wetland	2277.231	bc	
7	Deciduous Forest	2216.77	bc	
8	Scrub/Shrub	2183.274	bc	
9	Palustrine Scrub/Shrub Wetland	2148.618	bc	
10	Estuarine Emergent Wetland	2132.895	bc	
11	Palustrine Emergent Wetland	2131.076	bc	
12	Pasture/Hay	2122.023	c	
13	Evergreen Forest	2108.149	c	
14	Grassland/Herbaceous	2091.439	c	
15	Unconsolidated Shore	2085.75	c	
16	Cultivated Crops	2074.499	c	
17	Bare Land	2062	c	
18	Palustrine Aquatic Bed	1996.889	c	
19	Estuarine Aquatic Bed	1996.6	c	
20	Mixed Forest	1969.573	c	
21	Open Water	1940.804	c	

Table 4.8 As in Table 4.5, but for 2010.

Degrees of Freedom	Number of Treatments	F	Scheffé	alpha
5673	21	1.572378	5.607813	0.05
Rankings	Land Class	Means	Groupings	
1	Developed, Medium Intensity	3037.882	a	
2	Developed, High Intensity	2734.273	ab	
3	Developed, Low Intensity	2537.545	ab	
4	Estuarine Aquatic Bed	2523.75	abc	
5	Estuarine Scrub/Shrub Wetland	2475	abc	
6	Developed, Open Space	2342.576	bc	
7	Palustrine Forested Wetland	2274.813	bc	
8	Evergreen Forest	2213.618	bc	
9	Deciduous Forest	2172.527	bc	
10	Scrub/Shrub	2160.984	c	
11	Palustrine Emergent Wetland	2133.588	c	
12	Estuarine Emergent Wetland	2127.178	c	
13	Pasture/Hay	2126.409	c	
14	Grassland/Herbaceous	2124.594	c	
15	Unconsolidated Shore	2110.455	c	
16	Evergreen Forest	2107.462	c	
17	Cultivated Crops	2070.917	c	
18	Bare Land	2007.25	c	
19	Mixed Forest	1981.288	c	
20	Open Water	1945.295	c	
21	Palustrine Aquatic Bed	1916.133	c	

each other. LULCs with multiple tags, such as “ab” or “abc”, have means that do not differ significantly from the means of any of the groups in their tags.

The LULC types with the five highest lightning frequencies generally remain consistent over the course of the 15-year study period. The LULCs that have the highest three means are “developed” (medium-, high-, and low-intensity, respectively). Outside of the top three, the significance in differences and changes in means fluctuate across the years. Between 1996 and 2001, changes occurred among the eight highest means, but with no significant changes of the groups. Between 2001 and 2006, although there are small fluctuations in lightning means, there are few significant changes in CG lightning groups. Between 2006 and 2010, there are a couple of significant changes in groupings. Estuarine aquatic bed is ranked 4th in 2010, but it was only ranked 19th in 2006. In addition, estuarine and palustrine emergent wetland, as well as scrub/shrub, fell to the third category (c) by 2010. Major changes from 1996 to 2010 are estuarine aquatic bed increasing in lightning frequency from among the lowest LULC types to among the highest. This could be due to a change in the amount of estuarine aquatic bed over time, but figure 3.9 states there was no change. Since it is known that Louisiana is experiencing coastal erosion (Williams et al., 2012; Visser et al., 2013), aquatic environments are changing constantly, and could result in changing land-air interactions as well.

4.4 Geographically Weighted Regression

Results from the GWR show static values between all four years of LULC classification data studied. Total lightning frequencies from 1995 to 2011 were utilized as the dependent variable, and the LULC classes for each year were the independent variable. Based on the weight placed on spatial coordinates by the GWR and the derivation of coordinates from raster data that were affixed to each 4 km x 4 km cell across the study region, few spatial differences in

coordinates occurred between years. Residual maps with associated R^2 and adjusted R^2 values for southern Louisiana (Figures 4.23–4.26) show little change in residuals for each LULC classification year studied. Results are only shown for southern Louisiana because of the extent of the data. This result corroborates the residual maps provided by the linear regression test, which showed little inter-annual variation in residuals, but only differences in p-values between lightning relationships and LULC classes. The Akaike Information Criterion (AIC; Fotheringham, 2002) determines the extent of the kernel used for calculating GWR. Conditional number determines if local collinearity is present. Any value above 30 represents collinearity (Fotheringham, 2002), which we do not see for any year examined. Local R^2 evaluates the fit of a local regression model fits, and the standard residuals and predicted values are used to measure over and under-prediction as well as accuracy of the model. Lastly, areas along the coast, and the Baton Rouge metropolitan area have high R^2 values compared to their surrounding locations. This is most likely due to a cluster of higher values and urban environments as seen in the lightning climatology and Scheffé's analysis.

Variable	Value
Bandwidth	49591.10953
Residual Squares	205761685.4
Effective Number	43.33715219
Sigma	190.8238073
AICc	75981.34628
R ²	0.274347414
R ² Adjusted	0.268910519

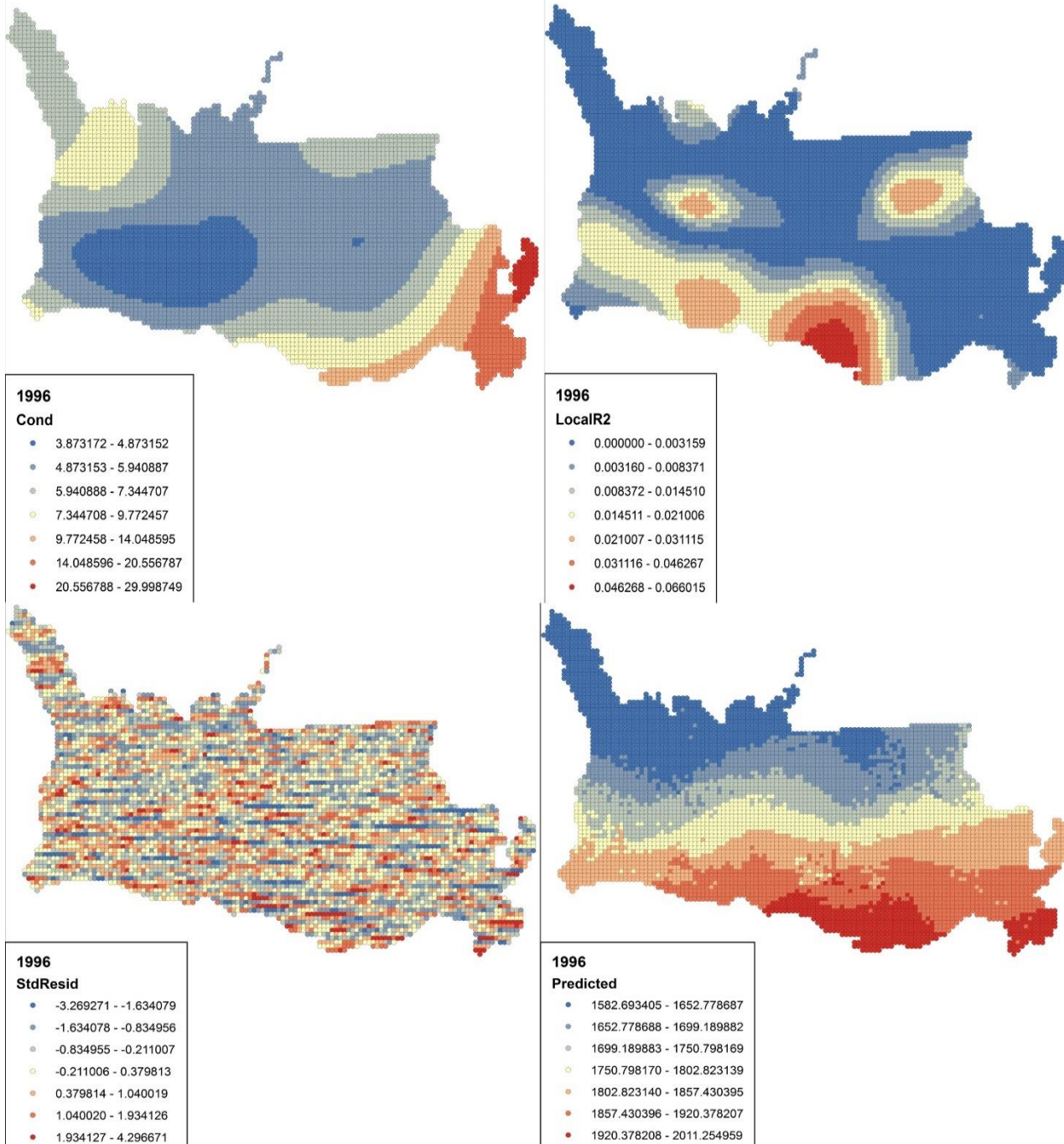


Figure 4.23 Resulting conditional number, local R², standard residuals, and predicted values from GWR output between total lightning frequency between 1996 land classes and total lightning.

Variable	Value
Bandwidth	49591.10953
Residual Squares	205761737.9
Effective Number	43.35031189
Sigma	190.8240538
AICc	75981.36291
R ²	0.274347229
R ² Adjusted	0.26890863

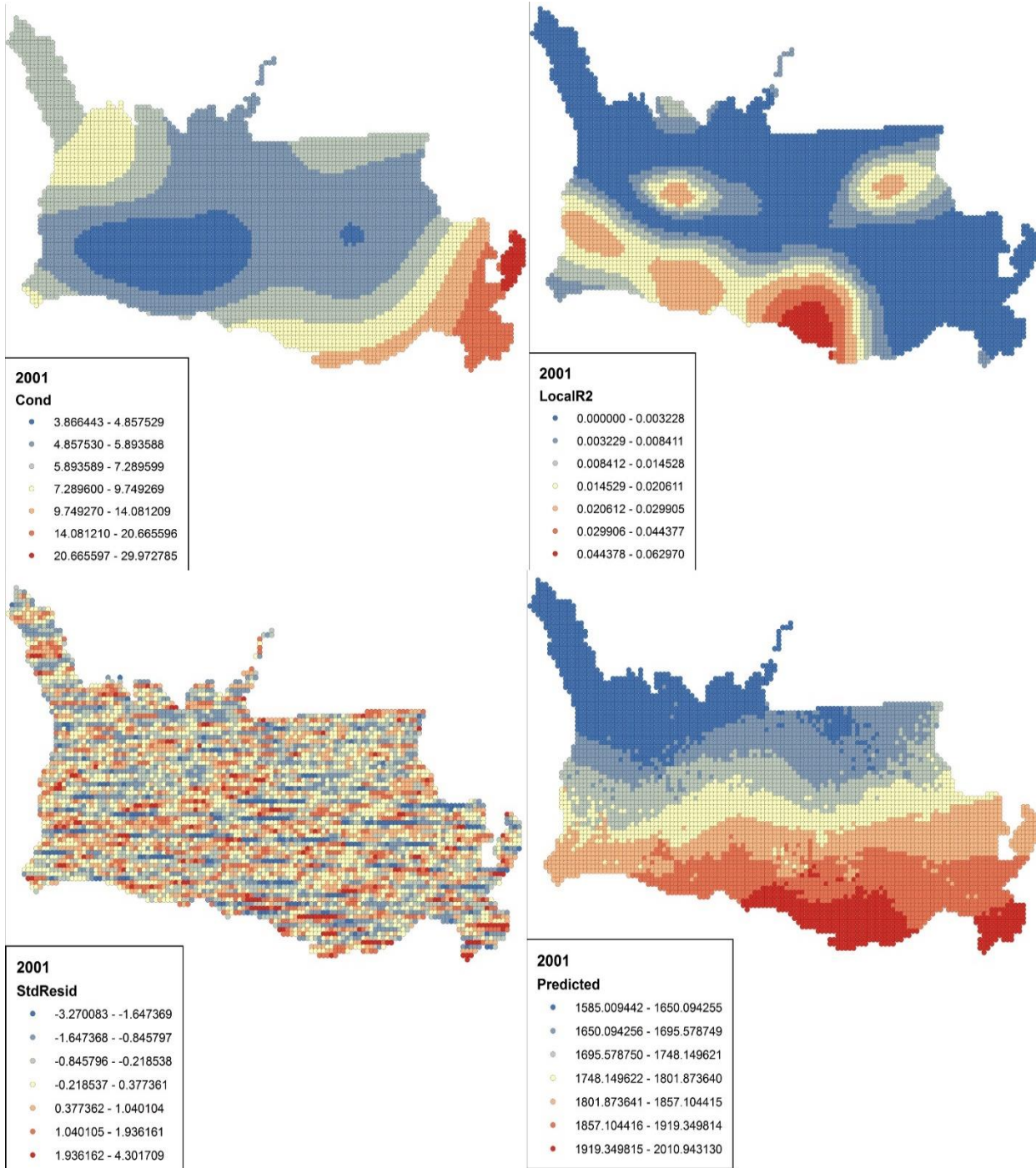


Figure 4.24 As in Figure 4.23 but for 2001.

Variable	Value
Bandwidth	49819.57837
Residual Squares	205814280.6
Effective Number	43.13758223
Sigma	190.8448241
AICc	75982.53375
R ²	0.274161929
R ² Adjusted	0.26874947

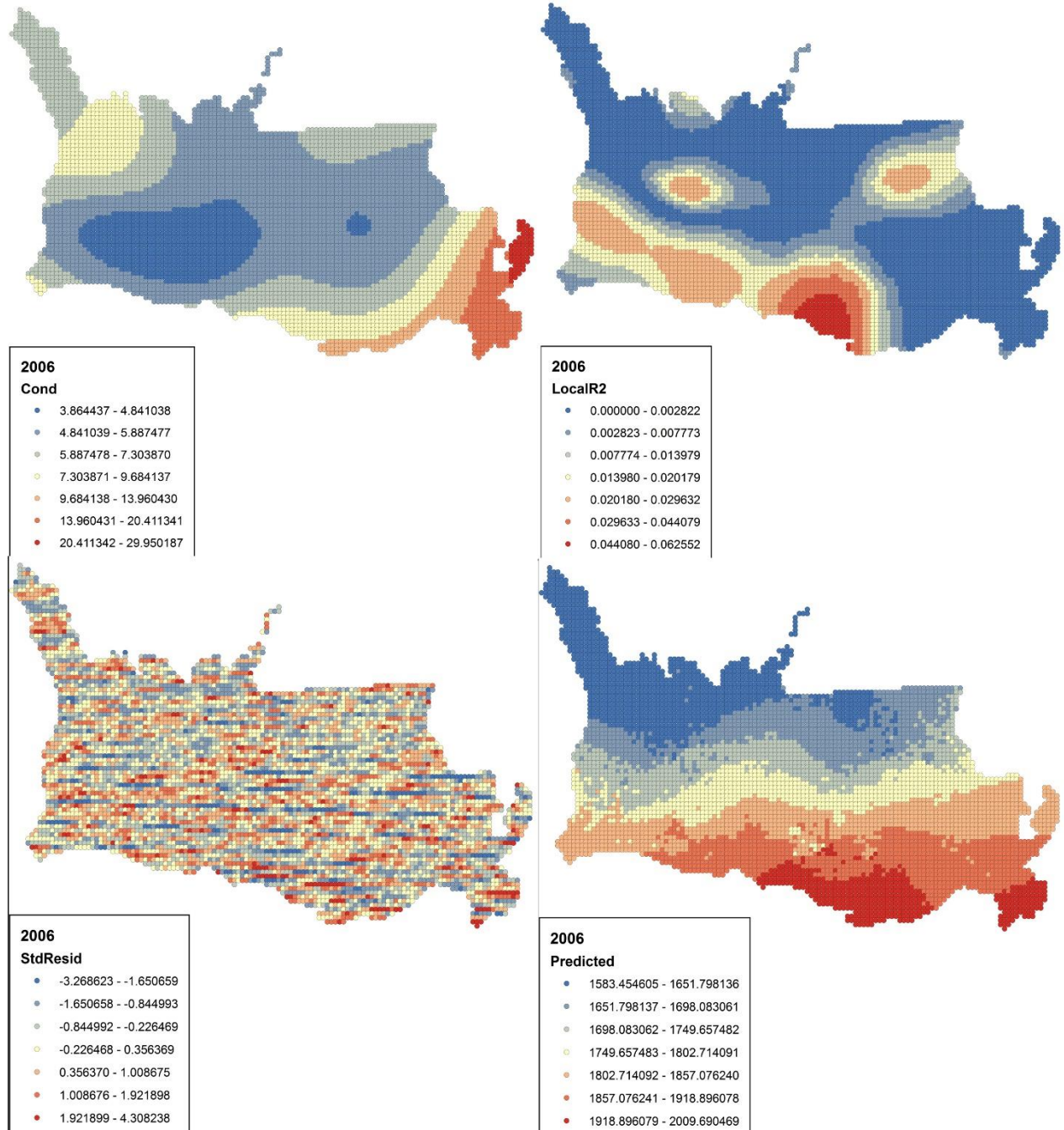


Figure 4.25 As in Figure 4.23 but for 2006.

Variable	Value
Bandwidth	49819.57837
Residual Squares	205886943.3
Effective Number	43.26697396
Sigma	190.8806953
AICc	75984.71472
R ²	0.273905672
R ² Adjusted	0.268474552

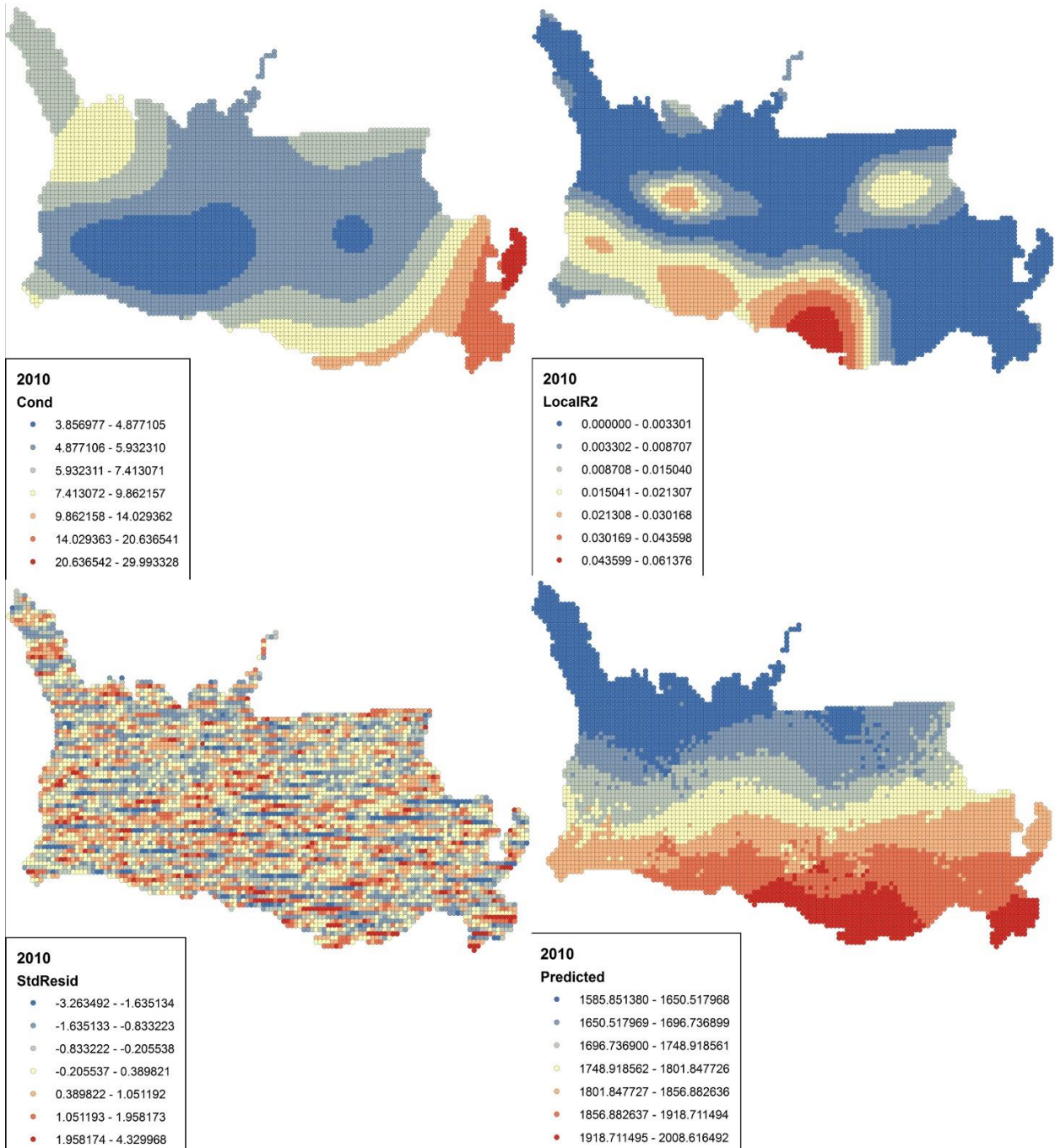


Figure 4.26 As in Figure 4.23 but for 2010.

Chapter 5. Summary/Conclusions

“I am turned into a sort of machine for observing facts and grinding out conclusions.”

– Charles Darwin

Lightning is one of the most dangerous hazards. Because the population of the central Gulf of Mexico coast region is growing, LULC is continually changing to satisfy the needs of residents, as well as enhance the area by providing new services to the public. On the other hand, human interaction and change of environments are impacting typical processes and patterns, including lightning, indirectly altering conditions across the region. While lightning deaths have decreased nationally (Curran et al., 2000; NWS, 2016), it is important to maintain an accurate assessment of all severe weather impacts in the U.S. to mitigate further damage.

The results of this study yielded insightful observations regarding the patterns and placement of CG lightning in southern Louisiana and its peripheral areas. The lightning climatology revealed inter-annual frequency and spatial fluctuations for the study area. One interesting feature is that CG lightning always appears to have its strongest values over land, which coincide with the results of previous research (Orville et al., 2001; LaJoie & Laing, 2008; Rose et al., 2008). Another interesting observation from the lightning climatology is the sudden increase in lightning totals leading up to 2005 when the Gulf Coast experienced an extreme hurricane season. While this study does not necessarily suggest there is a relationship between hurricanes and lightning, the environment around that time should be investigated further for any possible connection. After 2005, there was a sharp decrease in the frequency of CG lightning in the area. While the trend analysis was not statistically significant, an anomalous period of increased total lightning between 2003 and 2005 could generate questions about whether changes in temperature or meteorological forcing mechanisms influenced CG lightning in the region.

The results of the linear regression analysis showed strong relationships between all LULC classes and lightning frequency except for developed medium-intensity and estuarine forested wetland. Results from Scheffé's test showed that lightning frequencies in developed medium-intensity cells were the highest for all four years of LULC classification analyzed. Results from GWR showed very little change in relationship between LULC and lightning frequencies for the 1996–2010 period. However, this result could be influenced by the spatial constraint of the point data. Further analysis with point data would need to be completed to ascertain the true characteristics of the spatio-temporal patterns of lightning.

Among the other LULC categories, results were mostly consistent between years. This result is likely due to prevailing climatic patterns, which determine where electrified storms occur and how much lightning is experienced within that region, and/or the small number of years analyzed. While the highest means of lightning are in urbanized LULC types, there is some possibility that the result occurs not because of increased lightning rates over these types but instead because of increased frequency of thunderstorm tracks over urban areas (Maier et al., 1981; Nastos et al., 2014). It is in this regard that a higher-resolution data set could provide more insight into the location of CG lightning flashes over time.

The sudden increase in lightning frequency of the estuarine aquatic bed LULC type to the top three could again be due to a change in climate forcing mechanisms, or (more likely) due to the observed local changes in that LULC category (eg. Lightning rod installation or industrial equipment), thereby enhancing the amount of lightning observed over that class. On land, a temporal decrease in lightning frequency over deciduous forests occurred, along with an increase in evergreen forests. Again, these results could be due to changes in LULC, as shown in Figure 3.9.

Overall, the results of this thesis provided an abundance of information regarding LULC relationship to lightning frequency. While urbanized areas tend to have the highest mean lightning frequencies on a per-pixel basis, variation in other LULC means could lead to greater shifts in lightning amounts between LULC categories besides the urban types. In addition, with several ocean, coastal, and land modifications being undertaken in the area now, future trends could see an increase in urban lightning totals due to more development spurred by population growth. Ultimately, it is hoped that the results of this thesis will help inhabitants of the Gulf, particularly in Louisiana, to better prepare for severe thunderstorms and provide industrial management teams and environmental planners the information needed to establish greater safety measures to prevent or mitigate damages.

References

- Antonescu, B., & Burcea, S. (2010). A cloud-to-ground lightning climatology for Romania. *Monthly Weather Review*, 138(2), 579–591. doi:10.1175/2009mwr2975.1
- Ashley, W. S., Bentley, M. L., & Stallins, A. J. (2012). Urban-induced thunderstorm modification in the southeast United States. *Climatic Change*, 113(2), 481–498.
- Beirle, S., Koshak, W., Blakeslee, R., & Wagner, T. (2014). Global patterns of lightning properties derived by OTD and LIS. *Natural Hazards and Earth System Sciences*, 14(10), 2715–2726. doi:10.5194/nhess-14-2715-2014
- Bentley, M. L., & Stallins, J. A. (2005). Climatology of cloud-to-ground lightning in Georgia, USA, 1992–2003. *International Journal of Climatology*, 25(15), 1979–1996. doi:10.1002/joc.1227
- Biagi, C. J., Cummins, K. L., Kehoe, K. E., & Krider, E. P. (2007). National lightning detection network (NLDN) performance in southern Arizona, Texas, and Oklahoma in 2003–2004. *Journal of Geophysical Research-Atmospheres*, 112(D5), 17. doi:10.1029/2006jd007341
- Blakeslee, R. J., Mach, D. M., Bateman, M. G., & Bailey, J. C. (2014). Seasonal variations in the lightning diurnal cycle global electric circuit. *Atmospheric Research*, 135, 228–243. doi:10.1016/j.atmosres.2012.09.023
- Boccippio, D. J., Koshak, W., Blakeslee, R., Driscoll, K., Mach, D., Buechler, D., Goodman, S. J. (2000). The optical transient detector (OTD): Instrument characteristics and cross-sensor validation. *Journal of Atmospheric and Oceanic Technology*, 17(4), 441–458. doi:10.1175/1520-0426(2000)017<0441:totdoi>2.0.co;2
- Boccippio, D. J., Koshak, W. J., & Blakeslee, R. J. (2002). Performance assessment of the optical transient detector and lightning imaging sensor. Part I: Predicted diurnal variability. *Journal of Atmospheric and Oceanic Technology*, 19(9), 1318–1332. doi:10.1175/1520-0426(2002)019<1318:paotot>2.0.co;2
- Buechler, D. E., Koshak, W. J., Christian, H. J., & Goodman, S. J. (2014). Assessing the performance of the lightning imaging sensor (LIS) using deep convective clouds. *Atmospheric Research*, 135, 397–403. doi:10.1016/j.atmosres.2012.09.008
- Burrows, W. R., King, P., Lewis, P. J., Kochtubajda, B., Snyder, B., & Turcotte, V. (2002). Lightning occurrence patterns over Canada and adjacent United States from lightning detection network observations. *Atmosphere-Ocean*, 40(1), 59–80. doi:10.3137/ao.400104

Burrows, W. R., & Kochtubajda, B. (2010). A decade of cloud-to-ground lightning in Canada: 1999–2008. Part 1: Flash density and occurrence. *Atmosphere-Ocean*, 48(3), 177–194. doi:10.3137/ao1118.2010

Cardille, J. A., & Foley, J. A. (2003). Agricultural land-use change in Brazilian Amazonia between 1980 and 1995: Evidence from integrated satellite and census data. *Remote Sensing of Environment*, 87(4), 551–562. doi:10.1016/j.rse.2002.09.001

Carey, L. D., & Rutledge, S. A. (2003). Characteristics of cloud-to-ground lightning in severe and nonsevere storms over the central United States from 1989–1998. *Journal of Geophysical Research-Atmospheres*, 108(D15), 21. doi:10.1029/2002jd002951

Cecil, D. J., Buechler, D. E., & Blakeslee, R. J. (2014). Gridded lightning climatology from TRMM-LIS and OTD: Dataset description. *Atmospheric Research*, 135, 404–414. doi:10.1016/j.atmosres.2012.06.028

Contiu, S., & Groza, A. (2016). Improving remote sensing crop classification by argumentation-based conflict resolution in ensemble learning. *Expert Systems with Applications*, 64, 269–286. doi:10.1016/j.eswa.2016.07.037

Changnon, S. A. (1988a). Climatography of thunder events in the conterminous United States. Part I: Temporal aspects. *Journal of Climate*, 1(4), 389–398. doi:10.1175/1520-0442(1988)001<389:coteit>2.0.co;2

Changnon, S. A. (1988b). Climatography of thunder events in the conterminous United States. Part II: Spatial aspects. *Journal of Climate*, 1(4), 399–405. doi:10.1175/1520-0442(1988)001<399:coteit>2.0.co;2

Chen, X. L., Zhao, H. M., Li, P. X., & Yin, Z. Y. (2006). Remote sensing image-based analysis of the relationship between urban heat island and land use/cover changes. *Remote Sensing of Environment*, 104(2), 133–146. doi:10.1016/j.rse.2005.11.016

Collier, A. B., Hughes, A. R. W., Lichtenberger, J., & Steinbach, P. (2006). Seasonal and diurnal variation of lightning activity over southern Africa and correlation with European whistler observations. *Annales Geophysicae*, 24(2), 529–542.

Cooray, V. (2015). *An Introduction to Lightning*. <http://dx.doi.org/10.1007/978-94-017-8938-7>. Dordrecht, Netherlands: Springer, 386 pp.

Cummins, K. L., & Murphy, M. J. (2009). An overview of lightning locating systems: History, techniques, and data uses, with an in-depth look at the U.S. NLDN. *IEEE Transactions on Electromagnetic Compatibility*, 51(3), 499–518. doi:10.1109/temc.2009.2023450

Curran, E. B., Holle, R. L., & López, R. E. (2000). Lightning casualties and damages in the United States from 1959 to 1994. *Journal of Climate*, 13(19), 3448–3464. doi:10.1175/1520-0442(2000)013<3448:LCADIT>2.0.CO;2

- Cramer, J. A., & Cummins, K. L. (2014, March). Evaluating location accuracy of lightning location networks using tall towers. In *23rd International Lightning Detection Conference & 5th International Lightning Meteorology Conference*, 18–21.
- Demetriades, N. W., Murphy, M. J., & Cramer, J. A. (2010, April). Validation of Vaisala's global lightning dataset (GLD360) over the continental United States. In *Preprints, 29th Conference on Hurricanes and Tropical Meteorology, Tucson, AZ, American Meteorological Society D* (Vol. 16).
- Dewan, A. M., & Yamaguchi, Y. (2009). Land use and land cover change in greater Dhaka, Bangladesh: Using remote sensing to promote sustainable urbanization. *Applied Geography*, 29(3), 390-401. doi:10.1016/j.apgeog.2008.12.005
- Dowdy, A. J. (2016). Seasonal forecasting of lightning and thunderstorm activity in tropical and temperate regions of the world. *Scientific Reports*, 6. doi:10.1038/srep20874
- Dowdy, A. J., & Kuleshov, Y. (2014). Climatology of lightning activity in Australia: Spatial and seasonal variability. *Australian Meteorological and Oceanographic Journal*, 64(2), 103–108.
- Easterling, D. R., & Robinson, P. J. (1985). The diurnal-variation of thunderstorm activity in the United-States. *Journal of Climate and Applied Meteorology*, 24(10), 1048–1058. doi:10.1175/1520-0450(1985)024<1048:tdvota>2.0.co;2
- Esri. (2016). Raster processing toolset: resample. *Tool Reference*. <https://pro.arcgis.com/en/pro-app/tool-reference/data-management/resample.html>
- Fan, F. L., Weng, Q. H., & Wang, Y. P. (2007). Land use and land cover change in Guangzhou, China, from 1998 to 2003, based on Landsat TM/ETM+ imagery. *Sensors*, 7(7), 1323–1342. doi:10.3390/s7071323
- Freund, R. J., Wilson, W. J., & Mohr, D. L. (2010). *Statistical Methods*. Third edition. Burlington, MA: Academic Press, 824 pp.
- Fotheringham, A. S., Brunsdon, C., & Charlton, M. (2002). *Geographically Weighted Regression: The Analysis of Spatially Varying Relationships*. West Sussex, UK: Wiley. 284 pp.
- GISpopsci. (2016). Geographically weighted regression: Introduction to Geographically Weighted Regression. In *Advanced Spatial Analysis*. <http://gispopsci.org/geographically-weighted-regression/>
- Haberlie, A. M., Ashley, W. S., & Pingel, T. J. (2015). The effect of urbanisation on the climatology of thunderstorm initiation. *Quarterly Journal of the Royal Meteorological Society*, 141(688), 663–675. doi:10.1002/qj.2499

- Hodanish, S., Sharp, D., Collins, W., Paxton, C., & Orville, R. E. (1997). A 10-yr monthly lightning climatology of Florida: 1986–95. *Weather and Forecasting*, 12(3), 439–448. doi:10.1175/1520-0434(1997)012<439:aymlco>2.0.co;2
- Holle, R. L. (2014). Diurnal variations of NLDN-reported cloud-to-ground lightning in the United States. *Monthly Weather Review*, 142(3), 1037–1052. doi:10.1175/mwr-d-13-00121.1
- Holle, R. L., & Murphy, M. J. (2015). Lightning in the North American monsoon: An exploratory climatology. *Monthly Weather Review*, 143(5), 1970–1977. doi:10.1175/mwr-d-14-00363.1
- Holle, R. (2016). Lightning fatalities by state, 2005–2014. *Vaisala Inc.* http://www.lightningsafety.noaa.gov/stats/05-14deaths_by_state_maps.pdf
- Hu, H., Wang, J., & Pan, J. (2014). The characteristics of lightning risk and zoning in Beijing simulated by a risk assessment model. *Natural Hazards and Earth System Sciences*, 14(8), 1985–1997. doi:10.5194/nhess-14-1985-2014
- Huang, C. Q., Goward, S. N., Schleeweis, K., Thomas, N., Masek, J. G., & Zhu, Z. L. (2009). Dynamics of national forests assessed using the Landsat record: Case studies in eastern United States. *Remote Sensing of Environment*, 113(7), 1430–1442. doi:10.1016/j.rse.2008.06.016
- Huffines, G. R., & Orville, R. E. (1999). Lightning ground flash density and thunderstorm duration in the continental United States: 1989–96. *Journal of Applied Meteorology*, 38(7), 1013–1019. doi:10.1175/1520-0450(1999)038<1013:lgfdat>2.0.co;2
- Idone, V. P., Davis, D. A., Moore, P. K., Wang, Y., Henderson, R. W., Ries, M., & Jamason, P. F. (1998). Performance evaluation of the US national lightning detection network in eastern New York - 1. Detection efficiency. *Journal of Geophysical Research-Atmospheres*, 103(D8), 9045–9055. doi:10.1029/98jd00154
- Jacobson, A. R., Holzworth, R., Harlin, J., Dowden, R., & Lay, E. (2006). Performance assessment of the world-wide lightning location network (WWLLN), using the Los Alamos sferic array (LASA) as ground truth. *Journal of Atmospheric and Oceanic Technology*, 23(8), 1082–1092. doi:10.1175/jtech1902.1
- James, G., Witten, D., Hastie, T., and Tibshirani, R. (2013). *An Introduction to Statistical Learning with Applications in R*. Springer, New York.
- Jensen, J. R. (1981). Urban change detection mapping using Landsat digital data. *American Cartographer*, 8(2), 127–147.

- Ju, J. C., & Roy, D. P. (2008). The availability of cloud-free Landsat ETM plus data over the conterminous United States and globally. *Remote Sensing of Environment*, 112(3), 1196–1211. doi:10.1016/j.rse.2007.08.011
- Kalnay, E., & Cai, M. (2003). Impact of urbanization and land-use change on climate. *Nature*, 423(6939), 528–531. doi:10.1038/nature01675
- Koshak, W. J., Cummins, K. L., Buechler, D. E., Vant-Hull, B., Blakeslee, R. J., Williams, E. R., & Peterson, H. S. (2015). Variability of CONUS lightning in 2003–12 and associated impacts. *Journal of Applied Meteorology and Climatology*, 54(1), 15–41. doi:10.1175/jamc-d-14-0072.1
- Laing, A., LaJoie, M., Reader, S., & Pfeiffer, K. (2008). The influence of the El Niño-Southern Oscillation on cloud-to-ground lightning activity along the Gulf Coast. Part II: Monthly correlations. *Monthly Weather Review*, 136(7), 2544–2556. doi:10.1175/2007mwr2228.1
- LaJoie, M., & Laing, A. (2008). The influence of the El Niño-Southern Oscillation on cloud-to-ground lightning activity along the Gulf Coast. Part I: Lightning climatology. *Monthly Weather Review*, 136(7), 2523–2542. doi:10.1175/2007mwr2227.1
- Lericos, T. P., Fuelberg, H. E., Watson, A. I., & Holle, R. L. (2002). Warm season lightning distributions over the Florida peninsula as related to synoptic patterns. *Weather and Forecasting*, 17(1), 83–98. doi:10.1175/1520-0434(2002)017<0083:wsldot>2.0.co;2
- Liu, J. Y., Liu, M. L., Tian, H. Q., Zhuang, D. F., Zhang, Z. X., Zhang, W., . . . Deng, X. Z. (2005). Spatial and temporal patterns of China's cropland during 1990–2000: An analysis based on Landsat TM data. *Remote Sensing of Environment*, 98(4), 442–456. doi:10.1016/j.rse.2005.08.012
- Lyon, J. G., Yuan, D., Lunetta, R. S., & Elvidge, C. D. (1998). A change detection experiment using vegetation indices. *Photogrammetric Engineering and Remote Sensing*, 64(2), 143–150.
- López, R. E., & Holle, R. L. (1998). Changes in the number of lightning deaths in the United States during the twentieth century. *Journal of Climate*, 11(8), 2070–2077. doi:doi:10.1175/1520-0442-11.8.2070
- Mach, D. M., Christian, H. J., Blakeslee, R. J., Boccippio, D. J., Goodman, S. J., & Boeck, W. L. (2007). Performance assessment of the optical transient detector and lightning imaging sensor. *Journal of Geophysical Research-Atmospheres*, 112(D9), 16. doi:10.1029/2006jd007787
- MacLaurin, G. J., & Leyk, S. (2016). Extending the geographic extent of existing land cover data using active machine learning and covariate shift corrective sampling. *International Journal of Remote Sensing*, 37(21), 5213–5233. doi:10.1080/01431161.2016.1230285

- Maier, M. W., & Piotrowicz, J. M. (1981). A lightning ground flash density climatology for the United-States. *Bulletin of the American Meteorological Society*, 62(9), 1403–1403.
- Makela, A., Rossi, P., & Schultz, D. M. (2011). The daily cloud-to-ground lightning flash density in the contiguous United States and Finland. *Monthly Weather Review*, 139(5), 1323–1337. doi:10.1175/2010mwr3517.1
- Mallick, S., Rakov, V. A., Hill, J. D., Ngin, T., Gamerota, W. R., Pilkey, J. T., Nag, A. (2014). Performance characteristics of the NLDN for return strokes and pulses superimposed on steady currents, based on rocket-triggered lightning data acquired in Florida in 2004–2012. *Journal of Geophysical Research-Atmospheres*, 119(7), 3825–3856. doi:10.1002/2013jd021401
- Massey, F. J. (1951). The kolmogorov-smirnov test for goodness of fit. *Journal of the American Statistical Association*, 46(253), 68-78. doi:10.1080/01621459.1951.10500769
- Murphy, M. S., & Konrad, C. E. (2005). Spatial and temporal patterns of thunderstorm events that produce cloud-to-ground lightning in the interior southeastern United States. *Monthly Weather Review*, 133(6), 1417–1430. doi:10.1175/mwr2924.1
- Naccarato, K. P., Pinto, O., & Pinto, I. (2003). Evidence of thermal and aerosol effects on the cloud-to-ground lightning density and polarity over large urban areas of southeastern Brazil. *Geophysical Research Letters*, 30(1674). doi:10.1029/2003gl017496, 13
- NASA. (2016). Lightning and Atmospheric Electricity Research. *Global Hydrology Resource Center*. https://lightning.nsstc.nasa.gov/data/data_lis-otd-climatology.html.
- Nastos, P. T., Matsangouras, I. T., & Chronis, T. G. (2014). Spatio-temporal analysis of lightning activity over Greece - preliminary results derived from the recent state precision lightning network. *Atmospheric Research*, 144, 207–217. doi:10.1016/j.atmosres.2013.10.021
- NWS. (2015). How dangerous is lightning?. *National Oceanic and Atmospheric Administration and National Weather Service*. <http://www.lightningsafety.noaa.gov/odds.shtml>
- NWS. (2016). United States lightning deaths. *National Weather Service*. <http://www.lightningsafety.noaa.gov/fatalities.shtml>
- Orville, R. E., Huffines, G., Nielsen-Gammon, J., Zhang, R. Y., Ely, B., Steiger, S., Read, W. (2001). Enhancement of cloud-to-ground lightning over Houston, Texas. *Geophysical Research Letters*, 28(13), 2597–2600. doi:10.1029/2001gl012990
- Orville, R. E., & Huffines, G. R. (1999). Lightning ground flash measurements over the contiguous United States: 1995-97. *Monthly Weather Review*, 127(11), 2693–2703. doi:10.1175/1520-0493(1999)127<2693:lgfmot>2.0.co;2

- Pinto, O., Pinto, I., & Naccarato, K. P. (2007). Maximum cloud-to-ground lightning flash densities observed by lightning location systems in the tropical region: A review. *Atmospheric Research*, 84(3), 189–200. doi:10.1016/j.atmosres.2006.11.007
- Rakov, V. A., & Uman, M. A. (2003). *Lightning: Physics and Effects*: Cambridge University Press. Pp. 1-700.
- Roeder, W. P., Cummins, B. H., Cummins, K. L., Holle, R. L., & Ashley, W. S. (2015). Lightning fatality risk map of the contiguous United States. *Natural Hazards*, 79(3), 1681–1692. doi:10.1007/s11069-015-1920-6
- Rose, L. S., Stallins, J. A., & Bentley, M. L. (2008). Concurrent cloud-to-ground lightning and precipitation enhancement in the Atlanta, Georgia (United States), urban region. *Earth Interactions*, 12. doi:10.1175/2008ei265.1
- Rudlosky, S. D., & Shea, D. T. (2013). Evaluating WWLLN performance relative to trmm/lis. *Geophysical Research Letters*, 40(10), 2344–2348. doi:10.1002/grl.50428
- Scanlon, B. R., Reedy, R. C., Stonestrom, D. A., Prudic, D. E., & Dennehy, K. F. (2005). Impact of land use and land cover change on groundwater recharge and quality in the southwestern us. *Global Change Biology*, 11(10), 1577–1593. doi:10.1111/j.1365-2486.2005.01026.x
- Scheffé, H. (1959). *The Analysis of Variance*. New York: John Wiley. 477 pp.
- Schultz, C. J., Petersen, W. A., & Carey, L. D. (2011). Lightning and severe weather: A comparison between total and cloud-to-ground lightning trends. *Weather and Forecasting*, 26(5), 744–755. doi:10.1175/waf-d-10-05026.1
- Sen Roy, S., & Balling, R. C. (2013). Spatial patterns of diurnal variations in summer-season lightning activity across the tropical and subtropical regions of the northern hemispheric Americas. *Meteorology and Atmospheric Physics*, 121(3–4), 199–206. doi:10.1007/s00703-013-0259-3
- Seneviratne, S. I., Luthi, D., Litschi, M., & Schar, C. (2006). Land-atmosphere coupling and climate change in Europe. *Nature*, 443(7108), 205–209. doi:10.1038/nature05095
- Seto, K. C., Woodcock, C. E., Song, C., Huang, X., Lu, J., & Kaufmann, R. K. (2002). Monitoring land-use change in the Pearl River delta using Landsat TM. *International Journal of Remote Sensing*, 23(10), 1985–2004. doi:10.1080/01431160110075532
- Shalaby, A., & Tateishi, R. (2007). Remote sensing and GIS for mapping and monitoring land cover and land-use changes in the northwestern coastal zone of Egypt. *Applied Geography*, 27(1), 28–41. doi:10.1016/j.apgeog.2006.09.004

- Singh, A. (1988). Digital change detection techniques using remotely-sensed data. *International Journal of Remote Sensing*, 10(6), 983–1003.
doi:<http://dx.doi.org/10.1080/01431168908903939>
- Smith, J. R., Fuelberg, H. E., & Watson, A. I. (2005). Warm season lightning distributions over the northern Gulf of Mexico coast and their relation to synoptic-scale and mesoscale environments. *Weather and Forecasting*, 20(4), 415–438. doi:10.1175/WAF870.1
- Stallins, J. A., & Bentley, M. L. (2006). Urban lightning climatology and GIS: An analytical framework from the case study of Atlanta, Georgia. *Applied Geography*, 26(3-4), 242–259. doi:10.1016/j.apgeog.2006.09.008
- Steiger, S. M., Orville, R. E., & Huffines, G. (2002). Cloud-to-ground lightning characteristics over Houston, Texas: 1989–2000. *Journal of Geophysical Research-Atmospheres*, 107(D11), 18. doi:10.1029/2001jd001142
- Tan, K. C., Lim, H. S., MatJafri, M. Z., & Abdullah, K. (2010). Landsat data to evaluate urban expansion and determine land use/land cover changes in Penang Island, Malaysia. *Environmental Earth Sciences*, 60(7), 1509–1521. doi:10.1007/s12665-009-0286-z
- Tang, Z., Engel, B. A., Pijanowski, B. C., & Lim, K. J. (2005). Forecasting land use change and its environmental impact at a watershed scale. *Journal of Environmental Management*, 76(1), 35–45. doi:10.1016/j.jenvman.2005.01.006
- Timmaker, M. I. R., Aslam, M. Y., & Chate, D. M. (2014). Climatology of lightning activity over the Indian seas. *Atmosphere-Ocean*, 52(4), 314–320.
doi:10.1080/07055900.2014.941323
- Todd, W. J. (1977). Urban and regional land-use change detected by using Landsat data. *Journal of Research of the U.S. Geological Survey*, 5(5), 529–534.
- Ushio, T., Heckman, S., Driscoll, K., Boccippio, D., Christian, H., & Kawasaki, Z. (2002). Cross-sensor comparison of the lightning imaging sensor (LIS). *International Journal of Remote Sensing*, 23(13), 2703–2712. doi:10.1080/01431160110107789
- Villarini, G., & Smith, J. A. (2013). Spatial and temporal variability of cloud-to-ground lightning over the continental US during the period 1995–2010. *Atmospheric Research*, 124, 137–148. doi:10.1016/j.atmosres.2012.12.017
- Virts, K. S., Wallace, J. M., Hutchins, M. L., & Holzworth, R. H. (2013). Highlights of a new ground-based, hourly global lightning climatology. *Bulletin of the American Meteorological Society*, 94(9), 1381–1391. doi:10.1175/bams-d-12-00082.1
- Virts, K. S., Wallace, J. M., Hutchins, M. L., & Holzworth, R. H. (2015). Diurnal and seasonal lightning variability over the Gulf Stream and the Gulf of Mexico. *Journal of the Atmospheric Sciences*, 72(7), 2657–2665. doi:10.1175/jas-d-14-0233.1

Visser, J. M., Duke-Sylvester, S. M., Carter, J., & Broussard III, W. P. (2013). A computer model to forecast wetland vegetation changes resulting from restoration and protection in coastal Louisiana. *Journal of Coastal Research*, 67(sp1), 51-59.

Vogelmann, J. E., Sohl, T. L., Campbell, P. V., & Shaw, D. M. (1998). Regional land cover characterization using Landsat thematic mapper data and ancillary data sources. *Environmental Monitoring and Assessment*, 51(1-2), 415-428.
doi:10.1023/a:1005996900217

Wallace, J. M. (1975). Diurnal variations in precipitation and thunderstorm frequency over the conterminous United States. *Monthly Weather Review*, 103(5), 406–419.
doi:10.1175/1520-0493(1975)103<406:DVIPAT>2.0.CO;2

Watson, A. I., & Holle, R. L. (1996). An eight-year lightning climatology of the southeast United States prepared for the 1996 summer olympics. *Bulletin of the American Meteorological Society*, 77(5), 883–890. doi:10.1175/1520-0477(1996)077<883:aeylco>2.0.co;2

Westcott, N. E. (1995). Summertime cloud-to-ground lightning activity around major midwestern urban areas. *Journal of Applied Meteorology*, 34(7), 1633–1642.
doi:10.1175/1520-0450-34.7.1633

Williams, E. R. (2005). Lightning and climate: A review. *Atmospheric Research*, 76(1-4), 272–287. doi:10.1016/j.atmosres.2004.11.014

Williams, S. J., Stone, G. W., & Burruss, A. E. (2012). A perspective on the Louisiana wetland loss and coastal erosion problem. *Journal of Coastal Research*, 13(3), 593–594.

Yang, H., Pasko, V. P., & Sátori, G. (2009). Seasonal variations of global lightning activity extracted from Schumann resonances using a genetic algorithm method. *Journal of Geophysical Research-Atmospheres*, 114(D01103). doi:10.1029/2008jd009961

Yuan, F., Sawaya, K. E., Loeffelholz, B. C., & Bauer, M. E. (2005). Land cover classification and change analysis of the twin cities (Minnesota) metropolitan area by multitemporal Landsat remote sensing. *Remote Sensing of Environment*, 98(2-3), 317–328.
doi:10.1016/j.rse.2005.08.006

Zajac, B. A., & Rutledge, S. A. (2001). Cloud-to-ground lightning activity in the contiguous United States from 1995 to 1999. *Monthly Weather Review*, 129(5), 999–1019.
doi:10.1175/1520-0493(2001)129<999:CTGLAI>2.0.CO;2

Zhang, Q., Wang, J., Peng, X., Gong, P., & Shi, P. (2002). Urban built-up land change detection with road density and spectral information from multi-temporal Landsat TM data. *International Journal of Remote Sensing*, 23(15), 3057–3078.
doi:10.1080/01431160110104728

Zhu, Y. N., Rakov, V. A., Mallick, S., & Tran, M. D. (2015). Characterization of negative cloud-to-ground lightning in florida. *Journal of Atmospheric and Solar-Terrestrial Physics*, 136, 8-15. doi:10.1016/j.jastp.2015.08.006

Vita

Nicholas Sokol was born in Charleston, South Carolina, and was raised in several states including Delaware, Florida, Maryland, New Jersey, North Carolina, Pennsylvania, and South Carolina. He earned a Bachelor of Science in geography and environmental planning from Towson University in May 2015. Immediately after his commencement Nicholas attended Louisiana State University to pursue the M.S. in geography in the Fall 2015. He will receive the Master of Science degree in Fall 2016.